dynamic software & engineering

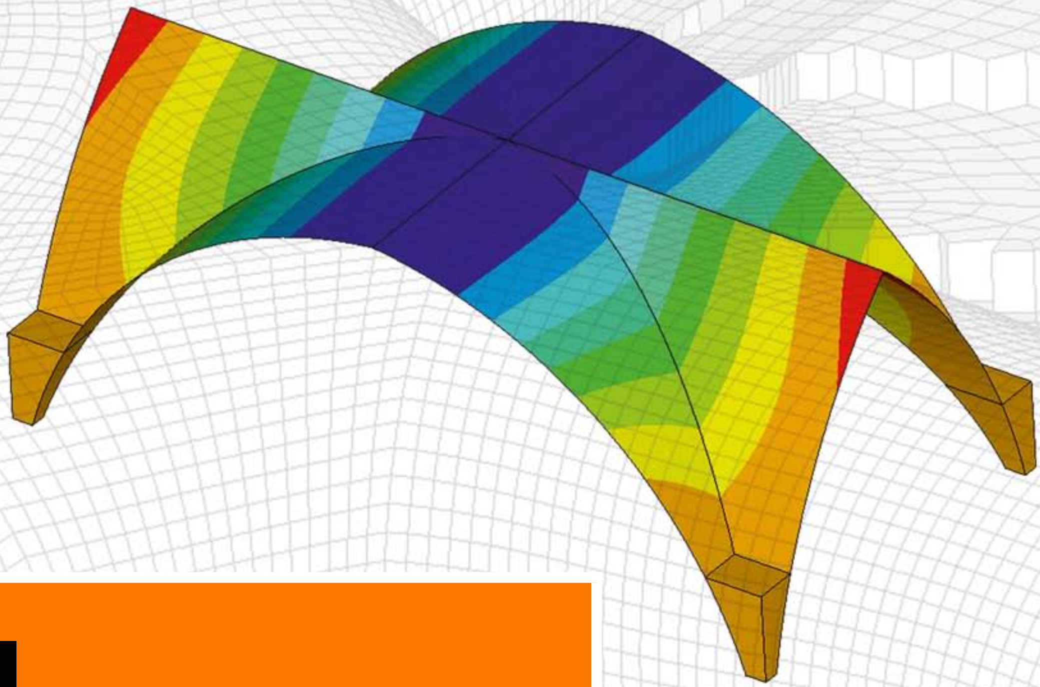

User's Manual

multiPlas

Release 4.1.8 for ANSYS 14.5

January 2013, Rev. 1

Elasto-plastic material models for ANSYS

General multisurface plasticity

multiPlas

CONTENT

1 INTRODUCTION

This manual describes the use of Dynardo's software product ***multiPlas*** for ANSYS. multiPlas is a library of elasto-plastic material models for ANSYS.

The elasto-plastic material models in multiPlas, enable the user to simulate elasto-plastic effects of artificial materials, e.g. steel or concrete, and natural born materials, e.g. soil or rock, in geotechnics, civil engineering - as well as - mechanical engineering.

In the context of finite element calculations with ANSYS, multiPlas provides an efficient and robust algorithm for the handling of single and multi-surface plasticity. The material models are based on elasto-plastic flow functions with associated and non-associated flow rules. One special feature of the multiPlas material models is the combination of isotropic and anisotropic yield conditions.

The multiPlas material models are available for structural volume elements (e.g. SOLID 45, SOLID 95), for structural shell elements (e.g. SHELL 43, SHELL 93) and structural plane elements (e.g. PLANE 42, PLANE 82).

The following material models and features are provided:

Model	Application	Flow Rule	Stress-Strain Response	Temperature Dependency
isotropic Material Models:				
Tresca	Steel, ...	associative	bilinear, ideal elastic-plastic	
Mohr-Coulomb	Soil, Rock, Stone, Masonry, ...	non-associative	bilinear, residual strength	yes
von Mises	Steel, ...	associative	bilinear, ideal elastic-plastic	
Drucker-Prager	Soil, Stone, ...	associative	bilinear, ideal elastic-plastic	
modified Drucker-Prager	Stone, Cement, Concrete, ...	associative	bilinear, ideal elastic-plastic	yes
Concrete	Concrete, Cement, Stone, Brick, ...	non-associative	nonlinear hardening and softening	yes
Tension cut off	rotated cracking	associative	residual strength	
anisotropic Material Models:				
Mohr-Coulomb	Joints, jointed Rock, Cohesive Zones, ...	non-associative	bilinear, residual strength	
Masonry_Ganz	Masonry, ...	non-associative	nonlinear hardening and softening	yes
Tsai / Wu	Wood, ...	associative	bilinear, ideal elastic-plastic	
boxed value	Wood, ...	associative	multilinear hardening and softening	
Tension cut off	fixed cracking, Cohesive Zones	associative	residual strength / exponential softening	

Additionally, all Mohr-Coulomb Models are coupled with a tension cut-off yield surface.

In simulations of joint materials (e.g. jointed rock), it is possible to arrange the joint sets arbitrarily. Isotropic and anisotropic Mohr-Coulomb yield surfaces can be combined in manifold ways. Up to 4 joint sets can be associated with an isotropic strength definition.

MultiPlas has been successfully applied in nonlinear simulations of and concrete as well as in stability analysis of soil or jointed rock.

2 INSTALLATION INSTRUCTIONS

multiPlas provides a customized executable (ANSYS.EXE) for ANSYS. The multiPlas package is delivered as a single zip-file, e.g. multiPlas_418_ansys145_64bit.zip. Please extract this file into an arbitrary directory, e.g. C:\Program Files\ANSYS Inc\v145. A new sub-directory, multiPlas_4.1.8 is created. Please notice the full path to your multiPlas installation. There is no further installation required for multiPlas.

In addition the multiPlas license file, e.g. *dynardo_client.lic*, must be copied into one of the following directories:

- the application installation directory
- the "%Program Files%/Dynardo/Common files" directory (Unix: "~/.config/Dynardo/Common")
- the users home directory (Unix: $HOME, Windows: %HOMEPATH%)
- the current working directory

For any further questions of licensing, please contact your system administrator or write an E-mail to support@dynardo.de

2.1 How to start ANSYS Mechanical APDL with multiPlas

The ANSYS Mechanical APDL Product Launcher can be used to start ANSYS Mechanical APDL with multiPlas. After starting the launcher, choose the “Customization/Preferences” tab. In the field “Custom ANSYS executable” browse to the ANSYS.EXE in your multiPlas installation directory. This procedure is summarized in Fig. 2-1.

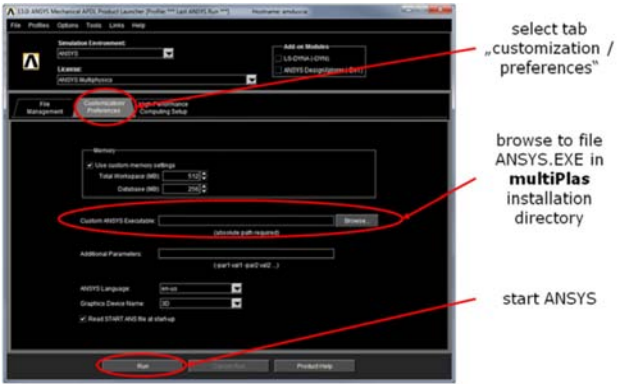

Fig. 2-1: start multiPlas in ANSYS Mechanical APDL via launcher

Another possibility is to start ANSYS Mechanical APDL from command line using the option “–custom <multiPlasDir>\ANSYS.EXE”, where <multiPlasDir> must be replaced by the full (absolute) path to your multiPlas installation.

The following command line starts ANSYS Mechanical APDL with multiPlas in graphical mode:
"C:\Programme\ANSYS Inc\v145\ansys\bin\winx64\ansys.exe" –g –custom “<multiPlasDir>\ANSYS.EXE”

The corresponding command line for batch mode is:
"C:\Programme\ANSYS Inc\v145\ansys\bin\winx64\ansys.exe" –b –i <InputFile> -o <OutputFile> –custom “<multiPlasDir>\ANSYS.EXE”

An example of the windows-batch script is included in the shipment.

Note: The path to the customized multiPlas executable must be enclosed in quotation marks.

For any further command line options please take a look at the ANSYS operations guide:
Operations Guide, chapter 3, Running the ANSYS Program, 3.1.
Starting an ANSYS Session from the Command Level

2.2 How to use ANSYS Workbench with multiPlas

In order to enable multiPlas in ANSYS Workbench the solver settings in Mechanical must be customized. In ANSYS Mechanical:

- Select “**Solve Process Settings…**“ from menu “**Tools**“
- Choose the solver settings to be modified and select **“Advanced…”**
- Add the following option to the field **“Additional Command Line Arguments”:** –custom “<multiPlasDir>\ANSYS.EXE”

3 THEORY OF THE MULTIPLAS MATERIAL MODELS IN ANSYS

3.1 Basics of elasto-plasticity in multiPlas

The material models in multiPlas uses a rate-independent plasticity. The material models are characterized by the irreversible strain that occurs once yield criteria are violated. It is assumed that the total strain vector can be divided into a elastic and a plastic component.

$$\{\varepsilon\}^{tot} = \{\varepsilon\}^{el} + \{\varepsilon\}^{pl} \tag{3-1}$$

where:

$\{\varepsilon\}^{el}$ – elastic strain vector (EPEL)
$\{\varepsilon\}^{pl}$ – plastic strain vector (EPPL)

The plastic strains are assumed to develop instantaneously, that is, independent of time.

The yield criterion

$$F(\{\sigma\},\kappa) \le 0 \tag{3-2}$$

where:

$\{\sigma\}$ - stress vector
κ - hardening parameter

limit the stress domain. If the computed stress, using the elastic deformation matrix, exceeds the yield criteria (F>0), then plastic strain occurs. Plastic strains will computed by flow rule

$$d\varepsilon^{pl} = \lambda \frac{\partial Q}{\partial \sigma} \tag{3-3}$$

where:

λ - plastic multiplier (which determines the amount of plastic straining)
Q - plastic potential (which determines the direction of plastic straining)

The plastic strains reduce the stress state so that it satisfies the yield criterion (F=0). By using associated flow rules, the plastic potential is equal the yield criterion and the vector of plastic strains is arranged perpendicularly to the yield surface.

$$Q = F \tag{3-4}$$

By using non-associated flow rules

$$Q \neq F \tag{3-5}$$

effects that are known from experiments like dilatancy can be controlled more realistically.

The hardening / softening function $\Omega(\kappa)$ describes the expansion and the reduction of the initial yield surface dependant on the load path, as well as the translation of the yield criterion in the stress domain. For the strain driven hardening/softening equations in multiPlas the scalar value κ serves as a weighting factor for plastic strain.

$$d\kappa = d\kappa(\varepsilon^{pl}) = d\varepsilon_{eq}^{pl} \tag{3-6}$$

The introduction of a separate softening function for each strength parameter made it possible to formulate an orthotropic softening model that is dependent from the failure mode. Existing relations, for example shear-tension interaction (mixed mode), were recognised.

The numerical implementation of the plasticity models is carried out using the return-mapping method [6-17], [6-18], [6-22]. The return mapping procedure is used at the integration point for the local iterative stress relaxation. It consists of two steps:

1. elastic predictor step:

$$\sigma_{i+1}^{trial} = \sigma_i^* + D\, d\varepsilon_{i+1}^{tot} \tag{3-7}$$

2. plastic corrector step (local iterative procedure):

$$\frac{d\sigma}{d\lambda} = -D\,\frac{\partial Q}{\partial \sigma} \tag{3-8}$$

3.2 Multisurface plasticity

The consideration of different failure modes rsp. failure mechanisms of a material is possible by a yield surface built up from several yield criteria. In the stress domain then a non-smooth multisurface yield criterion figure develops.

The elastic plastic algorithm has to deal with singularities at intersections from different yield criteria (e.g. F1 to F2 as represented in Fig. 3-1).

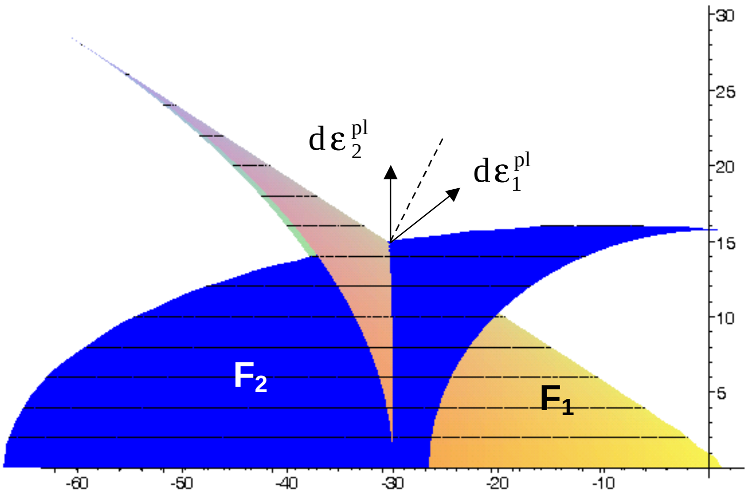

Fig. 3-1 Intersection between the two flow criteria F1 and F2

The consistent numerical treatment of the resulting multi-surface plasticity must deal with the possibility that many yield criteria are active simultaneously. This leads to a system of n=j equations:

$$\left\{\frac{\partial F_n}{\partial \sigma}\right\}^T D\, d\varepsilon = \sum_{j=1}^{Set\ of\ active\ YC} \left[\left\{\frac{\partial F_n}{\partial \sigma}\right\}^T D\,\frac{\partial Q_j}{\partial \sigma} - \frac{\partial F_n}{\partial \kappa_n}\frac{\partial \kappa_n}{\partial \lambda_j}\right] d\lambda_j \tag{3-9}$$

The solution of this system of equations generates the stress return to flow criteria or within the intersection of flow criterias. Contrary to single surface plasticity exceeding the flow criterion is no longer a sufficient criterion for activity of the plastic multiplier for each active yield criterion. An activity criterion needs to be checked.

$$d\lambda_j \geq 0 \tag{3-10}$$

This secures that the stress return within the intersection is reasonable from a physical point of view.

3.3 Computed yield surfaces

3.3.1 Introduction yield surfaces of basic material models

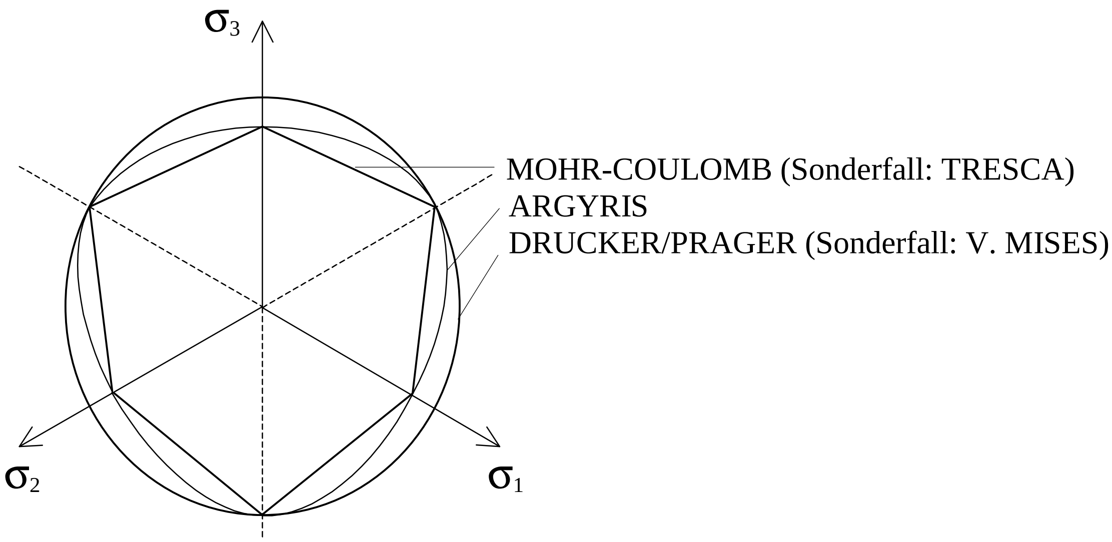

Fig. 3-2 Cut in the deviator plane of different flow figures

Miscellaneous yield criteriona of soil or rock mechanics generally describe flow figures which lie in between the flow figure of Mohr-Coulomb and of Drucker-Prager. . The difference in the area, surrounded by the yield surface (elastic stress domain) in the deviator-cut-plane, is 15% at its maximum.

In the standard literature of soil mechanics, the general usage of Mohr-Coulomb material models is suggested. Yield graphs according to Drucker and Prager do in fact generally overestimate the bearing strength.

For brittle materials (concrete/rock) composite flow conditions on the basis of Mohr-Coulomb as well as composite flow conditions on the basis of Drucker-Prager are used in the standard literature.

3.3.2 **MOHR-COULOMB isotropic yield criterion**

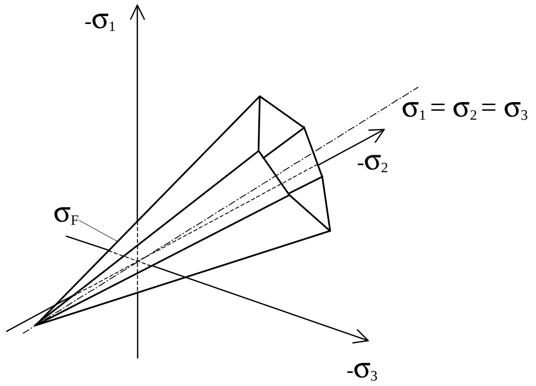

These yield criteria depend only on the two material parameters:

cohesion c and

inner friction angle φ

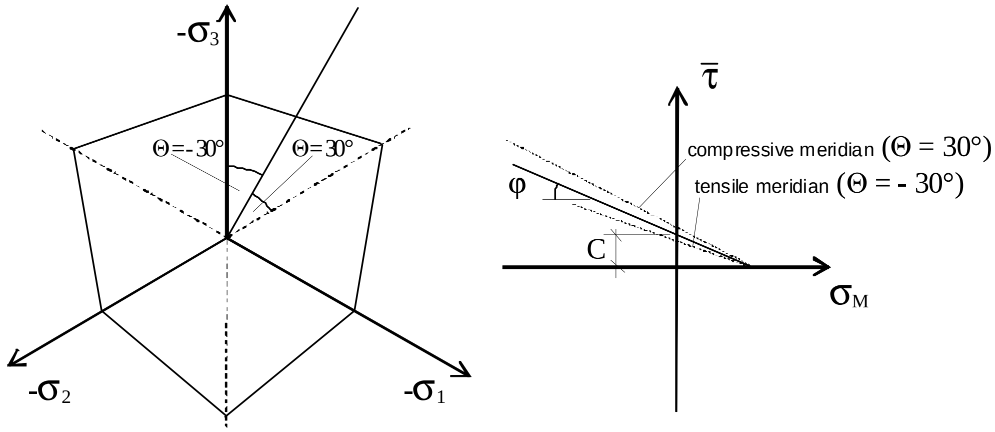

Fig. 3-3 MOHR-COULOMB isotropic yield criterion

The yield criterion is:

$$F = \sigma_m \sin\varphi + \sigma_S \left(\cos\Theta - \frac{\sin\Theta \sin\varphi}{\sqrt{3}} \right) - c \cos\varphi \tag{3-11}$$

where:

$$\sigma_m = \frac{\sigma_x + \sigma_y + \sigma_z}{3} \tag{3-12}$$

$$\sigma_S = \sqrt{I_2} \tag{3-13}$$

$$\sin(3\,\Theta) = -\frac{3\sqrt{3}}{2}\frac{I_3}{I_2^{3/2}} \tag{3-14}$$

σ_m hydrostatic stress
I_2 second invariant of the deviatoric main stresses
I_3 third invariant of the deviatoric main stresses
Θ Lode-angle

Necessary material parameters in the ANSYS material model MOHR-COULOMB isotropic:

φ – inner friction angle (phi)
C – cohesion
f_t – tensile strength (in case of tension cut off)
ψ – dilatancy angle (psi)

The residual strength can be defined. The residual strength is initiated after the yield strength has been exceeded.

The uniaxial compressive strength corresponds with the friction angle and cohesion as shown below:

$$f_c = c\frac{2\cos\varphi}{1-\sin\varphi} = 2c\tan\left(45+\frac{\varphi}{2}\right) \tag{3-15}$$

3.3.3 **MOHR-COULOMB anisotropic yield criterion**

For the definition of joints, separation planes or strength anisotropies the position of the yield surface depends on the position of the two joint-angles:

The two angles „First Angle“ (α) and „Second Angle“ (β) describe the position of the joint / separation plane.

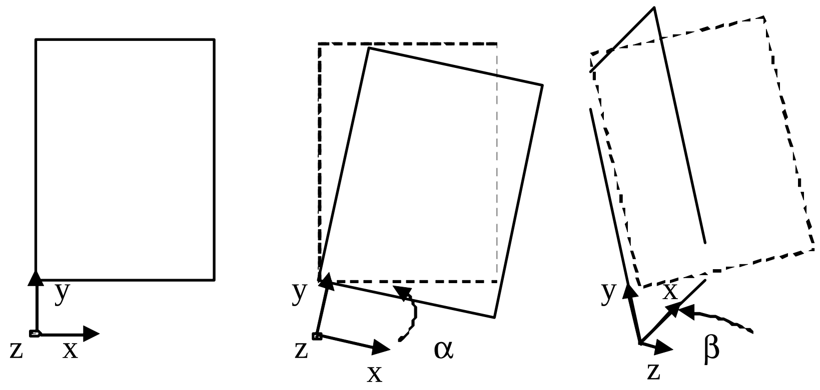

1. α - rotation against positive rotational direction about the z-axis
2. β - rotation in positive rotational direction about the y-axis

Fig. 3-4 Angle definition of the joint

The yield criterion is:

$$\left|\tau_{Res}\right| - \sigma_n \cdot \tan\varphi - C = 0 \qquad (3\text{-}16)$$

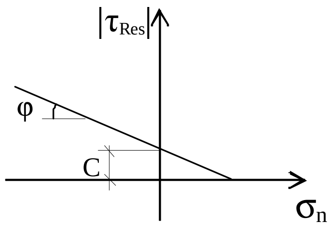

Fig. 3-5 MOHR-COULOMB anisotropic yield criterion

where:

τ_{Res} – shear stress in the joint

σ_n – normal stress perpendicular to the joint

Necessary material parameters in the ANSYS material model MOHR-COULOMB anisotropic:

α,β – position angle of the family or separation planes
φ – friction angle
C – cohesion
f_t – tensile strength (in case of tension cut off)
ψ – dilatancy angle

Residual strength can be defined. The residual strength is initiated after the yield strength has been exceeded.

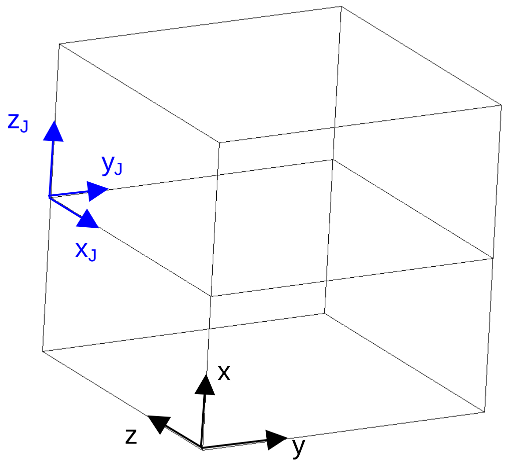

α=0°, β=90°

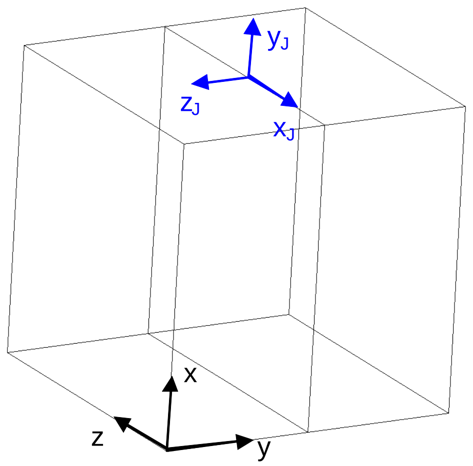

α=90°, β=90°

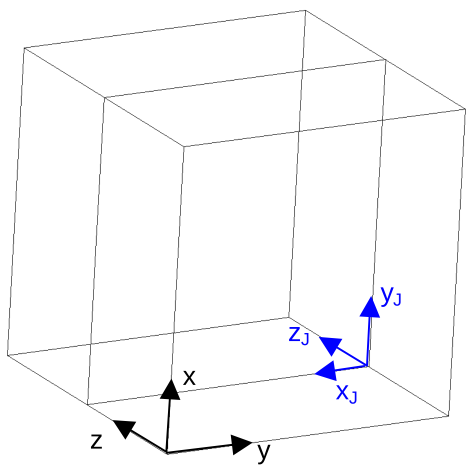

α=90°, β=0°

x, y, z – Element coordinate system

x_J, y_J, z_J – joint coordinate system

Fig. 3-6 Examples for the angle definition of joints

3.3.4 **Yield criterion according to DRUCKER-PRAGER**

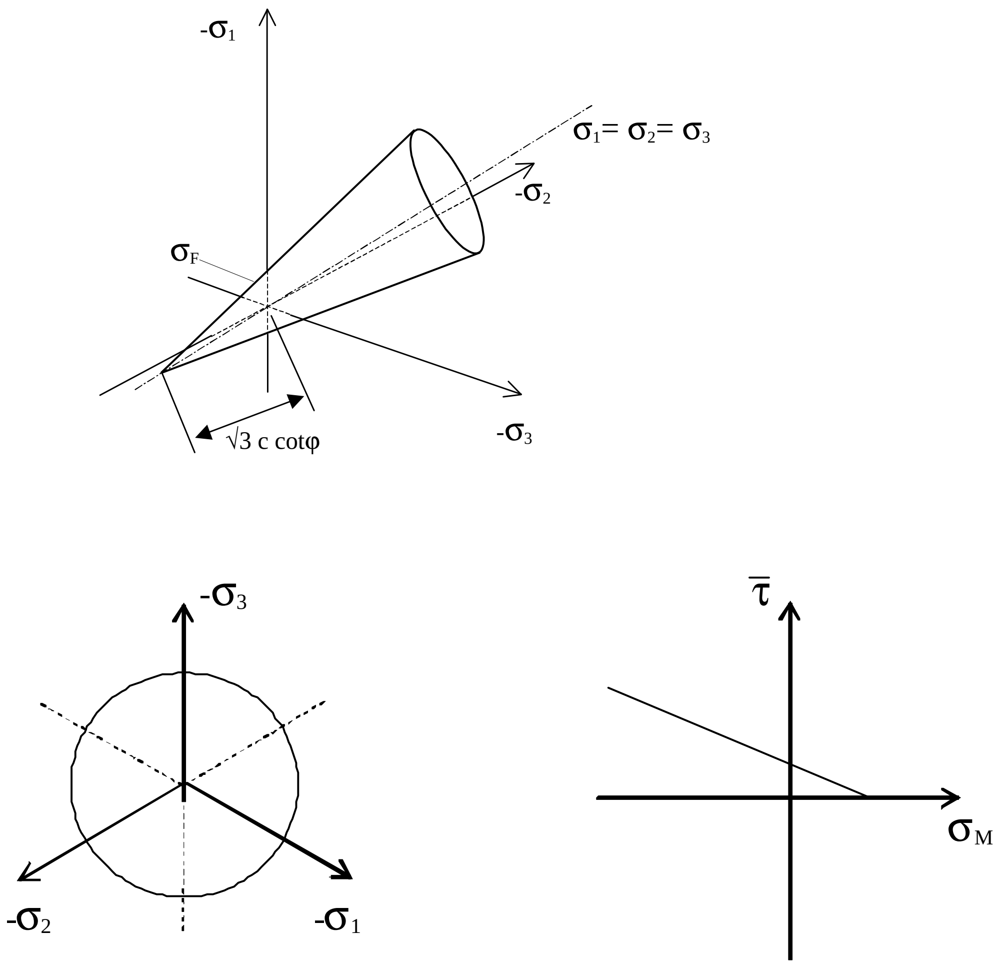

Fig. 3-7 Flow conditions according to DRUCKER-PRAGER

The Drucker-Prager yield criterion is:

$$F = \sigma_S + \beta\,\sigma_m - \tilde{\sigma}_{yt} \tag{3-17}$$

The plasticity potential is:

$$Q = \sigma_S + \beta\,\delta\,\sigma_m \tag{3-18}$$

where:

σ_m hydrostatic stress s. (3.12)
I_2 second invariant of the deviatoric main stresses s. (3.13)
δ dilatancy factor

The Drucker-Prager yield criterion can approximate the Mohr-Coulomb failure condition as circumlocutory cone or as inserted to a cone (see Fig. 3-8). Using the material library multiPlas calculation of arbitrary

interim values or blending with Mohr-Coulomb failure conditions are possible as well. Necessary material parameters in the ANSYS multiPlas material model DRUCKER/PRAGER are

β and $\tilde{\sigma}_y$.

Both parameters are connected to cohesion and angle of friction by the following formula:

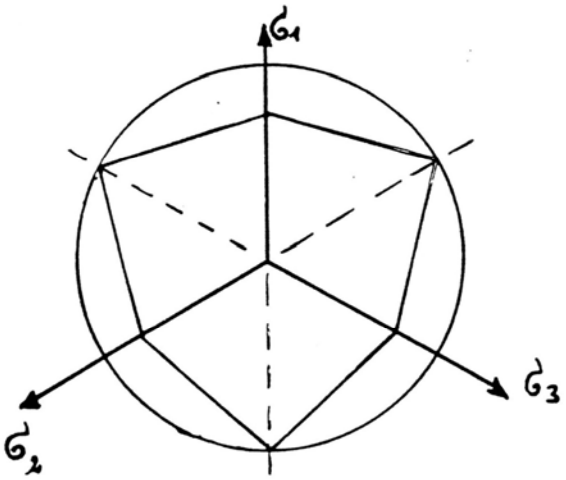

where:

$$\beta = \frac{6 \cdot \sin\varphi}{\sqrt{3}(3+\sin\varphi)} \qquad \beta = \frac{6 \cdot \sin\varphi}{\sqrt{3}(3-\sin\varphi)}$$

$$\tilde{\sigma}_y = \frac{6 \cdot c \cdot \cos\varphi}{\sqrt{3}(3+\sin\varphi)} \qquad \tilde{\sigma}_y = \frac{6 \cdot c \cdot \cos\varphi}{\sqrt{3}(3-\sin\varphi)}$$

Fig. 3-8 Drucker-Prager yield criterion as circumlocutory cone (left) or inserted to a cone (right).

3.3.5 **Combination of flow condition according to MOHR-COULOMB and DRUCKER-PRAGER or TRESCA and von MISES**

As shown in
Fig. **3-8** the MOHR-COULOMB and the DRUCKER-PRAGER yield criterion differ in the elastic stress domain. The difference of the surrounded area in the deviator cut plane is 15% at the maximum.

For some problem formulations it can be necessary to limit the elastic stress domain to the area given by the MOHR-COLOUMB yield criterion. In cases if MOHR-COULOMB or TRESCA alone lead to poor convergence or even divergence, it can be reasonable to use a combination of the yield criteria to stabilize the numerical computation.

It has to be kept in mind that this combination is reasonable only for numerical stabilization. It leads inevitably to differences in the results contratry to the sole usage of the yield criterion by MOHR-COULOMB. The return-mapping of the stress is not commutaded exactly for both criteria – MOHR-COULOMB and DRUCKER-PRAGER. Therefore, the permissibility of these result has to be checked individually!

3.3.6 **Concrete modelling using modified DRUCKER-PRAGER model**

The yield condition consists of two yield criteria (equations (3-19), (3-20)), whereby the concrete strength can be described closed to the reality as well in the compressive as in the tensile domain.

$$F_1 = \sigma_S + \beta_t \sigma_m - \tilde{\sigma}_{yt}\, \Omega_1 \tag{3-19}$$

$$\beta_t = \frac{\sqrt{3}\,(R_d - R_z)}{R_d + R_z} \qquad \tilde{\sigma}_{yt} = \frac{2\,R_d\,R_z}{\sqrt{3}\,(R_d + R_z)}$$

$$F_2 = \sigma_S + \beta_c \sigma_m - \tilde{\sigma}_{yc}\, \Omega_2 \tag{3-20}$$

$$\beta_c = \frac{\sqrt{3}\,(R_u - R_d)}{2R_u - R_d} \qquad \tilde{\sigma}_{yc} = \frac{R_u R_d}{\sqrt{3}\,(2R_u - R_d)}$$

where:

σ_m	hydrostatic stress
I_2	second invariant of the deviatoric main stresses
R_z	uniaxial tensile strength
R_d	uniaxial compression strength
R_u	biaxial compression strength
Ω	hardening and softening function (in the pressure domain $\Omega_1 = \Omega_2 = \Omega_c$, in the tensile domain $\Omega_1 = \Omega_t$).

The plasticity potentials are:

$$Q_1 = \sigma_S + \delta_t \beta_t \sigma_m$$

where: δt, δc are dilatancy factors (3-21)

$$Q_2 = \sigma_S + \delta_c \beta_c \sigma_m$$

The yield condition is shown in Fig. 3-9 and Fig. 3-10 in different coordinate systems. The comparison with the concrete model made by Ottosen [6-15] is shown in Fig. 3-9 and illustrates the advantages of the Drucker-Prager model consisting of two yield criteria. While there is a very good correspondence in the compressive domain, the chosen Drucker-Prager model can be well adjusted to realistic tensile strength. In opposite to that, the Ottosen model overestimates these areas significantly! A further advantage lies within the description of the yield condition using the three easily estimable and generally known parameters R_z, R_d and R_u.

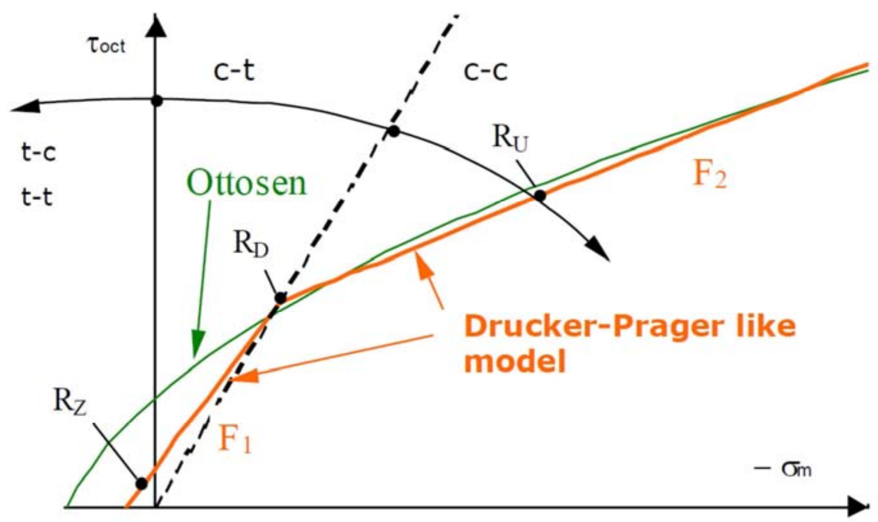

Fig. 3-9 Singular Drucker-Prager flow conditions – Illustrated in the octaeder system

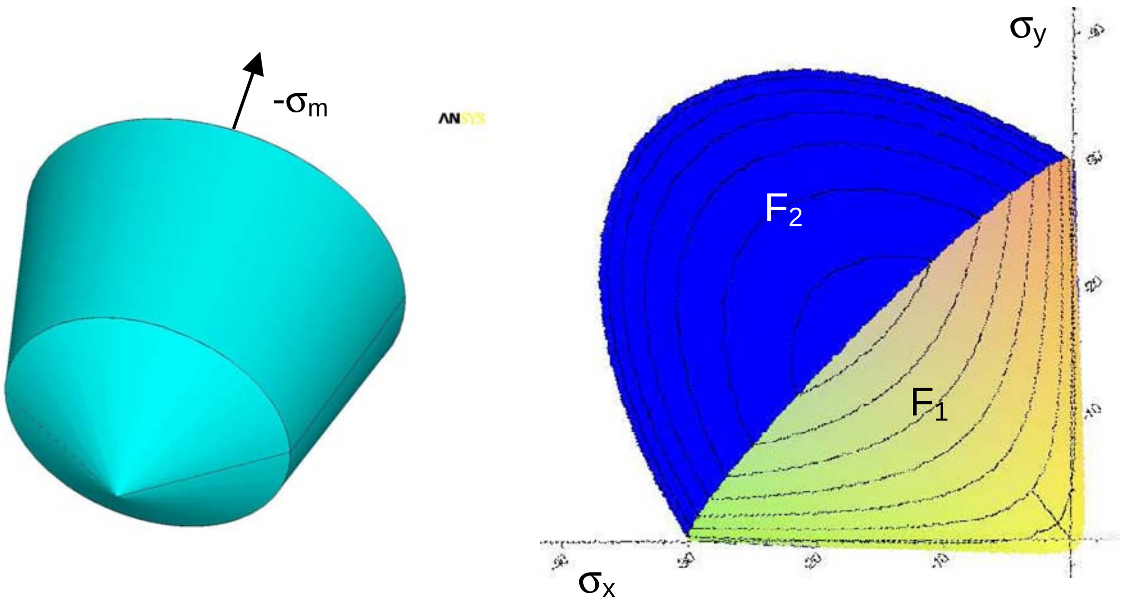

a) b)

Fig. 3-10 Singular Drucker-Prager flow condition:
a) yield surface in the main stress domain; b) Illustration in the σ_x-σ_y-τ_{xy}-space

3.3.6.1 Nonlinear deformation behaviour in case of pressure load

In general the uniaxial stress-strain relationship of concrete is characterized by three domains:

- A linear elastic domain which generally reaches up to about a third of the compressive strength.
- This is followed by an increasingly bent run until the compressive strength is reached. The nonlinear relation between stress and strain is caused by an initially small number of micro-cracks which merge with higher stress levels.
- The achievement of the compressive strength is associated with the forming of fracture surfaces and cracks which are aligned parallel to the largest main stress.
- The softening area is characterized by a decreasing strength. Finally, it leads to a low residual strain level. The slope of the decreasing branch is a measure for the brittleness of the material.

Fig. 3-11 shows the typical nonlinear stress-strain relation of normal concrete in uniaxial compressive tests [6-9].

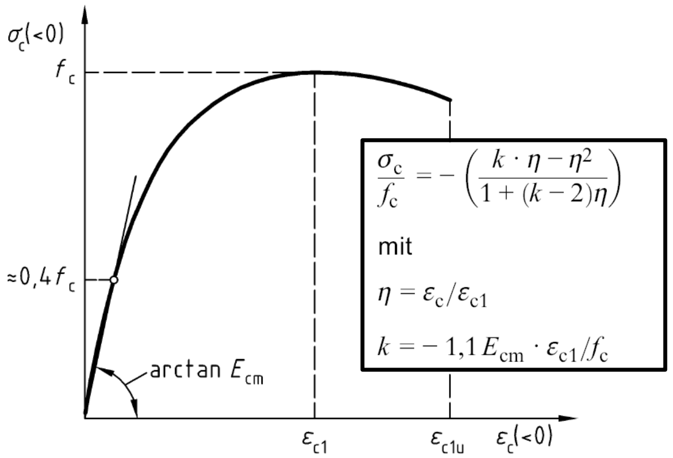

Fig. 3-11 Nonlinear stress-strain relation (uniaxial compression test) of normal concrete used in codes (DIN 1045-1 [6-9] and EC2 [6-10])

In Fig. 3-12 the stress-strain relation which is available in multiPlas is shown. Thereby linear softening (mlaw = 0, 2) or parabolic-exponential softening (mlaw = 1) can be chosen. Up to reaching the strain ε_u the parabola equation (as seen in Fig. 3-11) is used.

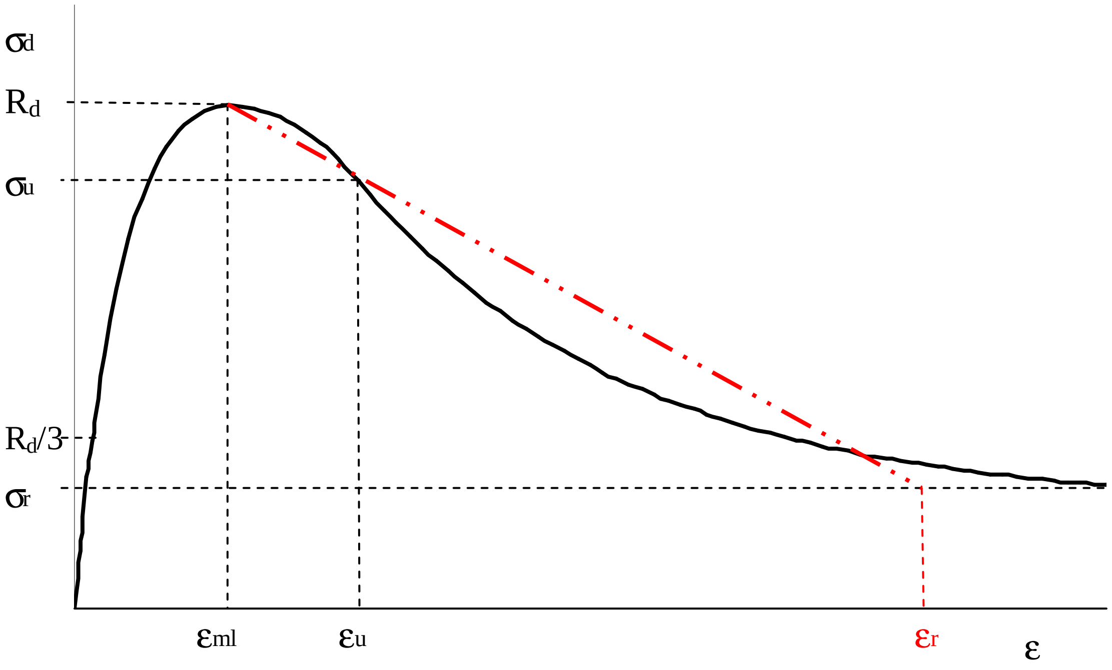

Fig. 3-12 stress-strain relation in multiPlas (mlaw=0,2; mlaw = 1)

3.3.6.2 Nonlinear deformation behaviour during tensile load

Concrete tends to soften relatively brittle with local appearances of cracks. For including this into the context of a continuum model, a homogenized crack and softening model is needed. The crack itself does not appear in the topology description of the structure - but is described by its impact on stress and deformation state [6-16],[6-21].

The softening process is formulated respectively to the energy dissipation caused by the occurance of cracks. For the complete cracking, the fracture energy concerning the crack surface has to be G_f-dissipated.

The used model has its origin within the crack band theory of Bažant / Oh [6-6]. It states that cracks develop within a local process zone. Its width h_{PR} (crack band width) is a material specific constant.
To avoid a mesh dependency of the softening and to assess the fracture energy correctly, a modification of the work equation is necessary. For a given width of the crack band and a given fracture energy, the volume fracture energy can be computed via:

$$g_f = \frac{G_f}{h_{PR}} \tag{3-22}$$

where:

g_f	volume fracture energy
G_f	fracture energy
h_{PR}	crack band width

For meshing of the structure with elements which are larger than the expected width of the crack band the stress-strain relationship has to be modified in such a way that the volume fracture energy reaches the following value:

$$g_{f,INT} = \frac{h_{PR}}{h} g_f = \frac{G_f}{h} \tag{3-23}$$

where: $g_{f,INT}$ volume fracture energy at the integration point
h equivalent length

This model guaranties a consistent dissipation of fracture energy during the softening process for different sizes of elements. The stress-strain lines available in multiPlas are shown in Fig. 3-13. Thereby, a linear elastic behaviour is assumed until the tensile strength is reached. After that, one of the following is assumed as consequence of tensile fracturing:

** linear softening until the strain limit is reached ε_{tr} (mlaw = 0, 2) or

** exponential softening (mlaw = 1)

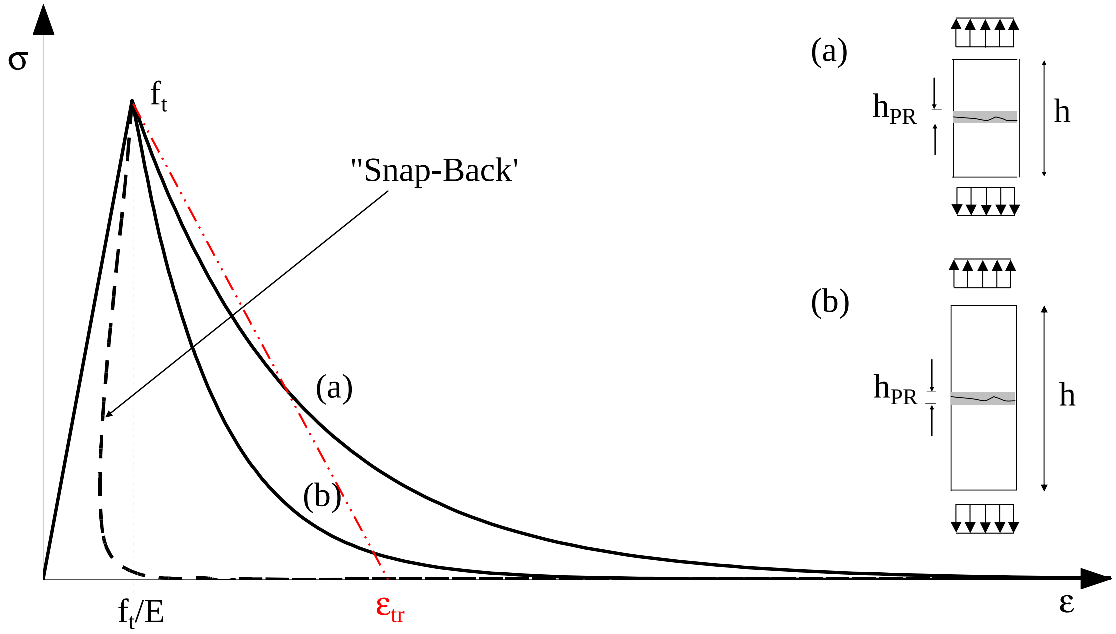

Fig. 3-13 Stress-strain relation in multiPlas (mlaw=0, 2; mlaw = 1)

For the exponential softening model (mlaw = 1) one should assume

$$h \leq \frac{G_f\, E}{f_t^2} \tag{3-24}$$

for the length h in order to avoid the numerically unstable „snap-back“ phenomena. This is preferably achieved by choosing a proper mesh size. In multiPlas, the equivalent length will calculated automatically.

3.3.6.3 Temperature dependency

Information on the temperature dependencies of the material behaviour are included in DIN EN 1992-1-2 [6-11]. As an example the temperature dependencies from pressure level are shown in Fig. 3-14, Fig. 3-15 and Tab. 3-1.

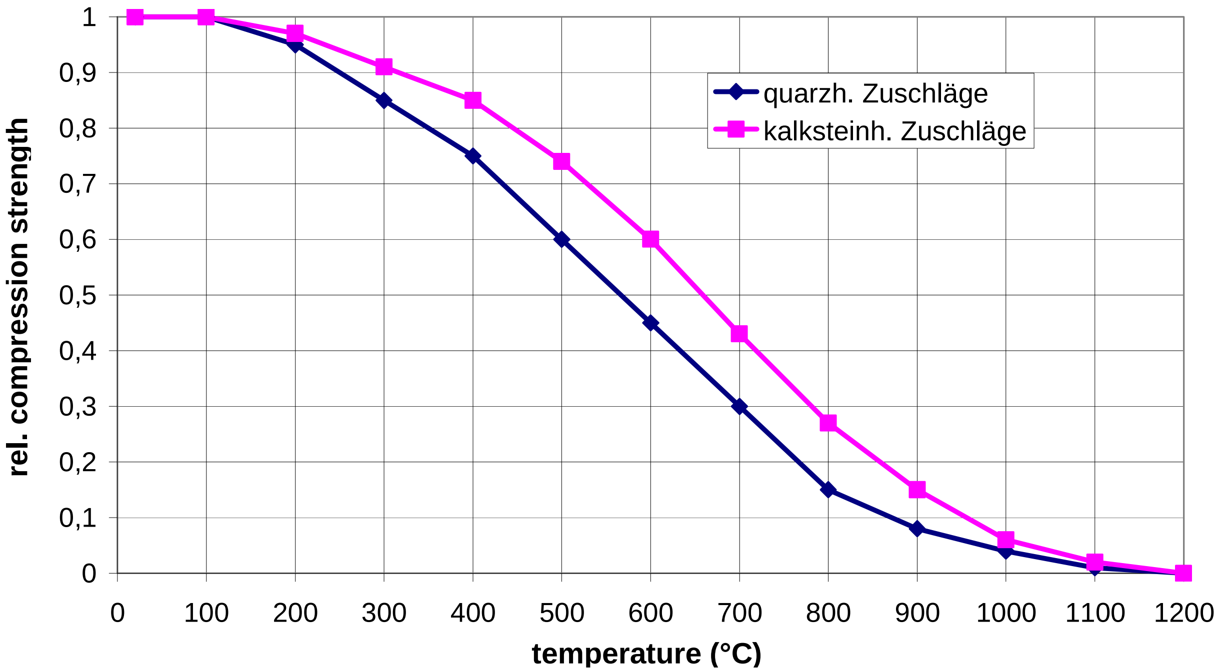

Fig. 3-14 Temperature dependency of concrete pressure resistance from [6-11]

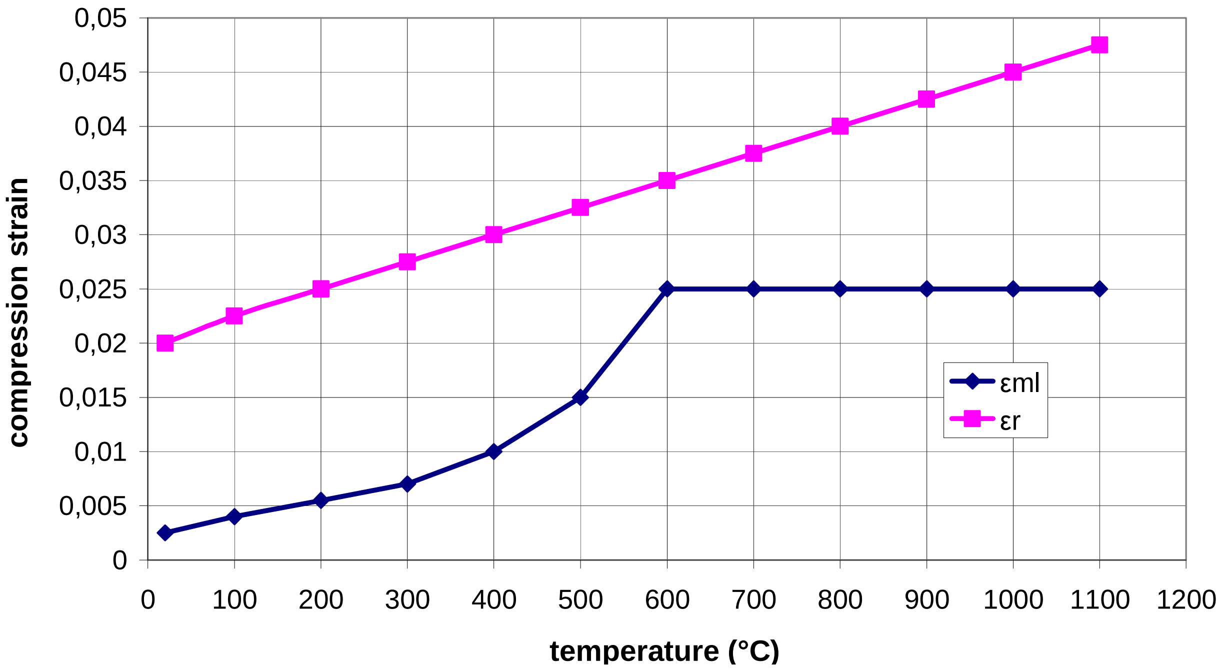

Fig. 3-15 Temperature dependency of concrete compression strain from [6-11]

Beton	quarzh. Zuschläge			kalksteinh. Zuschläge		
T (°C)	$R_d(T)/R_d$	ε_{ml}	ε_r	$R_d(T)/R_d$	ε_{ml}	ε_r
20	1	0,0025	0,02	1	0,0025	0,02
100	1	0,004	0,0225	1	0,004	0,0225
200	0,95	0,0055	0,025	0,97	0,0055	0,025
300	0,85	0,007	0,0275	0,91	0,007	0,0275
400	0,75	0,01	0,03	0,85	0,01	0,03
500	0,6	0,015	0,0325	0,74	0,015	0,0325
600	0,45	0,025	0,035	0,6	0,025	0,035
700	0,3	0,025	0,0375	0,43	0,025	0,0375
800	0,15	0,025	0,04	0,27	0,025	0,04
900	0,08	0,025	0,0425	0,15	0,025	0,0425
1000	0,04	0,025	0,045	0,06	0,025	0,045
1100	0,01	0,025	0,0475	0,02	0,025	0,0475
1200	0			0		

Tab. 3-1 Temperature dependency of concrete material values from [6-11]

In multiPlas up to 11 temperatures-pressure points and respective strains ε_m can be predefined. The associated limit strains are assumed according to Tab. 3-1. Interim values are linearly interpolated.
The temperature dependency of the concrete tensile strength is implemented in multiPlas using the Data from [6-11] (s. Fig. 3-16).

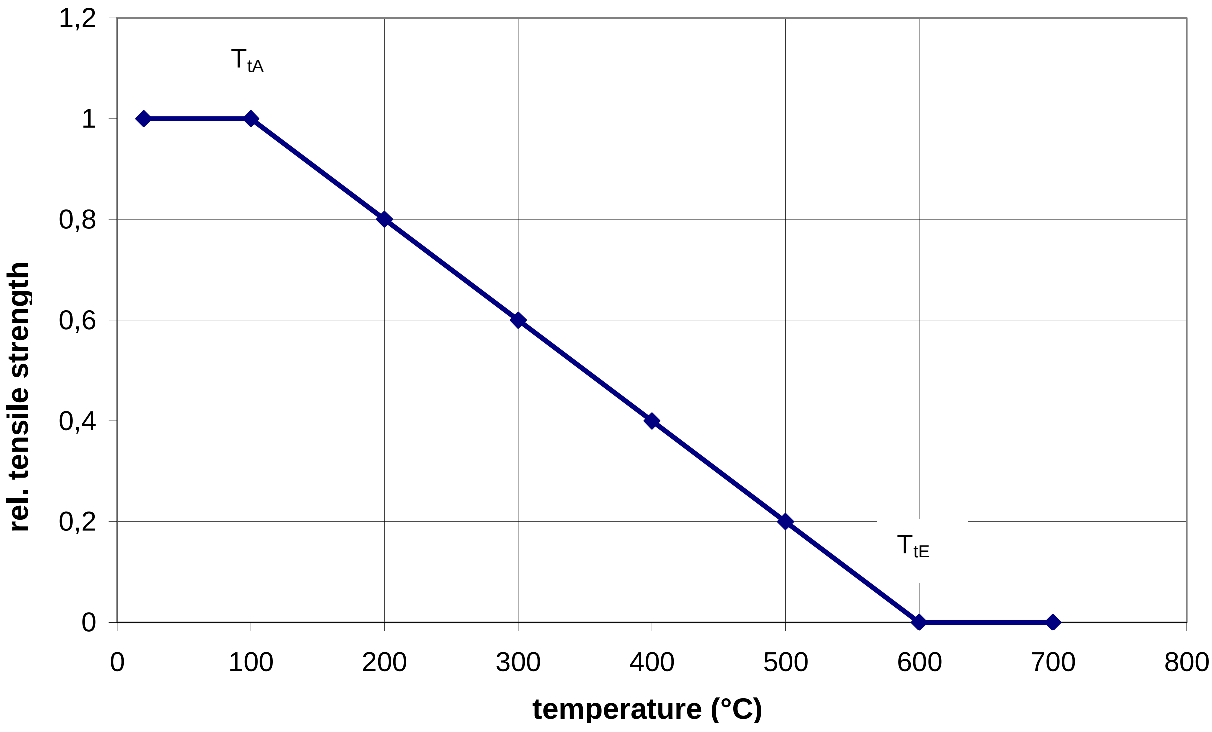

Fig. 3-16 Temperature dependency of the tensile strength of concrete from [6-11]

For the temperature dependency of steel reinforcement we refer to [6-11]. It can be taken into account by the standard parameters of ANSYS (tb,bkin oder tb,mkin).

3.3.7 **Simulation of regular masonry using the Ganz yield condition**

For describing the orthotropic strength of a regular masonry, an extended spatial masonry model was implemented which uses the Ganz yield criterion [6-23], [6-17]. It is the foundation of the Swiss masonry norm SIA 177/2 and complies with the fracturing model of Mann contained in DIN 1053 [6-24] as well as with the natural stone masonry model suggested by Berndt [6-25]. In the Ganz masonry model, an additionally interaction with a horizontal load (parallel to the longitudinal joint) is considered. The necessary material parameters of this model are compression- and tensile strength of the masonry, the friction angle and the cohesion between brick and joint as well as the brick dimensions. The multisurface yield condition (Fig. 3-17) represents the different failure mechanisms of regular masonry formation. The meaning of the yield criteria are given in Tab. 3-2.

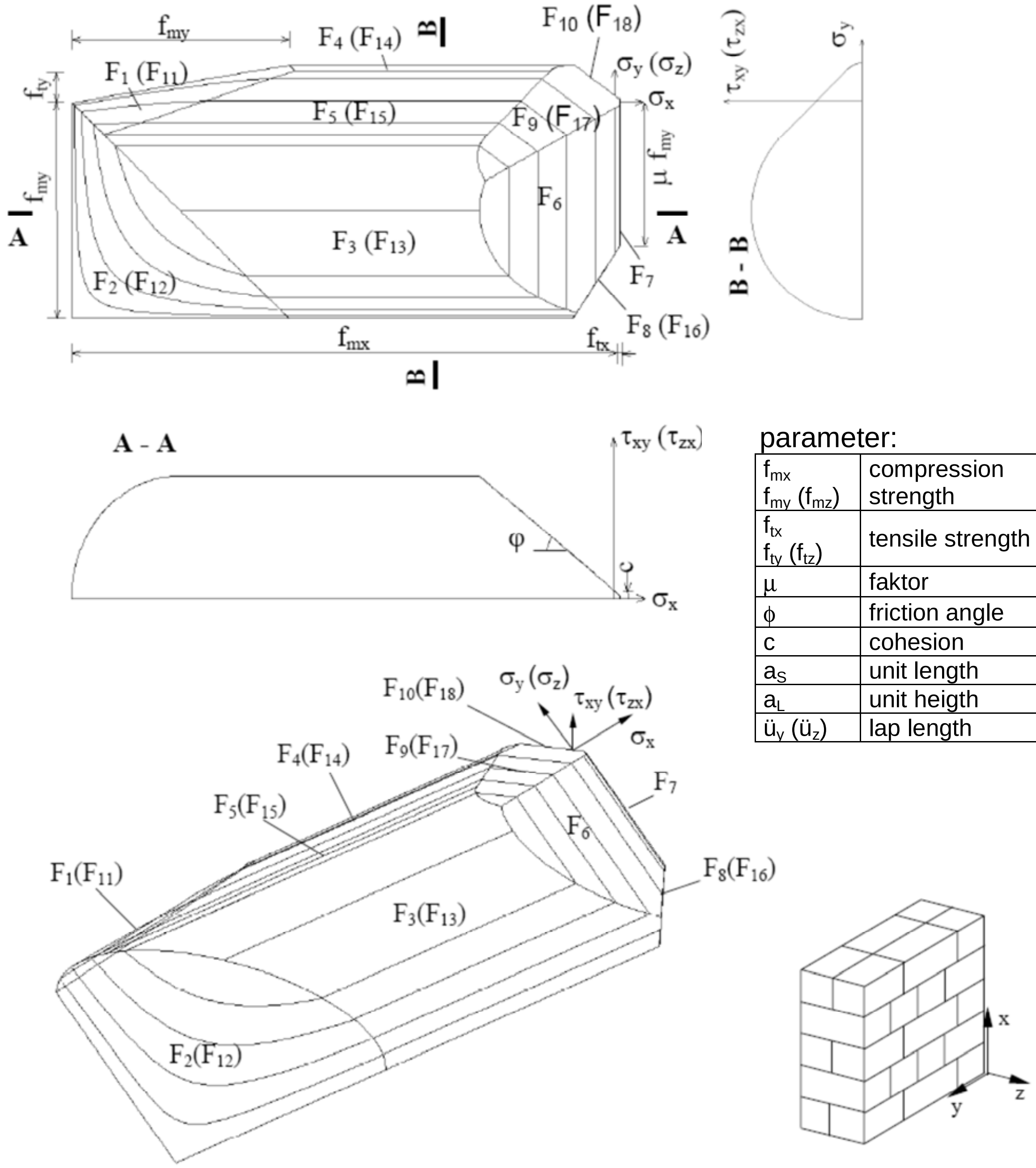

parameter:

f_{mx} f_{my} (f_{mz})	compression strength
f_{tx} f_{ty} (f_{tz})	tensile strength
μ	faktor
ϕ	friction angle
c	cohesion
a_S	unit length
a_L	unit heigth
$ü_y$ ($ü_z$)	lap length

Fig. 3-17 Ganz material model for masonry [6-17]

F1 (F11)	Tension failure brick
F2 (F12)	Compressive failure masonry
F3 (F13)	Shear failure masonry (brick failure)
F4 (F14)	Tension failure parallel to bed joint (brick failure)
F5 (F15)	Shear failure masonry
F6	Shear failure bed joint
F7	Tension failure bed joint
F8 (F16)	Tension failure bed joint under high horizontal pressure
F9 (F17)	Staircase-shaped shear failure
F10 (F18)	Tension failure of masonry parallel to bed joints (joint failure)

Tab. 3-2 Material model for masonry – meaning of the flow criteria

The orthotropic nonlinear stress-strain behaviour of masonry is described using the corresponding softening and hardening models [6-17].

3.3.7.1 Nonlinear stress-strain relation under pressure load

For simulation of a nonlinear stress-strain relation under pressure load two models are available (s. Fig. 3-18). The stress-strain relation complies with the DIN 1045-1 [Law 22] model for concrete shown in chapter 3.3.6.1 which also applies for vertical pressure load.
The model [Law 20] within Fig. 3-18 is often sufficiently accurate for practical applications.

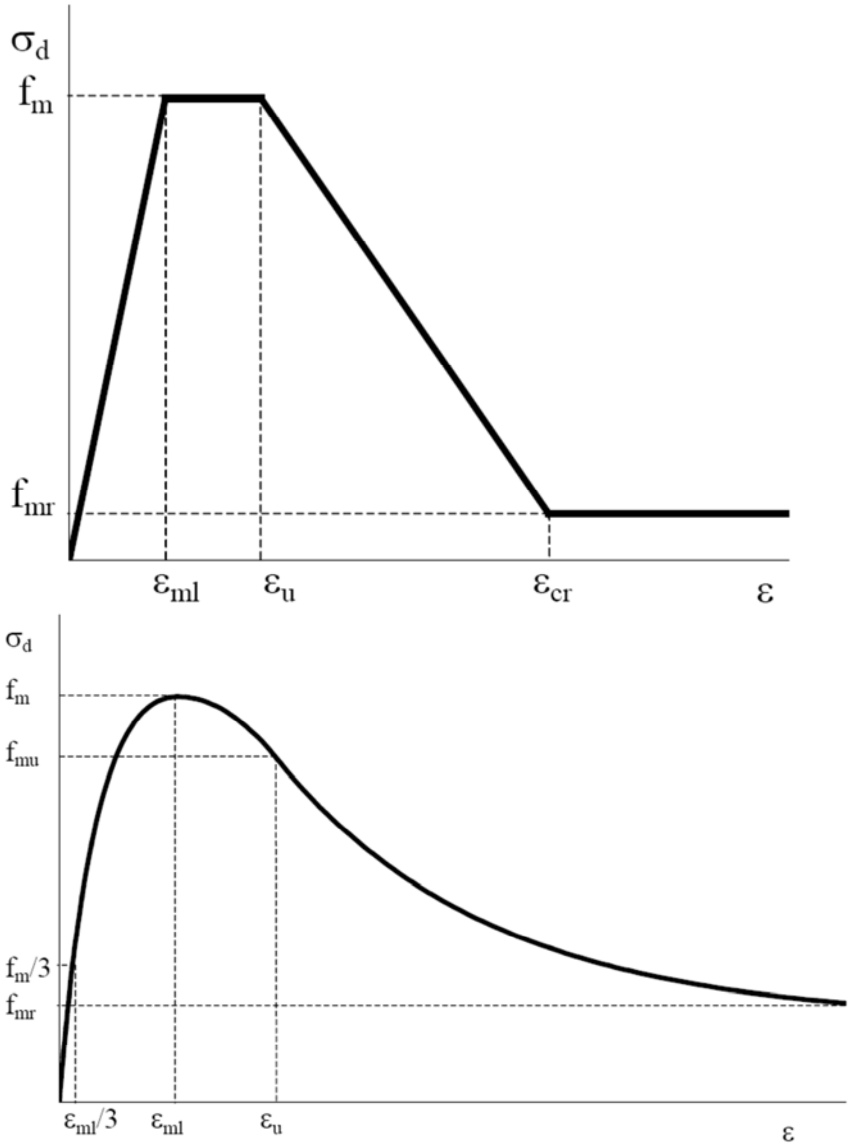

Fig. 3-18 models of the stress-strain relation in case of pressure load, above: LAW 20, below: LAW 22

3.3.7.2 Nonlinear stress-strain relation under tensile load perpendicular to the bed joints

For the behaviour under tensile stress perpendicular to the bed joints a stress-strain relation with exponential softening is available. The stress-strain relation is shown in Fig. 3-19. The conclusions, that are done in 3.3.6.2 are valid here as well.

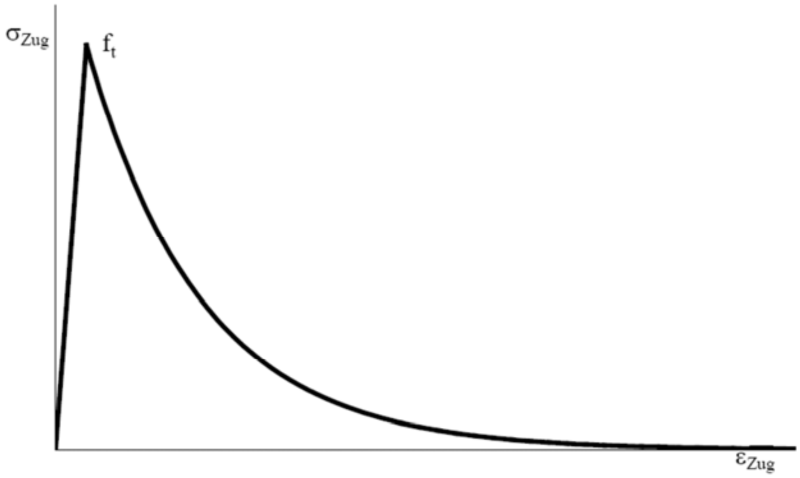

Fig. 3-19 stress-strain relation under tensile load perpendicular to the bed joints

3.3.7.3 Nonlinear stress-strain relation in case of shear load of bed joint

The shear failure of the bed joints, which could be observed in the test case, can be described by an exponential degradation of the cohesion C and linear reduction of the friction angle φ0 to a residual friction angle φr. The corresponding, assumed stress-strain line is shown in Fig. 3-20. The softening model for the cohesion C was chosen analogical to the approach described in chapter 3.3.6.2. Hereby it is assumed that for completely diminishing of the cohesion, a fracture energy G_{IIfJ} (mode II – adhesion-shear-strength) has to be dissipated. This has been experimentally established by van der Pluijm [6-27]. The tension and shear softening are synchronized.

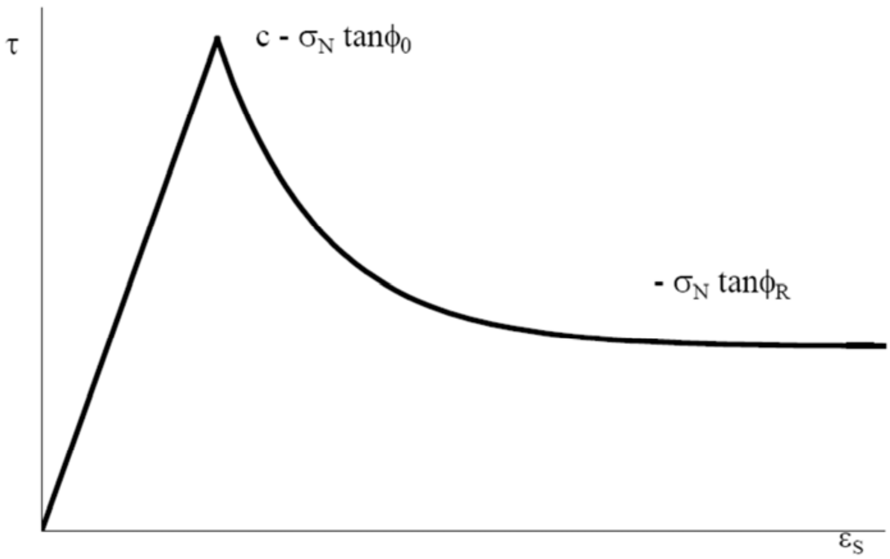

Fig. 3-20 Nonlinear stress-strain relation in case of shear of bed joint

3.3.8 **Wood modelling using a boxed-value-model**

The multi surface material model for wood is based on a boxed-value model from Grosse [6-26]. The orthotropic material model is implemented in multiPlas via LAW 33. It considers the interactions between the longitudinal, radial and tangential material behaviour of wood. The yield conditions are shown in Fig. 3-21 and Fig. 3-22. The stress and strain functions, implemented for describing the nonlinear deformation behaviour, are shown in chapter 3.3.8.1.

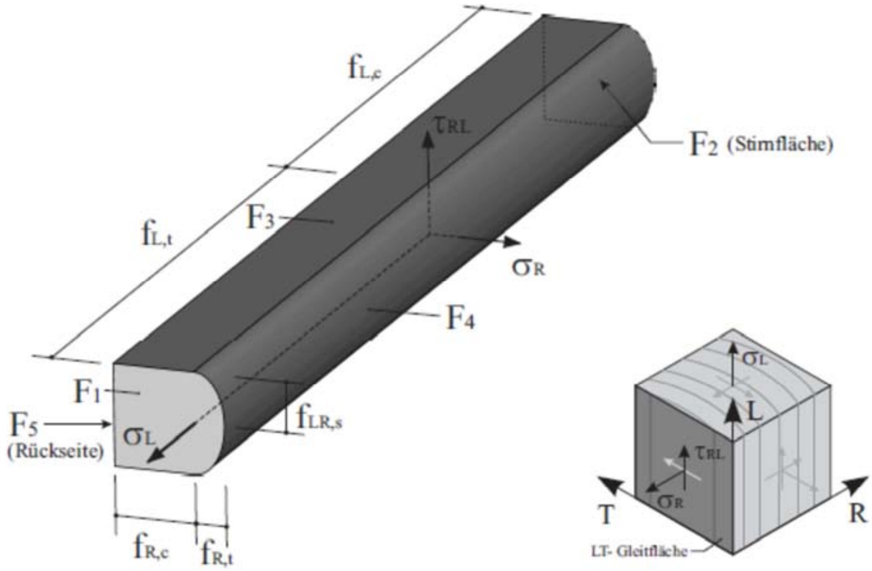

Fig. 3-21 yield condition – Interaction longitudinal vs. radial

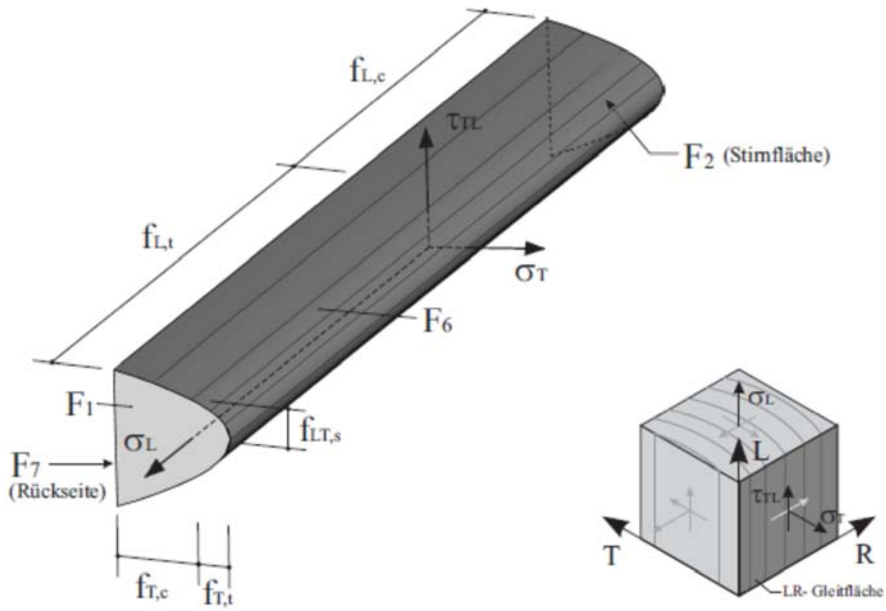

Fig. 3-22 yield condition – Interaction longitudinal vs. tangential

In multiPlas, the following conventions for the direction of wood fibre have been made:

Radial	=	X- Axis of element coordinate systems
Tangential	=	Y- Axis of element coordinate systems
Longitudinal	=	Z- Axis of element coordinate systems

This conventions hold for Cartesian and Cylindrical coordinate systems.

Following yield conditions are used:

Fiber rupture (tensile failure longitudinal)

$$F_1 = \sigma(3) - f_{Lt} \cdot \Omega_{Lt} = 0 \tag{3-25}$$

Fiber compressions (compression failure longitudinal)

$$F_2 = -\sigma(3) - f_{Lc} \cdot \Omega_{Lc} = 0 \tag{3-26}$$

Crack parallel to LT-Plane

$$F_3 = \left(\frac{\sigma(6)}{f_{RLs} \cdot \Omega_{RLs}}\right)^2 + \left(\frac{\sigma(4)}{f_{RTs} \cdot \Omega_{RTs}}\right)^2 - 1 = 0 \tag{3-27}$$

$$F_4 = \left(\frac{\sigma(1)}{f_{Rt} \cdot \Omega_{Rt}}\right)^2 + \left(\frac{\sigma(4)}{f_{RTs} \cdot \Omega_{RTs}}\right)^2 + \left(\frac{\sigma(6)}{f_{RLs} \cdot \Omega_{RLs}}\right)^2 - 1 = 0 \tag{3-28}$$

Radial Compression of fiber (compression failure radial)

$$F_5 = -\sigma(1) - f_{Rc} \cdot \Omega_{Rc} = 0 \tag{3-29}$$

Crack parallel to LR-Plane

$$F_6 = \left(\frac{\sigma(2)}{f_{Tt} \cdot \Omega_{Tt}}\right)^2 + \left(\frac{\sigma(4)}{f_{TRs} \cdot \Omega_{TRs}}\right)^2 + \left(\frac{\sigma(5)}{f_{TLs} \cdot \Omega_{TLs}}\right)^2 - 1 = 0 \tag{3-30}$$

Tangential Compression of fiber

$$F_7 = -\sigma(2) - f_{Tc} \cdot \Omega_{Tc} = 0 \tag{3-31}$$

3.3.8.1 Nonlinear deformation behaviour

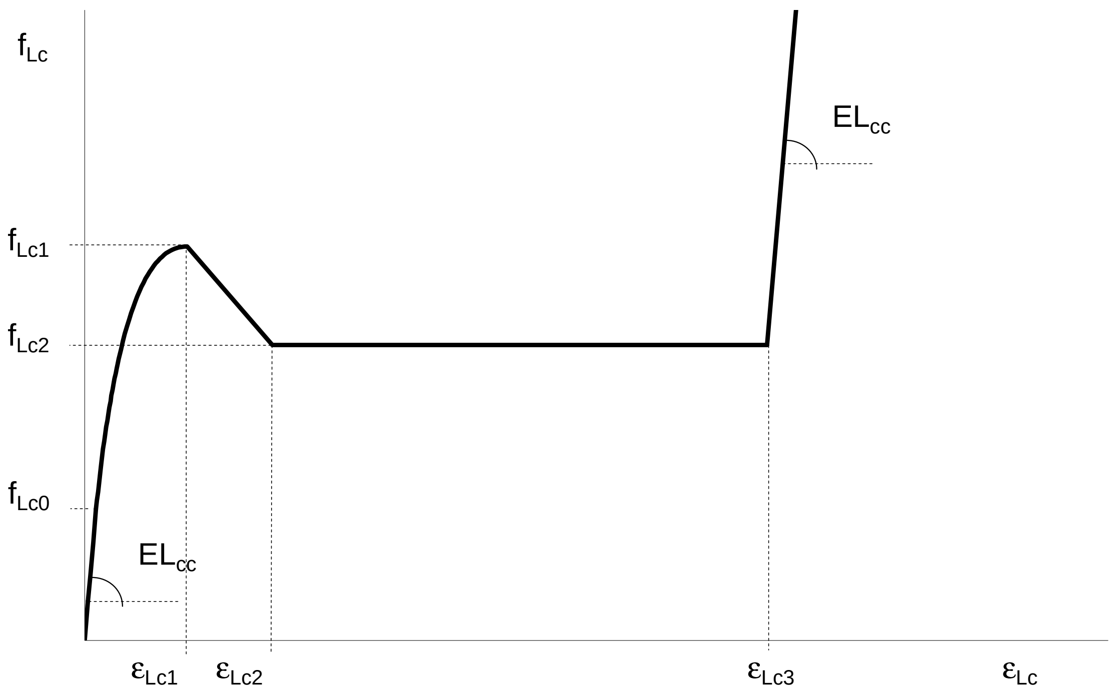

Fig. 3-23 Stress-strain relation - compression in fiber direction (longitudinal)

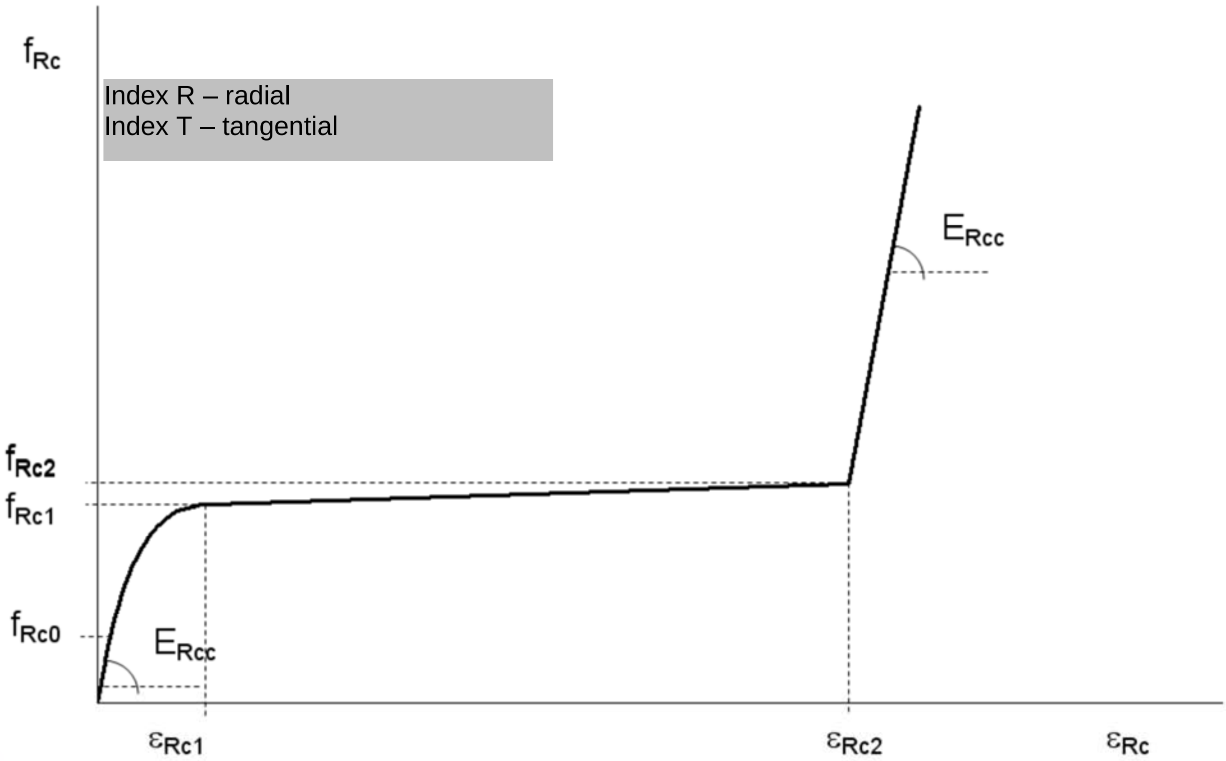

Fig. 3-24 Stress-strain relation - compression perpendicular to fiber direction (radial or tangential)

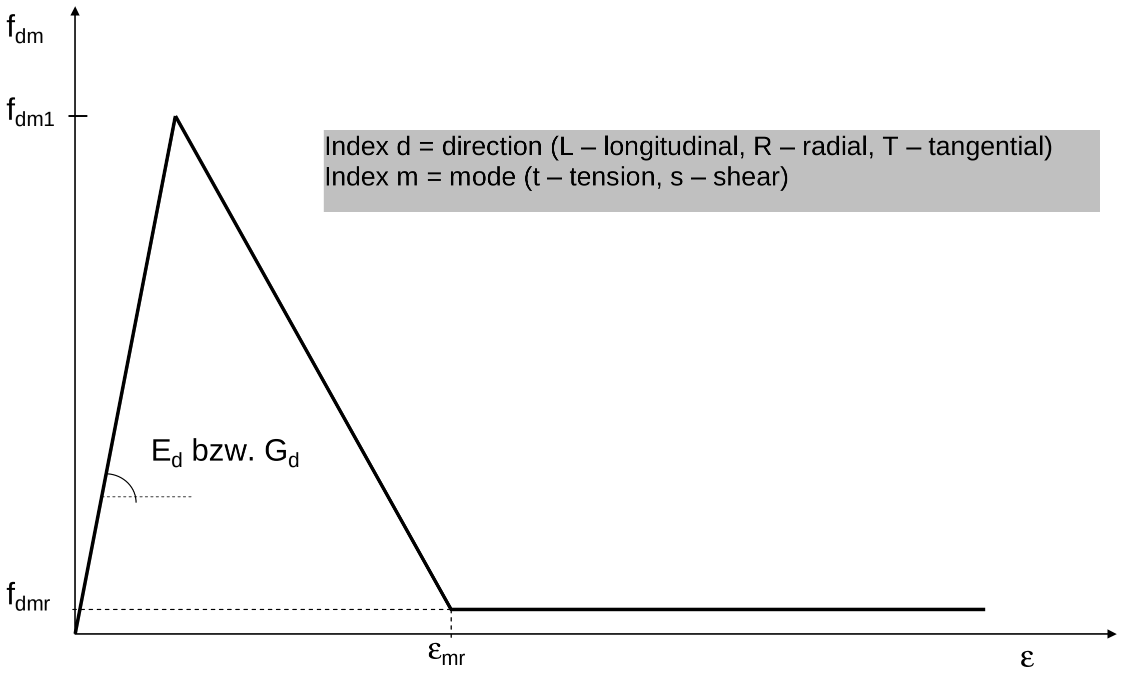

Fig. 3-25 Stress-strain relation for shear and tension

3.4 Dilatancy

The strict adherence of the stability postulations of Drucker usually requires an associated yield constitutive law (e.g. dilatancy angle = friction angle). But in reality, for some materials, the calculated volume strains are significantly larger than those, determined by experiments. In that cases, a deformation behaviour closer to reality can be described by using non-associated flow rules. The dilatancy angle describes the ratio of normal and shear translation in the Mohr-Coulomb shear criterion. It has two limits:

Dilatancy angle = friction angle => maximum plastic normal strain at shear strain, associated plasticity
Dilatancy angle = 0.0 => no plastic normal strain at shear (not recommended limit case because of resulting numerical problems)

By replacing the friction angle φ by the dilatancy angle ψ within the yield condition (rsp. plastic potential function), a non-associated flow rule is obtained. In addition to that it has to be considered, that the dilatancy angle is only physically reasonable for

dilatancy angle $\psi \leq$ friction angle φ.

A dilatancy angle larger than the friction angle leads to generation of energy within the system.

For the Drucker-Prager yield condition, the plastic deformation behaviour can be controlled via a non-associated flow rule by manipulating the dilatancy factor δ. Then the plastic potential is modified according to the equations ($Q = \sigma_S + \beta\,\delta\,\sigma_m$ (3-18) and ((3-21).
Thereby:

dilatancy factor δ = 1 => associated plasticity
dilatancy factor $\delta \leq 1$ => non-associated plasticity

For the compressive domain $0 \leq \delta_c \leq 1$ is true. In the tensile domain of the Drucker-Prager, a yield condition of δ_t = 0,1 ... 0,25 is recommended.

In case of prevalent shear strain, the dilatancy factor δ can be calculated via the ratio of the beta values from
Fig. **3-8** with the help of the friction angle φ and the dilatancy angle ψ. From equation (4.1), this could calculated by:

$$\beta(\varphi) = \frac{6 \cdot \sin\varphi}{\sqrt{3}(3+\sin\varphi)} \qquad \beta(\psi) = \frac{6 \cdot \sin\psi}{\sqrt{3}(3+\sin\psi)} \qquad \delta = \frac{\beta(\varphi)}{\beta(\psi)} \tag{3-32}$$

Please note that a non-associated flow rule however lead to asymmetric deformation matrices and may result in pure convergence behaviour.

4 COMMANDS

4.1 Material Models

LAW	Material Model
1	Mohr-Coulomb / Tresca (isotropic), tension cut off (isotropic) Mohr-Coulomb (anisotropic), tension cut off (anisotropic) for up to 4 joint sets
2	Drucker-Prager / modified Drucker-Prager (ideal elastic-plastic)
5	Drucker-Prager / modified Drucker-Prager, temperature dependent
8	Mortar / Cement (modified Drucker-Prager, stress dependent, nonlinear hardening / softening)
9	Concrete (nonlinear hardening / softening, Temperature Dependency)
10	Mohr-Coulomb (anisotropic), tension cut off (anisotropic) for up to 4 joints
11	fixed crack model (x-direction)
20	Masnory_Ganz (linear hardening /softening, Temperature Dependency)
22	Masonry_Ganz (nonlinear hardening / softening)
33	boxed value (orthotropic)
40	Drucker-Prager-Geo
41	Coupling Mohr-Coulomb and Drucker-Prager
99	usermpls

The material library multiPlas was implemented within the ANSYS-user-interface “userpl”. The activation is realized by using the tb-commands:

tb,user,*mat*,,80	*mat* – material number
tbda,1,LAW, , ,	allocation of the data field with the selected material model (LAW) and the material parameters (see the following sections 4.2)

4.2 TBDATA-Declaration

4.2.1 LAW = 1, 10 – Mohr Coulomb

	1	2	3	4	5	6	7	8	9	10
0-10 isotrop	LAW	phig	Cg	psig	phig*	Cg*	Tension		Tension*	number of joint sets
11-20 1. joint	Phi	C	psi	phi*	C*	Tension	alpha	beta	Tension*	
21-30 2. joint	Phi	C	psi	phi*	C*	Tension	alpha	beta	Tension*	
31-40 3. joint	Phi	C	psi	phi*	C*	Tension	alpha	beta	Tension*	
41-50 4. joint	Phi	C	psi	phi*	C*	Tension	alpha	beta	Tension*	tempd
51-60	T1	T2	β_{c2}	T3	β_{c3}	T4	β_{c4}	T5	β_{c5}	wr
61-70	Elem	Intpt	eps	geps	maxit	cutmax	dtmin	maxinc		ktuser
71-80										

Base material parameter Isotropic Mohr-Coulomb

phig	friction angle
Cg	cohesion
psig	dilatancy angle
phig*	residual friction angle
Cg*	residual cohesion
Tension	tensile strength -Tension cut off- (<=Cg/tan(phig)
Tension*	residual tensile strength (<=Cg*/tan(phig*)

Temperature dependency rsp. moisture dependency[1]

The temperature-dependent strength is realised over the temperature dependence of the cohesion

tempd	switch for temperature dependency =0: no temperature dependency =1: temperature dependence of the cohesion
T1	reference temperature with 100% strength, see Cg (field 3)
T2-5	temperatures at °C (in ascending order)
β_{ci}	relative cohesion Cg(Ti)/Cg

Anisotropic Mohr-Coulomb (up to 4 joint sets)

phi	joint friction angle
C	joint cohesion
psi	joint dilatancy angle
phi*	joint residual friction angle
C*	joint residual cohesion
Tension	joint tensile strength - Tension cut off- (<=Cg/tan(phi)
Tension*	joint residual tensile strength (<=Cg*/tan(phi*)

direction of anisotropic joint system

The transformation into the element coordinate system is defined by two angles (alpha, beta) see Fig. 3-4 and Fig. 3-6.

alpha	negative rotation about Z-axis
beta	positive rotation about Y-axis

[1] Volume-referred moisture as temperature equivalent interpreted

4.2.2 **LAW = 2 – Modified Drucker-Prager**

	1	2	3	4	5	6	7	8	9	10
0-10 isotrop	LAW	Rd	Rz	Ru						number of joint sets
11-20 1. joint	Phi	C	psi	phi*	C*	Tension	alpha	beta	Tension*	
21-30 2. joint	Phi	C	psi	phi*	C*	Tension	alpha	beta	Tension*	
31-40 3. joint	Phi	C	psi	phi*	C*	Tension	alpha	beta	Tension*	
41-50 4. joint	Phi	C	psi	phi*	C*	Tension	alpha	beta	Tension*	
51-60										wr
61-70	Elem	Intpt	eps	geps	maxit	cutmax	dtmin	maxinc		ktuser
71-80										

Base material parameter:

Rd uniaxial compression strength
Rz uniaxial tensile strength
Ru biaxial compression strength

(Remark: ideal elastic-plastic behaviour with associated flow rule)

Combination with joints / anisotropic Mohr-Coulomb (up to 4 joint sets)
phi joint friction angle
C joint cohesion
psi joint dilatancy angle
phi* joint residual friction angle
C* joint residual cohesion
Tension joint tensile strength -Tension cut off- (<=Cg/tan(phi)
Tension* joint residual tensile strength (<=Cg*/tan(phi*)

direction of anisotropic joint system
The transformation into the element coordinate system is defined by two angles (alpha, beta) see Fig. 3-4 and Fig. 3-6.
alpha negative rotation about Z-axis
beta positive rotation about Y-axis

4.2.3 **LAW = 5 – Modified Drucker-Prager, temperature dependent**

	1	2	3	4	5	6	7	8	9	10
0-10 isotrop	LAW	Rd	Rz	Ru						
11-20						T1				
21-30	T2	T3	T4	T5	T6	T7	T8	T9	T10	T11
31-40	β_{c2}	β_{c3}	β_{c4}	β_{c5}	β_{c6}	β_{c7}	β_{c8}	β_{c9}	β_{c10}	β_{c11}
41-50										
51-60				utz			T_{tS}	T_{tE}	β_{tE}	wr
61-70	Elem	Intpt	eps	geps	maxit	cutmax	dtmin	maxinc		ktuser
71-80										

Base material parameter:
for reference temperatur T1 (e.g. room-temperatur):

Rd	uniaxial compression strength
Rz	uniaxial tensile strength
Ru	biaxial compression strength

(Remark: ideal elastic-plastic behaviour with associated flow rule)

Temperature dependency

utz	switch for temperature dependency of tensile strength (=0 – off; =1 – on)
T_{tS}	temperature, at which a linear, temperature-dependent reduction of the tensile strength begins (see Fig. 3-16)
T_{tE}	temperature, up to which the linear, temperature-dependent reduction of the tensile strength takes place (see Fig. 3-16)
β_{tE}	residual plateau for tensile strength $Rz(T_{tE})/Rz$

T2-11	temperatures in °C (please enter in ascending order !!!)
β_{ci}	temperature-dependent, normalized compressive strength Rd(Ti)/Rd

4.2.4 LAW = 8 – Modified Drucker-Prager, calibrated stress dependent nonlinear hardening (Mortar / Cement)

	1	2	3	4	5	6	7	8	9	10
0-10	LAW	Rd	Rz	Ru	$\delta_{\psi t}$	$\delta_{\psi c}$	$\delta_{\psi c2}$	ε_{ml1}	ε_{u1}	O_{i1}
11-20	O_{u1}	O_{r1}	ε_{ml2}	ε_{u2}	O_{i2}	O_{u2}	O_{r2}	fst2	ε_{i3}	ε_{ml3}
21-30	ε_{u3}	O_{03}	O_{i3}	O_{u3}	$O_{r\,3}$	fst3	ε_{i4}	ε_{ml4}	ε_{u4}	O_{04}
31-40	O_{i4}	O_{u4}	$O_{r\,4}$	fst4	Ev					
41-50										
51-60	G_f	G_{fJ}^{I}	G_{fJ}^{II}							wr
61-70	Elem	Intpt	eps	geps	maxit	cutmax	dtmin	maxinc		ktuser
71-80										

Base material parameter:

Rd	uniaxial compression strength
Rz	uniaxial tensile strength
Ru	biaxial compression strength
$\delta_{\psi t}$	dilatancy factor in tensile stress domain $0 \le \delta_\psi \ge 1$
$\delta_{\psi c}$	dilatancy factor in compression stress domain $0 \le \delta_\psi \ge 1$ (recommendation $\delta_\psi = 1{,}00$)
Ev	elastic modulus
G_f	fracture energy (Mode 1 - tensile failure)

Nonlinear deformation behaviour under multiaxial compression (σm < 0)

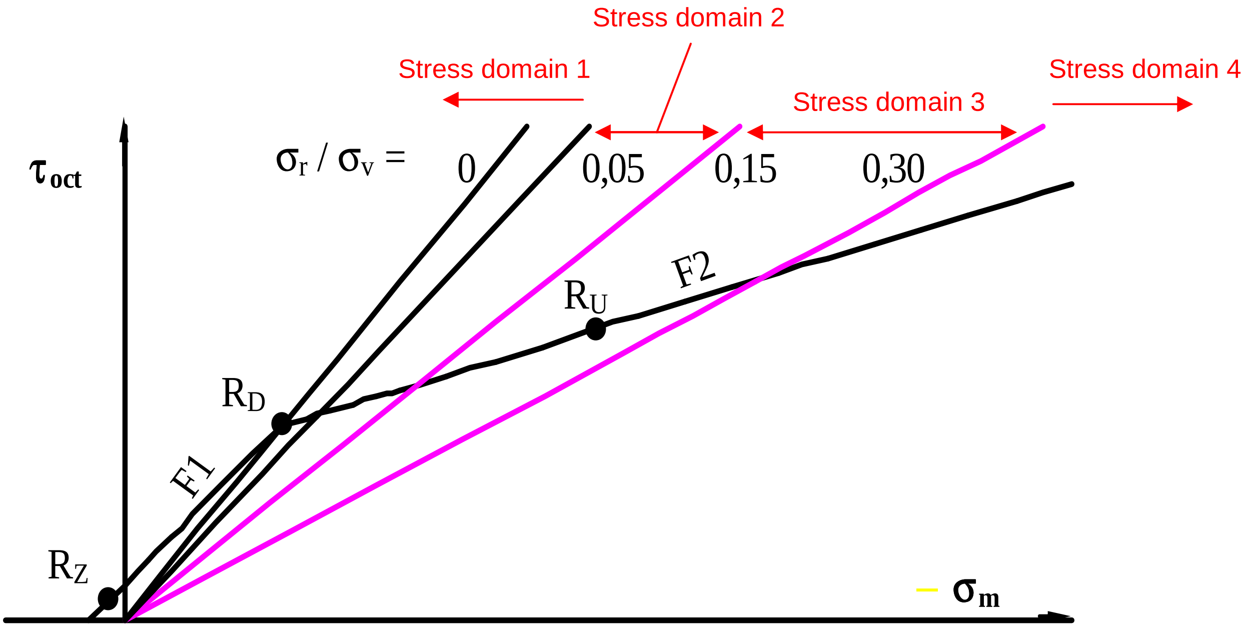

Fig. 4-1 Compression stress domains

Parameter for stress-strain-relations

Stress domain 1: (σr/σv<0,05) – uniaxial compression test

ε_{ml1}	strain at compression strength Rd
Ωi	start of nonlinear hardening
Ω_{u1}	compression stress level (see Fig. 4-2)
ε_{u1}	strain at softening up to Ω_{u1}
Ω_{r1}	residual stress plateau (see Fig. 4-2)

Stress domain 2: (0,05 ≥ σr/σv < 0,15)

Ω_{i2} start of nonlinear hardening
ε_{ml2} strain at compression strength

Ω_{u2} compression stress level (see Fig. 4-2)
ε_{u2} strain at softening up to Ω_{u2}
Ω_{r2} residual stress plateau (see Fig. 4-2)
fst2 factor increase in compressive strength

Stress domain 3: (0,15 ≥ σr/σv < 0,30)

Ω_{03} start of nonlinear hardening
Ω_{i3} compression stress level (see Fig. 4-2)
ε_{i3} strain at stress level Ω_{i3}
ε_{ml3} strain at compression strength
Ω_{u3} compression stress level (see Fig. 4-2)
ε_{u3} strain at stress level Ω_{u3}
Ω_{r3} residual stress plateau (see Fig. 4-2)
fst3 factor increase in compressive strength (at ε_{ml3})

Stress domain 4: (0,30 ≥ σr/σv)

Ω_{04} start of nonlinear hardening
Ω_{i4} compression stress level (see Fig. 4-2)
ε_{i4} strain at stress level Ω_{i4}
ε_{ml4} strain at compression strength
Ω_{u4} compression stress level (see Fig. 4-2)
ε_{u4} strain at stress level Ω_{u4}
Ω_{r4} residual stress plateau (see Fig. 4-2)
fst4 factor increase in compressive strength (at ε_{ml4})

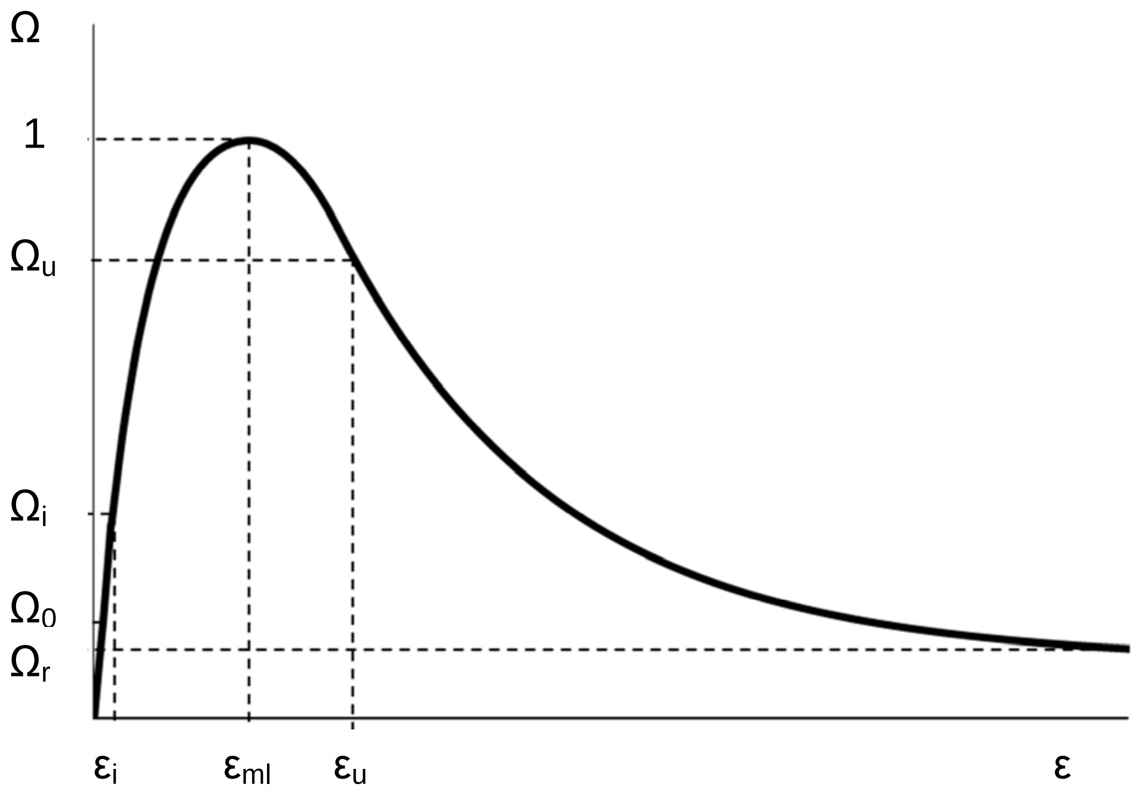

Fig. 4-2 Input parameter in compression stress domain

4.2.5 **LAW = 9 – Concrete**

	1	2	3	4	5	6	7	8	9	10
0-10	LAW	Rd	Rz	Ru	$\delta_{\psi t}$	$\delta_{\psi c}$				
11-20	κ_{m1}	κ_u	Ω_i	Ω_u	Ω_r	T1				
21-30	T2	T3	T4	T5	T6	T7	T8	T9	T10	T11
31-40	β_{c2}	β_{c3}	β_{c4}	β_{c5}	β_{c6}	β_{c7}	β_{c8}	β_{c9}	β_{c10}	β_{c11}
41-50	κ_{m2}	κ_{m3}	κ_{m4}	κ_{m5}	κ_{m6}	κ_{m7}	κ_{m8}	κ_{m9}	κ_{m10}	κ_{m11}
51-60	G_f	Ω_{tr}	κ_{tr}	utz		mlaw	T_{tS}	T_{tE}	β_{tE}	wr
61-70	Elem	Intpt	eps	geps	maxit	cutmax	dtmin	maxinc	EInt	ktuser
71-80										

Base material parameter:
for reference temperatur T1 (e.g. room-temperatur):

Rd — uniaxial compression strength
Rz — uniaxial tensile strength (recommendation Rz = 0,1 Rd for normal concrete)
Ru — biaxial compression strength (recommendation Ru = 1,2 Rd for normal concrete)
$\delta_{\psi t}$ — dilatancy factor in tensile stress domain $0 \leq \delta_\psi \geq 1$ (recommendation $\delta_{\psi t} = 0{,}25$)
$\delta_{\psi c}$ — dilatancy factor in compression stress domain $0 \leq \delta_\psi \geq 1$ (recommendation $\delta_{\psi c} = 1{,}00$)

Hardening- / softening function

mlaw — switch for softening function
= 0 – linear softening up to a predefined limit strain κ_{cr} after DIN EN 1992-1-2
= 1 – exponential softening with fracture energy
= 2 – like 0, but with mixed softening model (hydrostatic and deviatoric part)

Hardening and softening function (stress-strain-function) in compression stress domain

κ_{m1} — plastic strain at compression strength Rd ($\kappa_{m1} = \varepsilon_{ml} - Rd/E$)
Ω_i — start of nonlinear hardening (recommendation $\Omega_i = 0{,}33$)
Ω_r — residual stress plateau (recommendation $\Omega_r = 0{,}2$)
mlaw = 1:
κ_u — plastic strain at softening up to Ω_u ($\kappa_u = \varepsilon_u - \Omega_u * Rd/E$)
Ω_u — stress level see Fig. 4-3

Softening function (stress-strain-function) in tensile stress domain

mlaw = 0 bzw. 2:
Ω_{tr} — residual plateau
κ_{tr} — plastic limit strain
mlaw = 1:
G_f — fracture energy (Mode 1 - tensile failure)

Temperature dependency

Temperature dependency is available for mlaw = 0/2
utz — switch for temperature dependency of tensile strength (=0 – off; =1 – on)
T_{tS} — temperature, at which a linear, temperature-dependent reduction of the tensile strength begins (see Fig. 3-16)
T_{tE} — temperature, up to which the linear, temperature-dependent reduction of the tensile strength takes place (see Fig. 3-16)
β_{tE} — residual plateau for tensile strength $Rz(T_{tE})/Rz$

T2-11 — temperatures in °C (please enter in ascending order !!!)
β_{ci} — temperature-dependent, normalized compressive strength Rd(Ti)/Rd
κ_{mi} — plastic strain with reaching the compressive strength (for Ti)

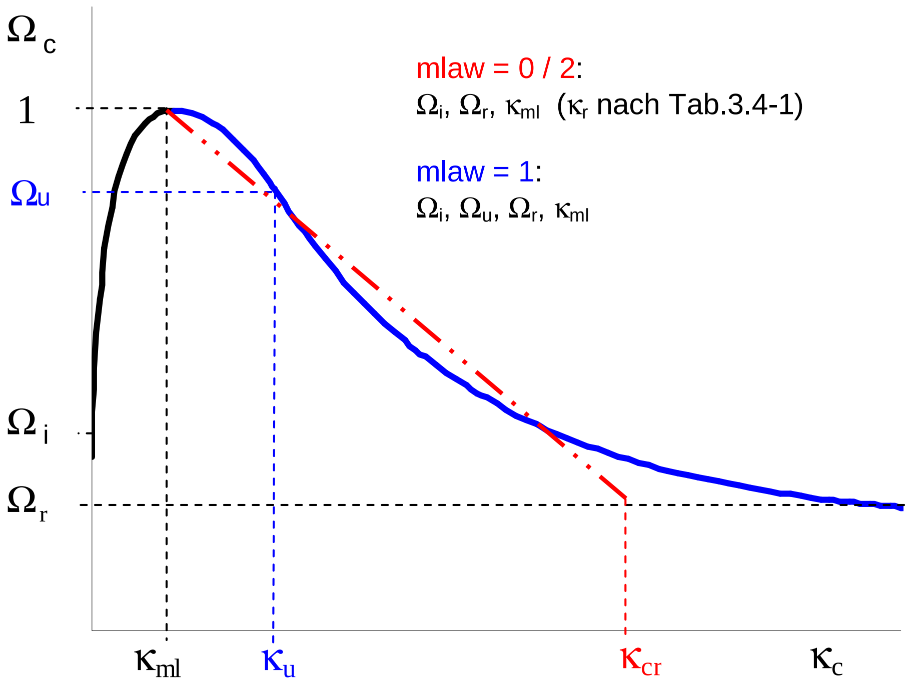

Fig. 4-3 Input parameter in compression stress domain

Overview input parameter of softening function in tensile stress domain

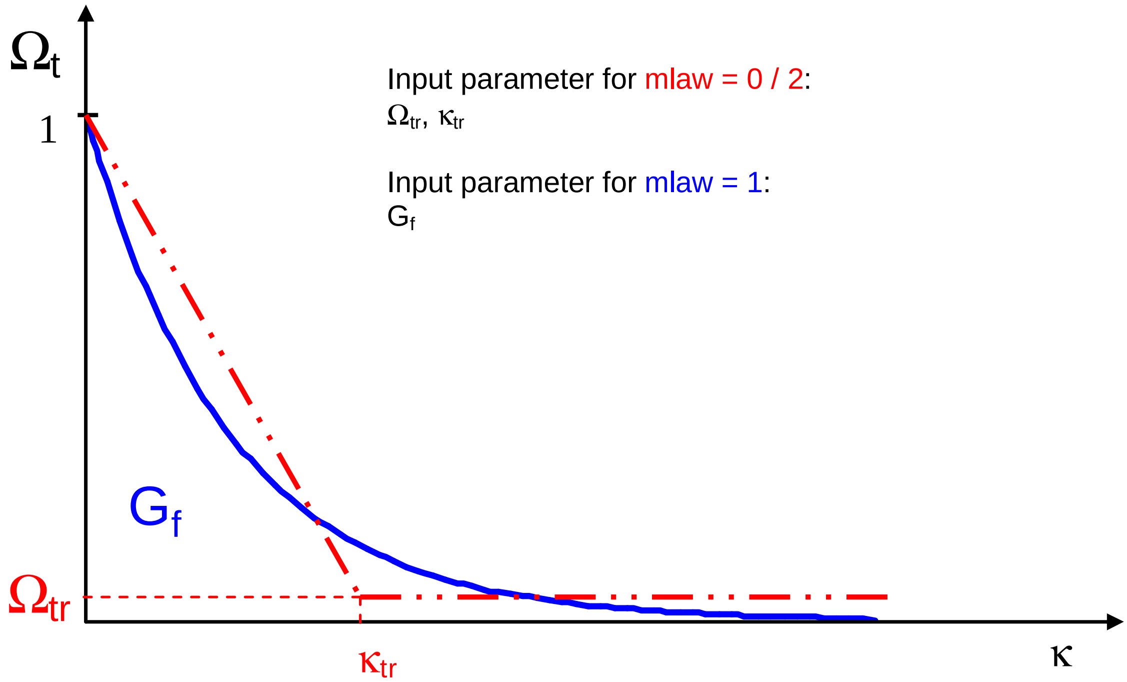

Fig. 4-4 Input parameter in tensile stress domain

Remark: switch to LAW = 5 (with same input like LAW=9) – for temperature dependency without mechanical softening

4.2.6 **LAW = 11 – Fixed Crack Model**

	1	2	3	4	5	6	7	8	9	10
0-10	LAW	ftx								
11-20										
21-30										
31-40										
41-50										
51-60	G^I_F						ftr			wr (Ausg)
61-70	Elem	Intpt	eps	geps	maxit	cutmax	dtmin	maxinc	EInt	ktuser
71-80										

Material parameter

ftx tensile strength in x-direction
G^I_{FJ} fracture energy (Mode 1 - tensile failure)
ftr residual tensile strength (for numerical stabilization)

Notes:
fixed and smeared crack model in x-direction with exponential softening

used equivalent length:

for volume elements: $h = \sqrt[3]{\frac{V_{El}}{n_{INT}}}$ for shell / plane elements: $h = \sqrt{\frac{A_{El}}{n_{INT}}}$

with
n_{INT} – number of integration points, V_{El} – element volume, A_{El} – element area

4.2.7 **LAW = 20 – Masonry Linear Softening**

	1	2	3	4	5	6	7	8	9	10
0-10	LAW	fmx	fmy	ftx	ftxx	fty	nue_y	ka_u	eta_r	as_y
11-20	al	ü_y	phi	c	phir	psi	direc	dreid	fmz	ftz
21-30	ftzz	nue_z	as_z	ü_z	tempd	T1	T2	β_{fm2}	ka_u2	T3
31-40	β_{fm3}	ka_u3	T4	β_{fm4}	ka_u4	T5	β_{fm5}	ka_u5	T6	β_{fm6}
41-50	ka_u6	T7	β_{fm7}	ka_u7	Tza	Tze	bte			
51-60	G^{I}_{FJ}	G^{I}_{FB}	G^{II}_{FJ}	G_m		cr	ftr	psir		wr (Ausg)
61-70	Elem	Intpt	eps	geps	maxit	cutmax	dtmin	maxinc	EInt	ktuser
71-80										

Material parameter

fmx	uniaxial compression strength of masonry normal to the bed joints
fmy	uniaxial compression strength of masonry normal to the head joints (fmy ≤ fmx !)
ftx	tensile strength normal to the bed joints (≤ C / tan(phi))
ftxx	ftxx=10*ftx (geometrical parameter for F_8)
fty	tensile strength normal to the head joints (= 50% of tensile strength of units)
nue_y	=0,9 (geometrical parameter for F_8)
as_y	distance of the head joints (mean value)
al	distance of the bed joints (mean value)
ü_y	lap length
phi	friction angle (bed joints)
c	cohesion (bed joints)
phir	residual friction angle (bed joints)
psi	dilatancy angle (usually 20°)
ka_u	plastic strain hence softening begins
eta_r	ratio of residual compressive strength / initial compressive strength
G^{I}_{FJ}	fracture energy MODE I tensile failure normal to bed joint(s)
G^{I}_{FB}	fracture energy MODE I tensile failure of stones (horizontal)
G^{II}_{FJ}	fracture energy MODE II shear failure of bed joint(s)
G_m	„strain energy“ (compressive failure)
direc	orientation of the joints in relation to the element coordinate system (0 = x – normal to bed joint; y – normal to head joint; z – normal to longitudinal joint 1 = z – normal to bed joint; y – normal to head joint; x – normal to longitudinal joint 2 = y – normal to bed joint; x – normal to head joint; z – normal to longitudinal joint)
dreid	switch for the three dimensional strength monitoring =0 for 2D F1 to F10 =1 for 2,5D F1 to F10, F6 with Tau_res =2 for 3D F1 to F18
if dreid = 2:	
fmz	compressive strength of the masonry normal to longitudinal joint
ftz	tensile strength normal to longitudinal joint (= ½ * stone tensile strength)
ftzz	geometric parameter of F_{16} (e.g. ftzz=10*ftx)
nue_z	value of decrease of the uniaxial horizontal MW-compressive strength fmz (s. F_{16})
as_z	distance of the longitudinal joints (stone breadth)
ü_z	amount of offset between longitudinal joints
cr	residual cohesion (for numerical stabilization)
ftr	residual tensile strength (for numerical stabilization)
psir	residual dilatancy (for numerical stabilization)

tempd	switch for temperature dependency	
	=0 or no entry:	no temperature dependency
	=1:	temperature dependency for compression and tension

Overview of input parameters of the softening function for the compressive space

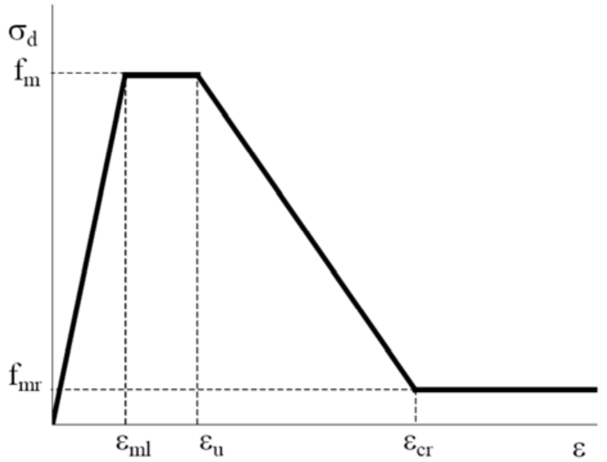

stress-strain relation

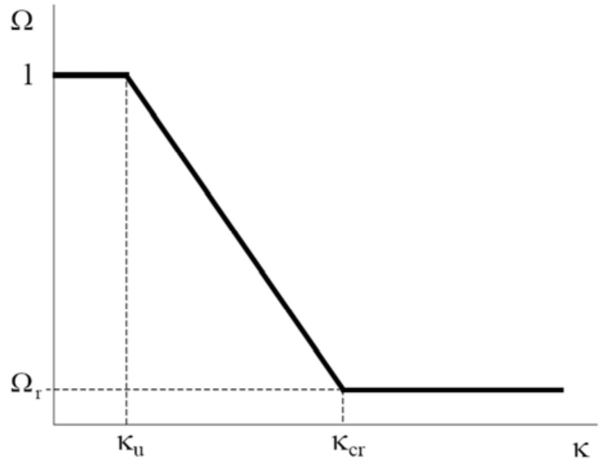

softening function

4.2.8 **LAW = 22 – Masonry Nonlinear Hardening/Softening**

	1	2	3	4	5	6	7	8	9	10
0-10	LAW	fmx	fmy	ftx	ftxx	fty	nue_y	ep_ml	Om_r	as_y
11-20	al	ü_y	phi	c	phir	psi	direc	dreid	fmz	ftz
21-30	ftzz	nue_z	as_z	ü_z		ep_u		Ev		
31-40										
41-50										
51-60	G^{I}_{FJ}	G^{I}_{FB}	G^{II}_{FJ}			cr	ftr	psir		wr (Ausg)
61-70	Elem	Intpt	eps	geps	maxit	cutmax	dtmin	maxinc	EInt	ktuser
71-80										

Material parameter

fmx	compressive strength of the masonry normal to the bed joint
fmy	compressive strength of the masonry normal to the head joint **fmy ≤ fmx !**
ftx	tensile strength normal to the bed joint (limit to C / tan(phi))
ftxx	geometric parameter for F_8 (e.g. ftxx=10*ftx)
fty	tensile strength normal to the head joint (= ½ * stone tensile strength)
nue_y	value of decrease of the uniaxial horizontal MW-tensile strength fmy (s. F_8)
as_y	distance of head joints (stone length)
al	distance of bed joints (stone height)
ü_y	amount of offset between head joints
phi	friction angle at the bed joint
c	cohesion at the bed joint
phir	residual strength - friction angle at the bed joint
psi	initial angle of dilatancy (usually = friction angle)
ep_ml	strain at reaching the uniaxial compressive strength of the masonry fmx
Om_r	ration residual compressive strength / initial compressive strength
ep_u	strain at softening in the pressure range at 0,85 fmx
Ev	Youngs' modulus normal to the bed joint
G^{I}_{FJ}	fracture energy MODE I tensile failure normal to the bed joint(s)
G^{I}_{FB}	fracture energy MODE I tensile failure of the stones (horizontal)
G^{II}_{FJ}	fracture energy MODE II shear failure of the bed joint(s)
direc	orientation of the joints in relation to the element coordinate system 0 = x – normal to bed joint; y – normal to head joint; z – normal to longitudinal joint 1 = z – normal to bed joint; y – normal to head joint; x – normal to longitudinal joint 2 = y – normal to bed joint; x – normal to head joint; z – normal to longitudinal joint
dreid	switch for the three dimensional strength monitoring = 0 for 2D F1 to F10 = 1 for 2,5D F1 to F10, F6 with Tau_res = 2 for 3D F1 to F18
if dreid = 2:	
fmz	compressive strength of the masonry normal to longitudinal joint
ftz	tensile strength normal to longitudinal joint (= ½ * stone tensile strength)
ftzz	geometric parameter of F_{16} (e.g. ftzz=10*ftx)
nue_z	value of decrease of the uniaxial horizontal MW-compressive strength fmz (s. F_{16})
as_z	distance of the longitudinal joints (stone breadth)
ü_z	amount of offset between longitudinal joints
cr	residual cohesion (for numerical stabilization)
ftr	residual tensile strength (for numerical stabilization)
psir	residual dilatancy (for numerical stabilization)

Overview input parameter of the relation of stress-strain in the compressive space

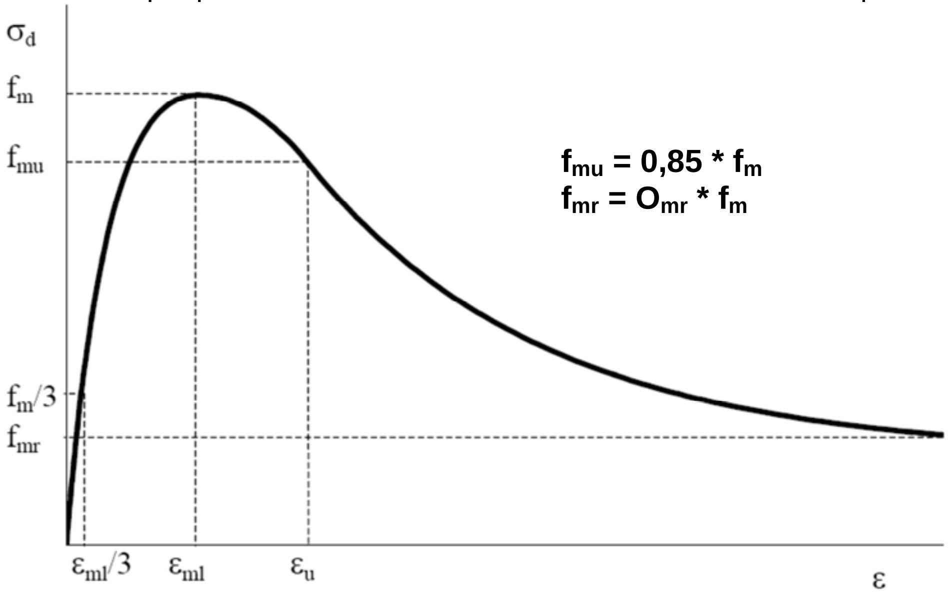

4.2.9 **LAW = 33 – Orthotropic Boxed Value Model**

	1	2	3	4	5	6	7	8	9	10
0-10	LAW	fLt	fLc	fRt	fRc	fTt	fTc	fRLs	fRTs	ntf
11-20	Phi	C	psi	phi*	C*	Tension	alpha	beta	Tension*	
21-30	Ω_{Lc0}	κ_{Lc1}	Ω_{Lc2}	κ_{Lc2}	κ_{Lc3}				fTLs	fTRs
31-40	Ω_{Rc0}	κ_{Rc1}	Ω_{Rc2}	κ_{Rc2}		Ω_{Tc0}	κ_{Tc1}	Ω_{Tc2}	κ_{Tc2}	
41-50	Ω_{Ltr}	κ_{Ltr}	Ω_{Rtr}	κ_{Rtr}	Ω_{Ttr}	κ_{Ttr}	Ω_{RLsr}	κ_{RLsr}	Ω_{RTsr}	κ_{RTsr}
51-60	Ω_{TLsr}	κ_{TLsr}	Ω_{TRsr}	κ_{TRsr}						wr (Ausg)
61-70	Elem	Intpt	eps	geps	maxit	cutmax	dtmin	maxinc		ktuser
71-80										

Material parameter

fLt uniaxial tensile strength longitudinal resp. parallel to the fiber direction
fLc uniaxial compressive strength longitudinal resp. parallel to the fiber direction
fRt uniaxial tensile strength radial
fRc uniaxial compressive strength radial
fTt uniaxial tensile strength tangential
fTc uniaxial compressive strength tangential
fRLs shear strength radial/longitudinal
fRTs shear strength radial/tangential
fTLs shear strength tangential/longitudinal
fTRs shear strength tangential/radial

relation of stress and strain, longitudinal, pressure domain

Ω_{Lc0} starting point of the parabolic hardening, longitudinal (stress ratio to fLc)
κ_{Lc1} plastic strain at reaching fLc
Ω_{Lc2} level of softening due to generation of knik bands
κ_{Lc2} plastic strain at reaching Ω_{Lc2}
κ_{Lc3} plastic strain at reaching the hardening due to compaction
E_{Lcc} Youngs' modulus in the hardening area due to compaction = E_L

relation of stress and strain, radial / tangential, pressure domain

Ω_{Rc0} starting point of the parabolic hardening, longitudinal (stress ratio to fLc)
κ_{Rc1} plastic strain at reaching fLc
Ω_{Rc2} evel of softening due to generation of knik bands
κ_{Rc2} plastic strain at reaching Ω_{Lc2}
E_{Rcc} Youngs' modulus in the hardening area due to compaction = E_R

Werte für tangentiale Richtung Index R $\rightarrow$ T

relation of stress and strain tensile area and shear domain

Ω_{dmr} ratio residual strength / initial strength
κ_{dmr} plastic strain at reaching the residual strength

For both dimensions applies:

Index d = direction (L – longitudinal, R – radial, T – tangential)
Index m = mode (t – tension, s – shear)

For graphical explanation of the material values see Fig. 3-23, Fig. 3-24 and Fig. 3-25.

4.2.10 LAW = 40 – Geological Drucker-Prager

	1	2	3	4	5	6	7	8	9	10
0-10	LAW									
11-20										
21-30										
31-40										
41-50										
51-60	beta	Sig_yt	delt							wr
61-70	Elem	Intpt	eps	geps	maxit	cutmax	dtmin	maxinc		ktuser
71-80										

DRUCKER-PRAGER

beta material parameter, that determines the ascent of the Drucker-Prager cone
Sig_yt strength value (analogue cohesion)
delt dilatancy factor

(note: ideal elasto-plastic material model with associated or non-associated flow rule)

4.2.11 LAW = 41 – Combination Mohr-Coulomb and Drucker-Prager resp. TRESCA vs. MISES

	1	2	3	4	5	6	7	8	9	10
0-10	LAW	phig	Cg	psig	phig*	Cg*	Tension		Tension*	
11-20										
21-30										
31-40										
41-50										
51-60	beta	Sig_yt	delt							wr
61-70	Elem	Intpt	eps	geps	max-it	cutmax	dtmin	maxinc		ktuser
71-80										

<u>Isotropic MOHR-COULOMB + DRUCKER-PRAGER</u>

phig	frictional angle
Cg	cohesion
psig	dilatancy angle
phig*	residual strength – frictional angle
Cg*	residual strength - cohesion
Tension	tension cut off (<=Cg/tan(phig)
Tension*	residual strength (<=Cg*/tan(phig*)
beta	material parameter, that determines the ascent of the Drucker-Prager cone
Sig_yt	strength value (analog cohesion)
delt	dilatancy factor

Remark:
Mohr Coulomb = Tresca if friction angle = 0
Drucker Prager = v Mises if beta = 0

4.3 Numerical control variables

eps	local convergence criteria Return Mapping
geps	criteria for singular systems of equations for multi-area activity
maxit	Maximum amount of local iterations of the return mapping process
cutmax	amount of local bisections prior the activation of a global bisection
maxinc	maximum incrementation of a load step (global + local)
dtmin	minimum time increment of the ANSYS-command (*deltim,,dtmin*)
ktuser =1	given setting to build the elasto-plastic tangent matrix at the local plane of the integration point (= 1)
EInt	switch for Element-Integration = 0: full integration = 1: reduced integration

activation of the output control (debug- resp. control-modus for developers or users when necessary)

wr	output key
Elem	element number
Intp	number of the integration point

4.3.1 Choice of the numerical control variables

eps:	10^{-6}, shall not be chosen to small (10^{-4} at KN and m);
maxit:	10 local iteration steps shall be enough (at least as many as active yield surfaces); but not to be chosen too small
geps:	10^{-20} for double precision;
maxinc:	must be larger than global and local load increments separately and also than the product e.g. at dtmin 0.05: maxinc > 1/0.05 > 20 and cutmax 5: maxinc > 2^5 > 32 maxinc > 20*32 > 640,
cutmax	4

output control

wr = 1 output of the violated yield criterias

```
*********** START mpls5 *********************************
Elem: 436 intpt= 1 KTFORM= 0TIMINC=0.5000 KFSTEQ= 0 KFIRST= 0 LAW= 1
*********** START LOCAL STRAIN INCREMENT *****************
*********** START LOCAL ITERATION ************************
*** Kontrollausgabe Fliesskriterien ***
1060 F-value 1-6:     70.165    0.000    0.000    0.000    0.000    96.647
1070 F-value 7-12:     0.000    0.000    0.000    0.000    0.000     0.000
1080 F-value 13-18:     0.000    0.000    0.000    0.000    0.000     0.000
1090 nfail=  2
```

wr =2 output of the local iteration sequence with trialstresses, violated yield criterias, plastic multiplicators, plastic and elastic increments of strain

Means:

<u>for LAW 1, 2, 10:</u>

F1	shear failure MOHR-COULOMB, isotropic
F2	shear failure 1. joint
F3	shear failure 2. joint
F4	shear failure 3. joint
F5	shear failure 4. joint
F6	tensile failure isotropic
F7	tensile failure 1. joint
F8	tensile failure 2. joint
F9	tensile failure 3. joint
F10	tensile failure 4. joint

<u>for LAW 9:</u>

F1	DRUCKER-PRAGER, F1 (tensile domain, tensile-compressive domain)
F2	DRUCKER-PRAGER, F2 (compressive-tensile domain, compressive domain)

<u>for LAW 20, 22:</u>

F1 (F11)	stone tensile failure
F2 (F12)	compression failure of the masonry
F3 (F13)	shear failure of the masonry, stone failure
F4 (F14)	tensile failure of the masonry, parallel to bed joint, stone failure
F5 (F15)	transition section between F1, F3, F4 resp. F11, F13, F14
F6	shear failure of bed joints
F7	tensile failure of bed joints
F8 (F16)	tensile failure of bed joints on horizontal compressive stress
F9 (F17)	staircase-shaped shear failure of bed- and head joints
F10 (F18)	tensile failure of the masonry parallel to the bed joint, joint failure

<u>for LAW 40:</u>

F2	DRUCKER-PRAGER

<u>for LAW 41:</u>

F1	shear failure MOHR-COULOMB, isotropic
F2	DRUCKER-PRAGER
F6	tensile failure isotropic

4.3.2 **Remarks for choosing the material parameters**

No material parameter should be ever set to 0.0. Even for residual strengths values above eps*100 should be chosen. Dilatancy angles close to zero imply ideally smooth friction surfaces in a physical sense and can lead to extreme convergence difficulties. This results from tension component which can not be removed in case of shear failure. The dilatancy angle therefore should always be set at least to 1°.
The tension strength is limited to the intersection point of the Mohr-Coulomb-line (-plane) and the normal friction axis (C /tan(phi)).

4.3.3 **Remarks and tips for using multiPlas in nonlinear structural analysis**

If an oscillation can be seen for a certain imbalance value, the convergence for the load step can be achieved by increasing the convergence criteria in ANSYS slightly above the oscillation value. In the following load case the convergence criteria can be set to the smaller value again.

In case of frequent error messages (**local return mapping failed**) the local number of iterations should be increased and the yield areas should be checked. This output only occurs if wr ≥ 1.

In case where problems occur from processing the polyhedral yield figure (in case of unfortunate physically problematic choice of parameters) the calculations sould be performed by using isotropic yield criteria with the whole load at first. Then a following calculation with activation of anisotropic yield criteria (this is especially the case for primary stress conditions) can be done.

Do never chose dilatancy or friction angle as 0.0 because this can lead to unbalanced forces which can not be relocated!

A cohesion c = 0 (e.g. sand) implies that the material does not have any uniaxial compressive or tensile strength. First, the material therefore has to be iterated into a stable position. This leads very often to convergence difficulties, so it is advised to use an adequately small value *instead* of zero for the cohesion while using the MOHR-COULOMB (LAW = 1) yield conditions.

The automatic time stepping is called directly from the routine (it can be switched on via: autots,on).

The global load step bisection can be disabled by choosing a large value for cutmax. In the case of a local bisection, no hints are written out.

Be careful not to use too large values for maxinc and simultaneous suppression of the global bisection. This may lead to a large computational effort in a Newton-Raphson-Equilibrium iteration! In this case, request the cause by use the global bisection!

Multi surface plasticity fundamentally is a physical path dependent phenomenon. Therefore a global incrementation in order to represent the relocation of force correctly is of utmost importance.

In the multi surface routines, softening (residual strength) is only introduced in at the equilibrium states (so only after reaching the global Newton-Raphson equilibrium). Therefore, a global incrementing is important in the case of softening.

The value dtmin in the tb-data-fiel has to be identical to the value of dtmin that is used by ANSYS in the solution-phase (deltim,dtanfang,dtmin,dtmax,...).

If no convergent solution could be found:

-decrease incrementation (dtmin,...)

-increase the global convergence criteria (cnvtol,f,...)

Newton-Raphson, full (usage of consistent elasto-plastic tangent) or Newton-Raphson, init (starting stiffness) is supported. For the practical problems Newton-Raphson, init is recommended. Especially when considering geometric nonlinearities or when working with EKILL / EALIVE the full Newton-Raphson method is necessary.

4.4 Remarks for Postprocessing

Plastic effective strain

EPPLEQV: The plastic effective strain shows the quantitative activity and is used for pointing out the areas in which local load shifting or material failure / crack forming take place.

$$\varepsilon_{pl,eqv} = \sqrt{\frac{2}{3}[\varepsilon^2_{pl,x} + \varepsilon^2_{pl,y} + \varepsilon^2_{pl,z} + \frac{1}{2}(\varepsilon^2_{pl,xy} + \varepsilon^2_{pl,yz} + \varepsilon^2_{pl,zx})]}$$

Plastic activity activity (NSLRAT)

The plastic activity shows which qualitative plastic activities are taking place in the current equilibrium state. They are used for illustration which of the flow criteria is active, that means not satisfied, within the respective are of the structure. This enables deducting the type and cause of the load shifting.

The pointer of the plastic activity is path depended. A plastic activity can be activated and deactivated more than once during a load case. The plastic activity is identified by a characteristic (nl,srat):

Output for LAW 1, 10:

scale	active yield criterion
1	shear failure MOHR-COULOMB, isotropic
10	shear failure 1. separation plane
100	shear failure 2. separation plane
1000	shear failure 3. separation plane
10 000	shear failure 4. separation plane
100 000	tensile failure isotropic
1 000 000	tensile failure 1. separation plane
10 000 000	tensile failure 2. separation plane
100 000 000	tensile failure 3. separation plane
1 000 000 000	tensile failure 4. separation plane

Output for LAW 2, 9:

scale	active yield criterion
1	DRUCKER-PRAGER, joint 1 (tensile space, tensile-compressive space)
10	DRUCKER-PRAGER, joint 2 (compressive-tensile space, compressive space)

Output for LAW 20, 22:

scale	active yield criterion
1	stone tensile failure
10	compressive failure of the masonry
100	shear failure of the masonry, stone failure
1000	tensile failure of the masonry parallel to bed joint, stone failure
10 000	transition section between F1, F3, F4 resp. F11, F13, F14
100 000	shear failure of bed joints
1 000 000	tensile failure of bed joints
10 000 000	tensile failure of bed joints on horizontal horizontal compressive stress
100 000 000	staircase-shaped shear failure of bed- and head joints
1 000 000 000	tensile failure of the masonry parallel to the bed joint, joint failure

Output for LAW 33:

scale	active yield criterion
1	F1 tensile failure longitudinal
10	F2 compressive failure longitudinal
100	F3 shear failure parallel to the LT plane
1000	F4 tensile / shear failure parallel to the LT plane
10 000	F5 compressive failure radial
100 000	F6 tensile- / shear fail parallel to the LR plane
1 000 000	F7 compressive failure tangential
10 000 000	shear failure separation plane
100 000 000	tensile failure separation plane

Output for LAW 40:

scale	active yield criterion
1	-
10	DRUCKER-PRAGER

Output for LAW 41:

scale	active yield criterion
1	tensile failure MOHR-COULOMB, isotropic
10	DRUCKER-PRAGER
100	-
1000	-
10 000	-
100 000	tensile failure isotropic

If several flow conditions are active at once then the activity pointer are added up. For example SRAT = 101 for LAW 1 with separation planes stands for shear failure MOHR-COULOMB isotropic and shear failure on the second separation plane.

The scaling settings for the output are done using the cval-command in ANSYS
(e.g.: /CVAL,all,0.5,1,10,100000
ples,nl,srat
for LAW 41)

5 VERIFICATION EXAMPLES

5.1 Example 1 – Earth pressure at rest

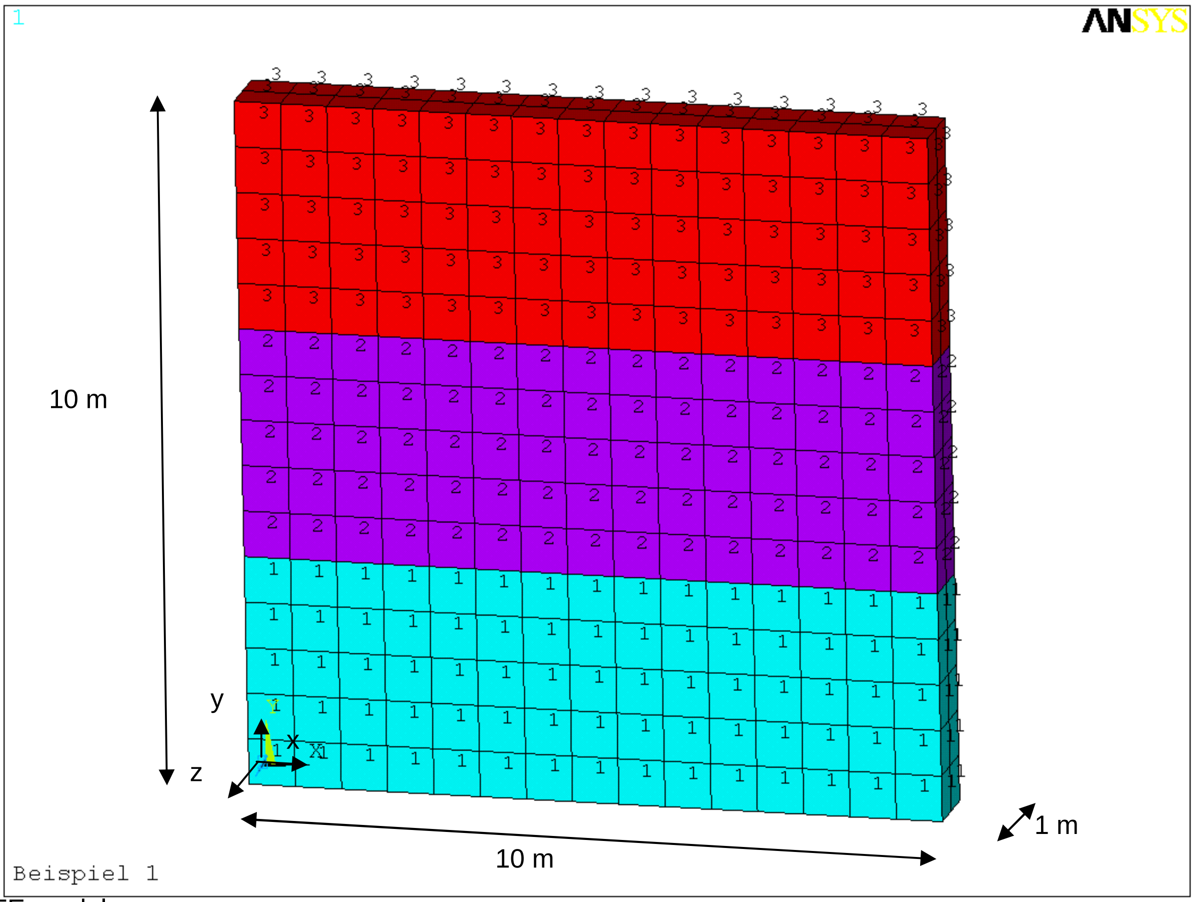

FE-model

Material assumptions (material 1 to 3), sand:

Angle of inner friction	$\varphi = 30°$
Cohesion	$c = 0$
Constrained modulus	$E_S = 40000$ kN/m²
Coefficient of earth pressure at rest	$k_0 = 0{,}5$
Density	$\rho = 1{,}8$ t/m³

Therefore:

Poisson's ratio: $\nu = \dfrac{k_0}{1+k_0} = 0{,}333$

Shear modulus: $G = \dfrac{1-2\nu}{2(1-\nu)} E_S = 10000$ kN/m²

theory see [6-19]

Young's modulus: $E = 2(1+\nu)G = 26670$ kN/m²

Boundary conditions:

lower boundary y = 0:	ux = uy = uz = 0
side boundary x = 0 bzw. 10:	ux = 0
side boundary z = 0 bzw. 1:	uz = 0

<u>Elements:</u> Solid45

<u>Load history:</u>

1st Load step: installation 1st layer (material 1)
2nd Load step: installation 2nd layer (material 2)
3rd Load step: installation 3rd layer (material 3)

<u>Reference solution:</u> (bsp1.dat) path plots along the boundary at x = 0

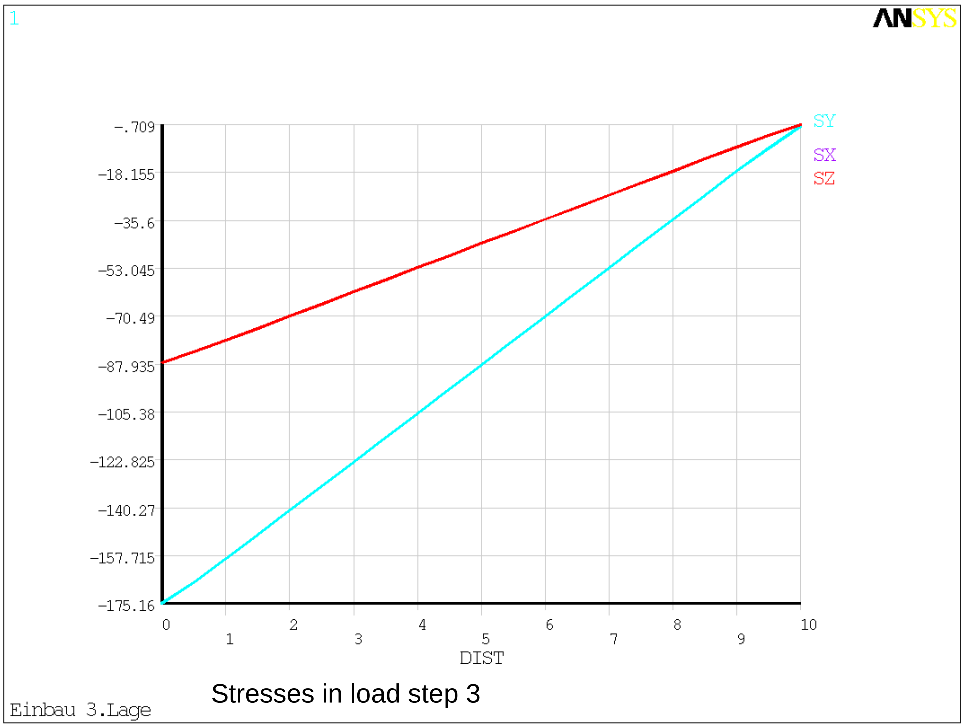

Stresses in load step 3

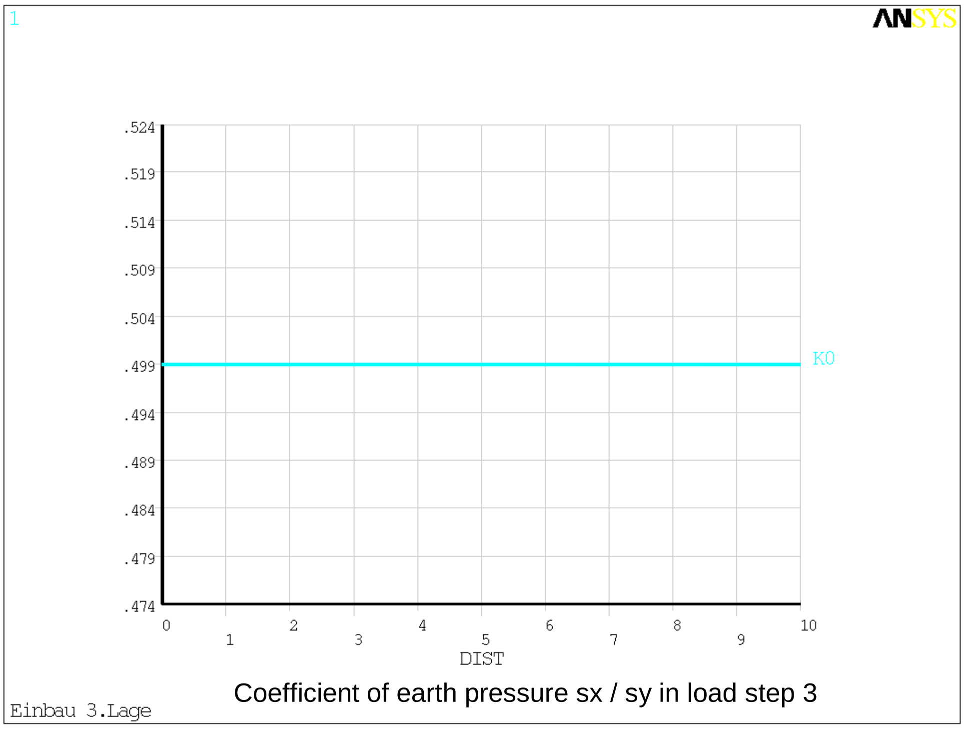

Coefficient of earth pressure sx / sy in load step 3

5.2 Examples 2 to 4 - Earth pressure at rest and active earth pressure

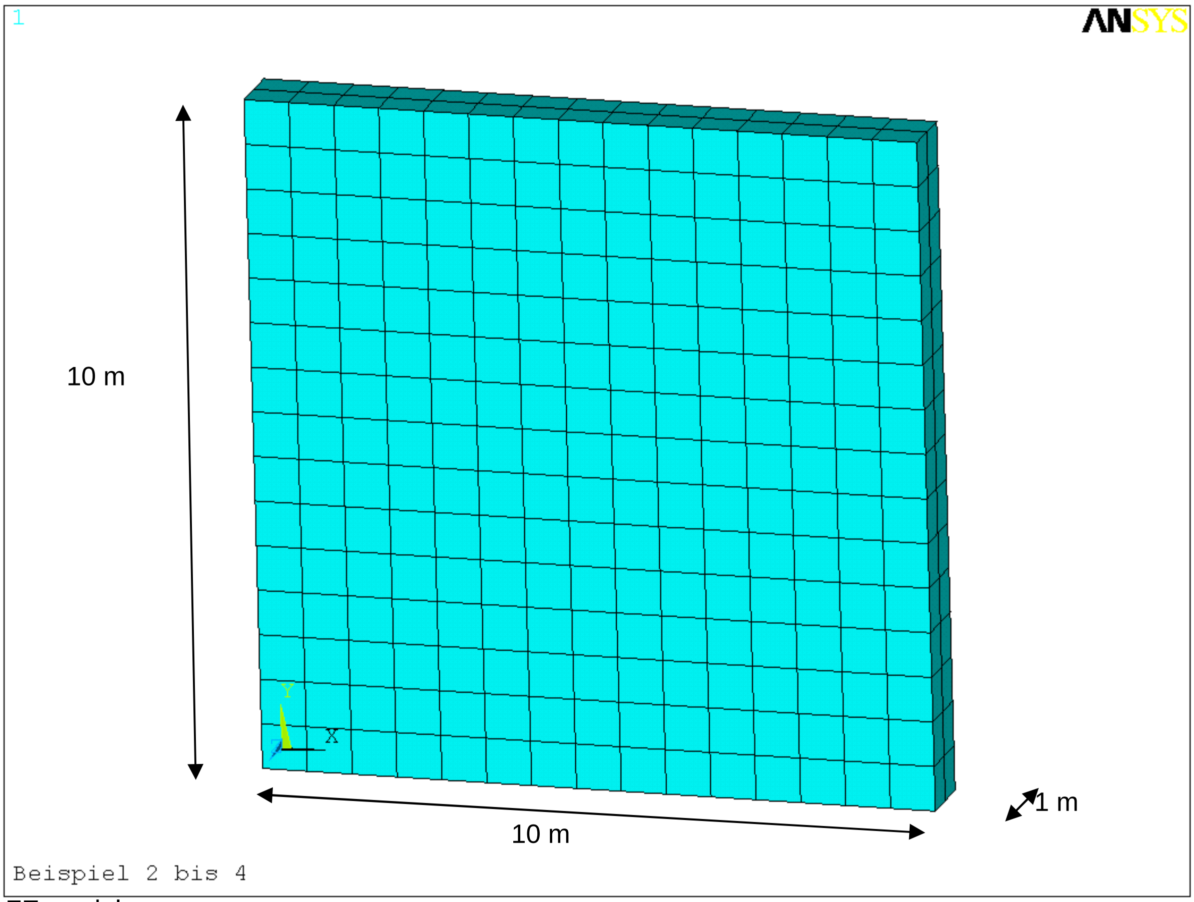

FE-model

<u>Material assumption (material 1):</u>

Angle of inner friction	φ = 30°; residual strength φr = 30°
Angle of dilatancy	ψ = 30°
Cohesion	c = 0
Elastic modulus	E_S = 40000 kN/m²
Coefficient of earth pressure at rest	k_0 = 0,5
Density	ρ = 1,8 t/m³

Therefore:

Poisson's ration:	ν = 0,333
Shear modulus:	G =10000 kN/m²
Young's modulus:	E =26670 kN/m²

<u>Elements:</u> Solid45

<u>Load history:</u>

1st Load step: Earth pressure in a result of the gravity

Boundary conditions:

lower boundary y = 0:	ux = uy = uz = 0
side boundary x = 0 bzw. 10:	ux = 0
side boundary z = 0 bzw. 1:	uz = 0

2nd load step: Activation of the active earth pressure by rotation of the side boundary x = 0 about the base point, horizontal top point displacement: 3cm

Reference solution: Example 2 - Calculation with LAW = 1 MOHR-COULOMB (bsp2.dat)

Number of substeps / iterations: 4 / 18
cpu-time: (1x 4-M CPU 1,70 GHz) 21,9 sec

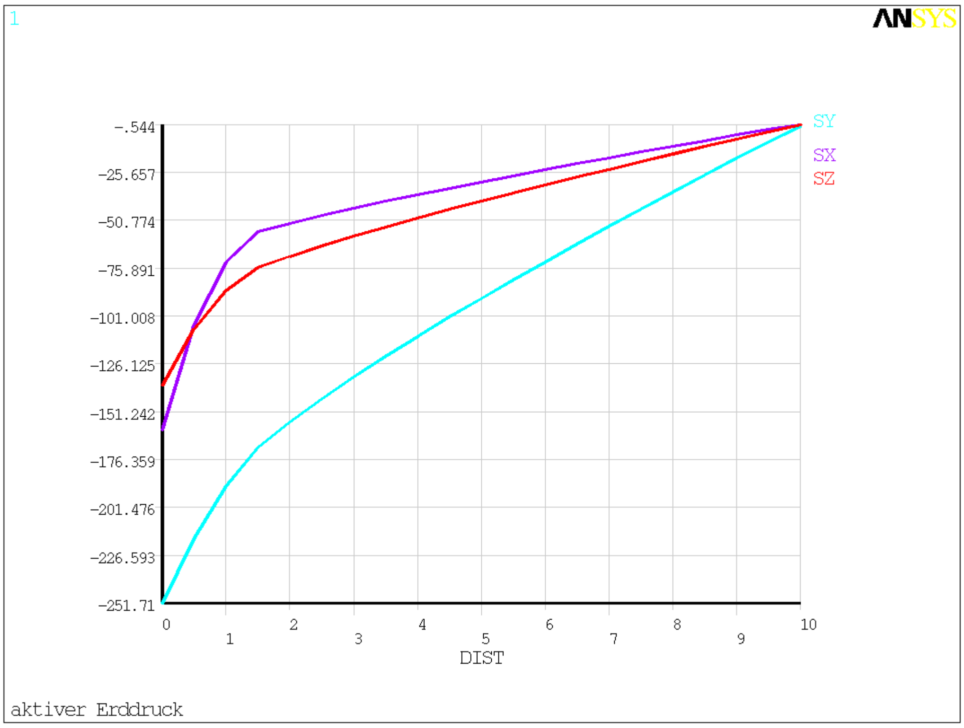

Stresses in load step 2 as path plots along the boundary x = 0

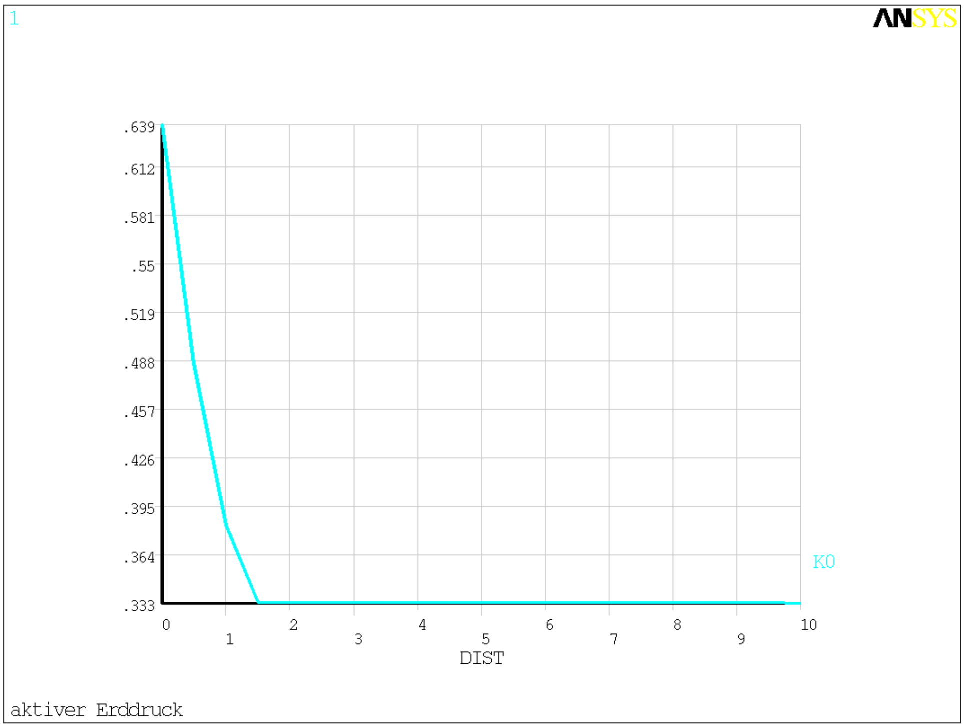

Coefficient of earth pressure sx / sy in load step 2 as a path plot along the border x = 0

U,sum = 0,047487 m
EPPL,EQV = 0,003927

Reference solution: Example 3 - Calculation with LAW = 40 DRUCKER-PRAGER (bsp3.dat)

Number of substeps / iterations: 4 / 8
cpu-time: (1x 4-M CPU 1,70 GHz) 13,4 sec

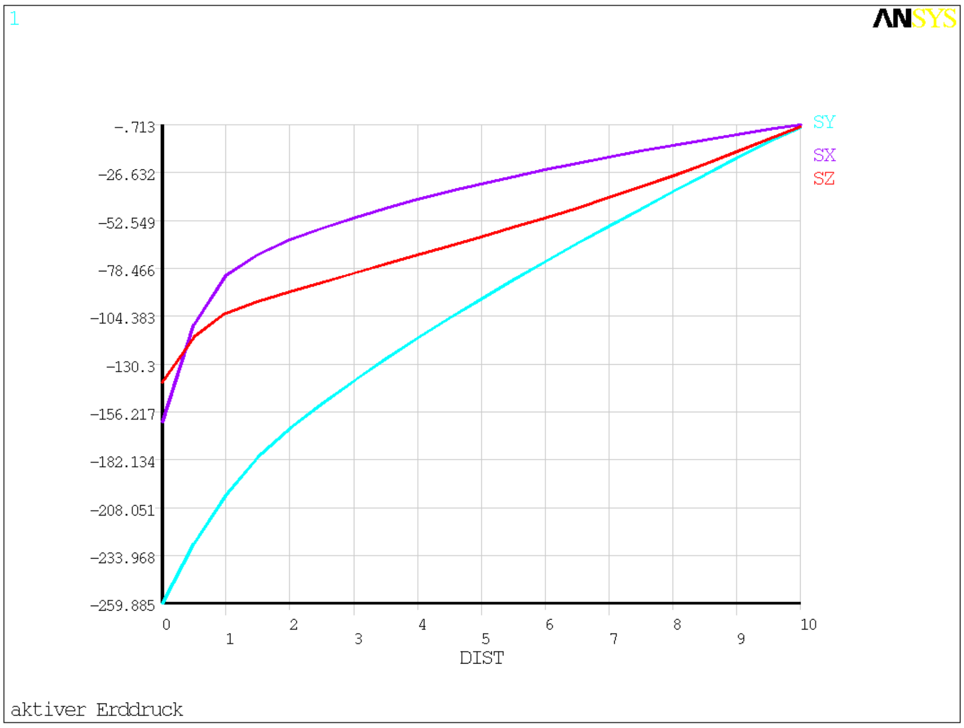

Stresses in load step 2 as path plots along the boundary x = 0

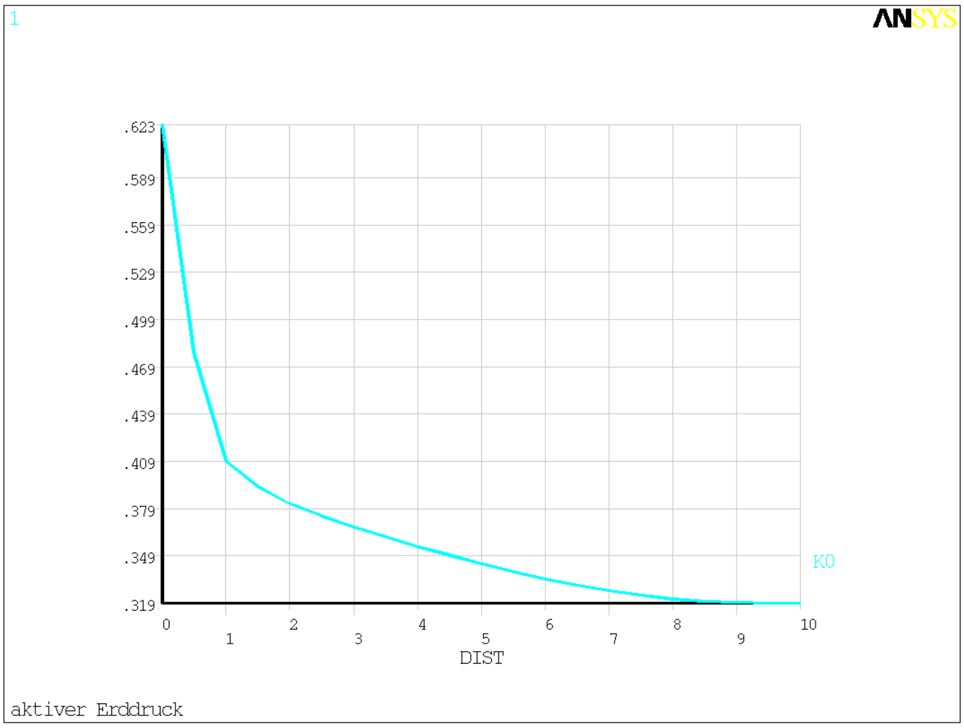

Coefficient of earth pressure sx / sy in load step 2 as a path plot along the border x = 0

U,sum = 0,046891 m
EPPL,EQV = 0,003238

Reference solution: Example 4 - Calculation with LAW = 41 MOHR-COULOMB+DRUCKER-PRAGER (bsp4.dat)

Number of substeps / iterations: 4 / 9
cpu-time: (1x 4-M CPU 1,70 GHz) 14,41 sec

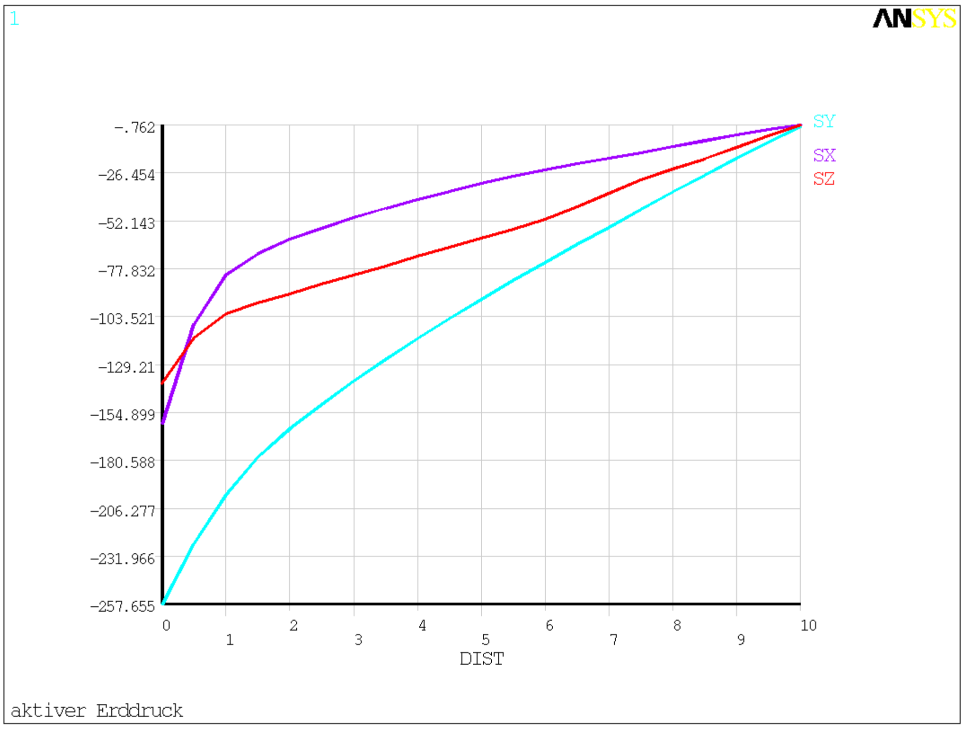

Stresses in load step 2 as path plots along the boundary x = 0

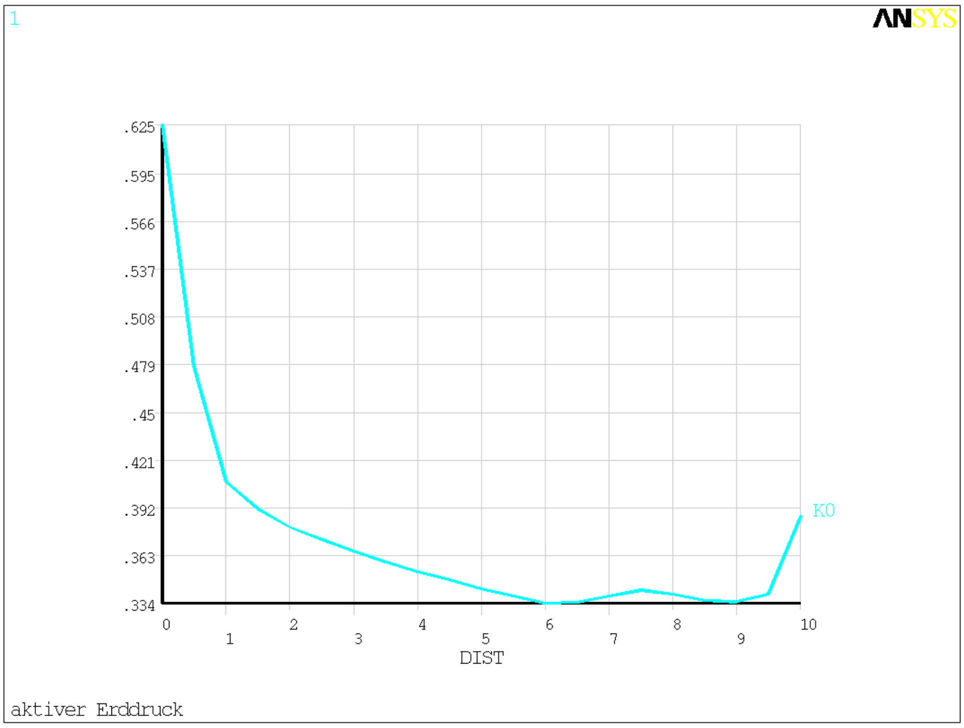

Coefficient of earth pressure sx / sy in load step 2 as a path plot along the border x = 0

maximale Gesamtverschiebung: U,sum = 0,047003 m
maximale plastische Vergleichsdehnung: EPPL,EQV = 0,003361

5.3 Examples 5 to 8 - Kienberger Experiment G6 [6-13]

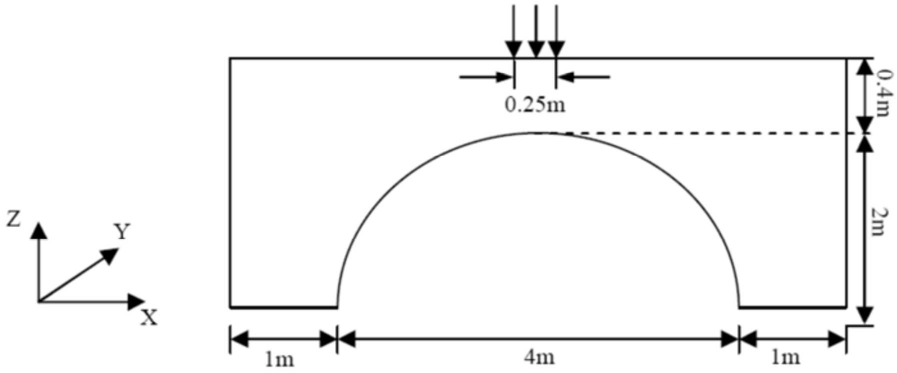

Figure 6. Geometry of laboratory testing.

Table 4. Soil characteristics.

Soil	E [MPa]	ν	Density [kg/m^3]	c [MPa]	φ [°]	ψ [°]
Sand	15	0.2	1800	0	45	15

Table 5. Steel profile characteristics.

Steel profile	E [GPa]	ν	Density [kg/m^3]	I [cm^4/m]	t [mm]	A [cm^2/m]
S235 W 152/50	210	0.3	7850	95.94	2.7	33.29

**Calculation:

- material and geometric nonlinear
- Convergence bound at 1% to 2% of the L2-norm of the residual forces.

In ANSYS, the convergence criterion is defined as default value of 0.1 % of the L2-norm of the residual forces. That means that all residual forces have to be transferred to the load vector except 0.1 % of the Root Mean Square. In the following calculations, a convergence criterion between 1% and 2% has been used. According to experience, convergence criteria between 1% and 2% are precisely enough, to verify equilibrium conditions.

(Cohesion = 0 means no tensile- resp. compressive strength of the material. Hence result convergence problems, so that the convergence bound has to be increased compared with the default value to achieve a solution.)

**Element types:

Solid45 und Shell63

**Load history

Load step 1: self-weight Sand
Load step 2: load

Reference solution: Example 5 - Calculation with LAW = 1 MOHR-COULOMB (bsp5.dat)

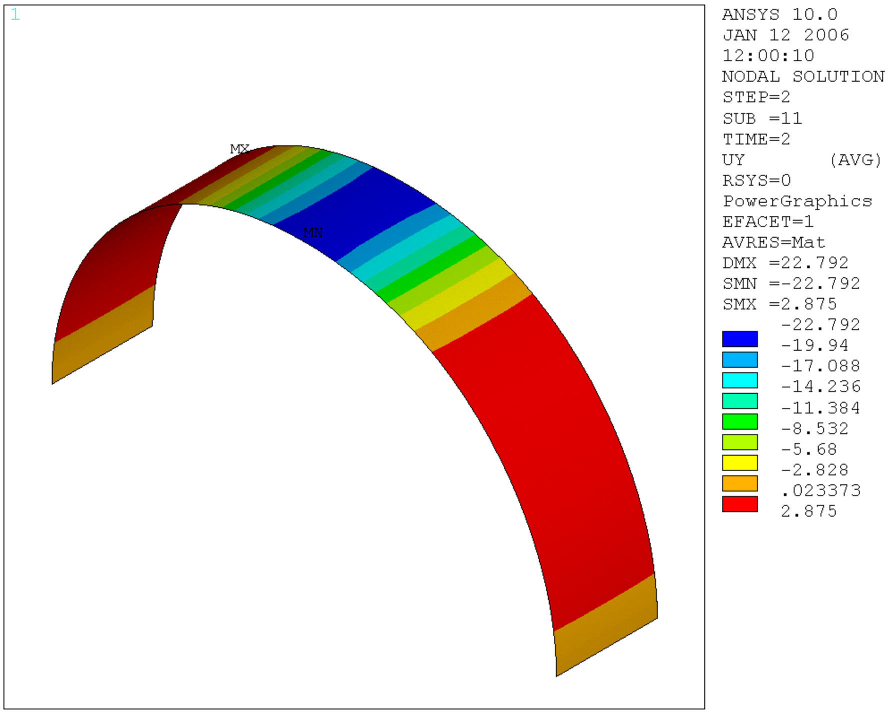

Vertical displacement uy (mm) of the steel tube - arc

Reference solution: Example 6 - Calculation with LAW = 40 DRUCKER_PRAGER (bsp6.dat)

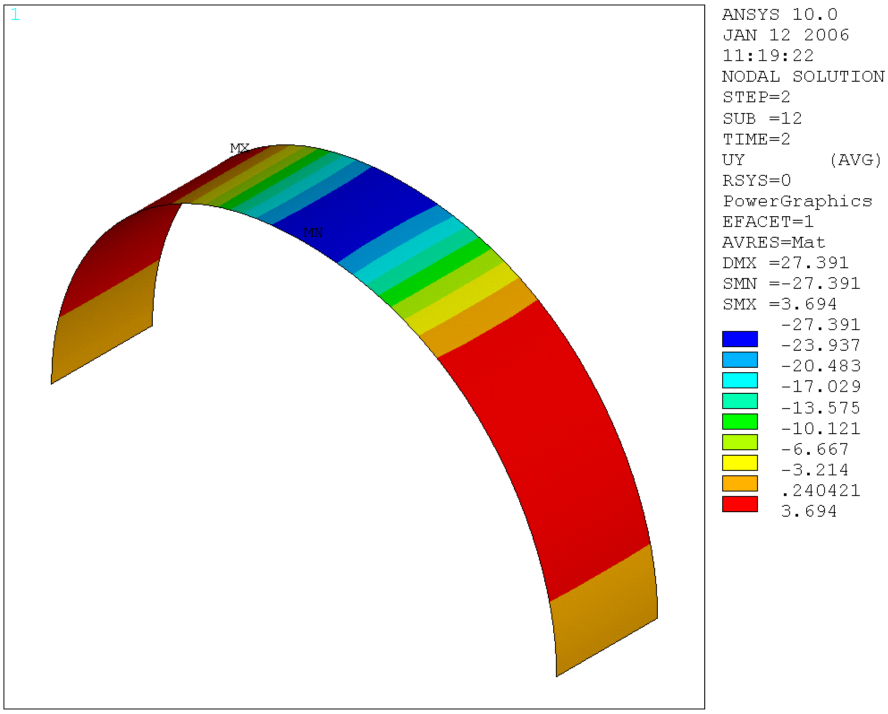

Vertical displacement uy (mm) of the steel tube - arc

Reference solution: Example 7 - Calculation with LAW = 41 MOHR-COULOMB+DRUCKER-PRAGER (bsp7.dat)

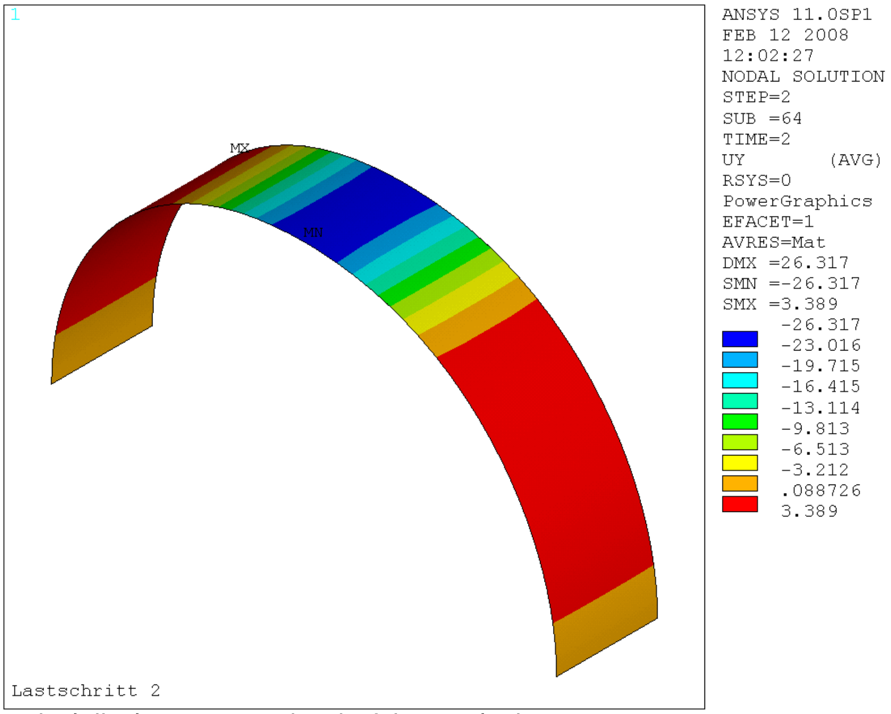

Vertical displacement uy (mm) of the steel tube - arc

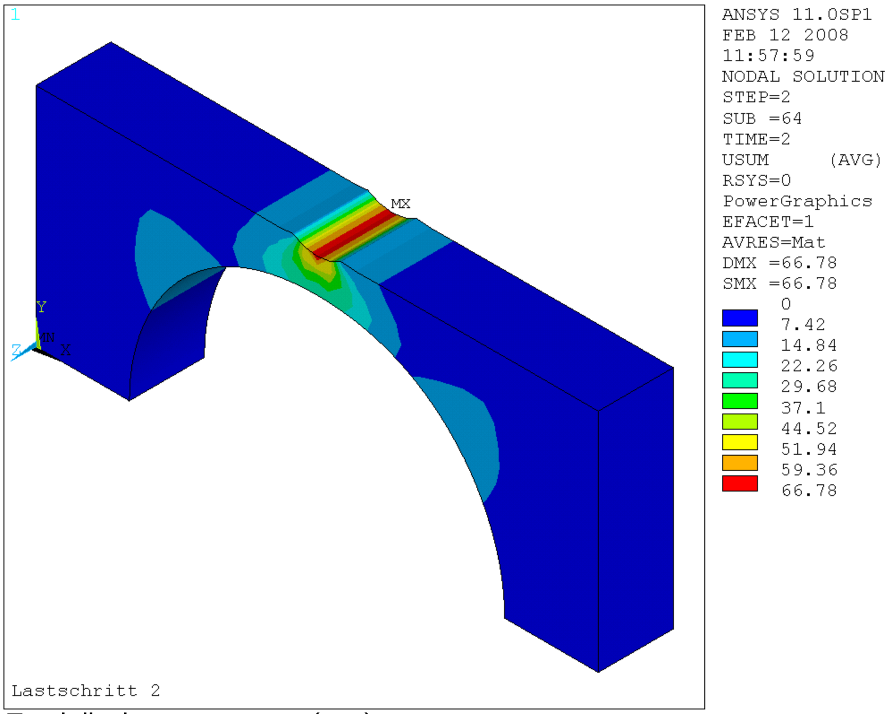

Total displacement usum (mm)

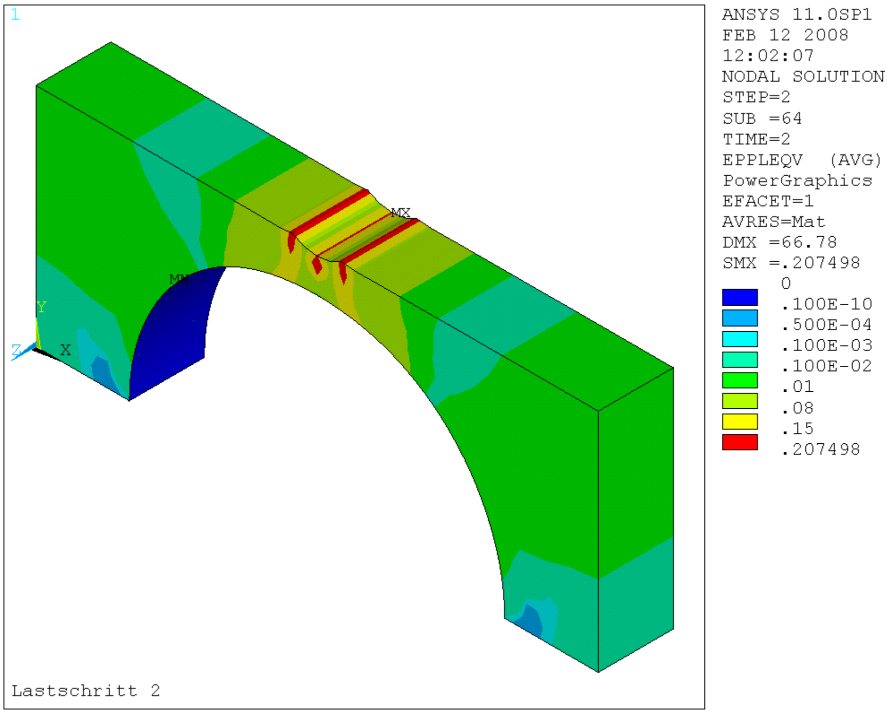

Equivalent plastic strain

Reference solution: Example 8 - Calculation with LAW = 40 DRUCKER-PRAGER (bsp8.dat)

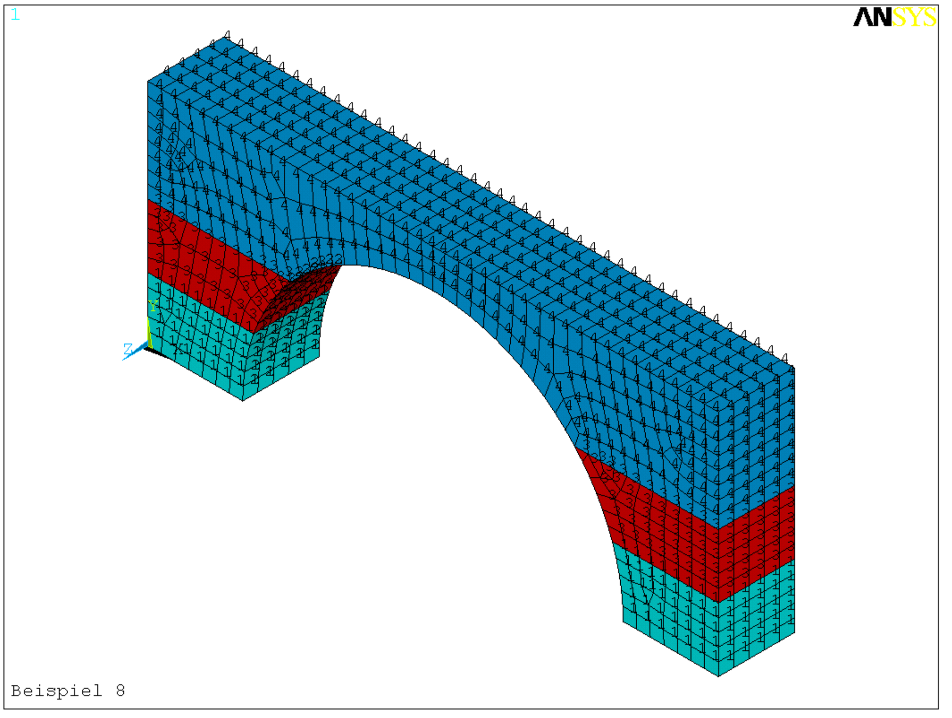

FE-Model

**Load history

Load step 1: Self-weight, Installation layer MAT1, steel tube – arc, stiffened
Load step 2: Self-weight, Installation layer MAT3, steel tube – arc, stiffened
Load step 3: Self-weight, Installation layer MAT4, steel tube – arc, stiffened
Load step 4: Load

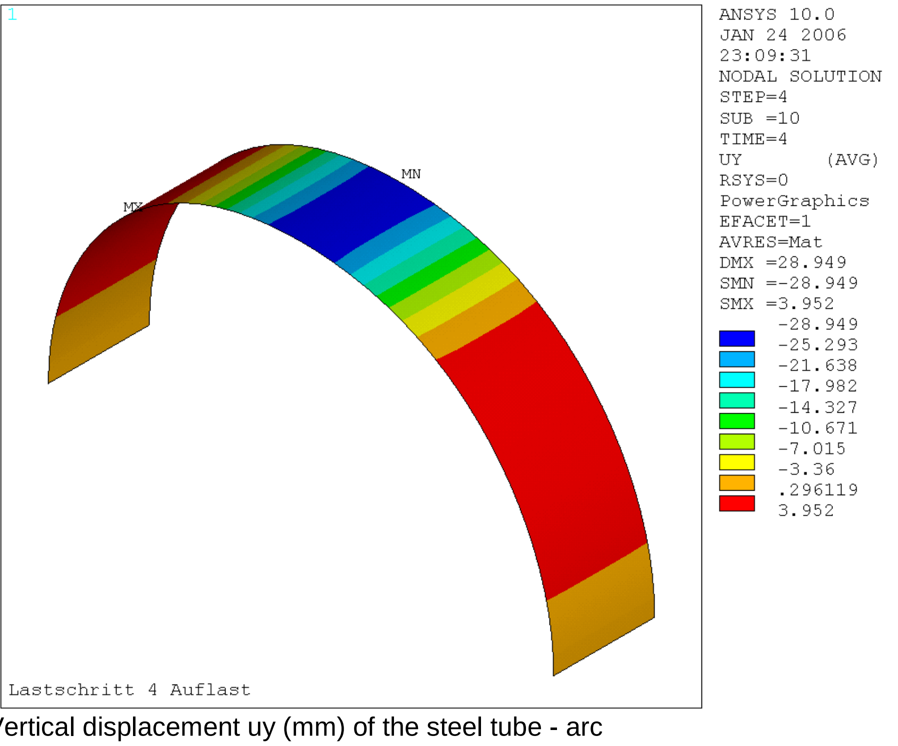

Vertical displacement uy (mm) of the steel tube - arc

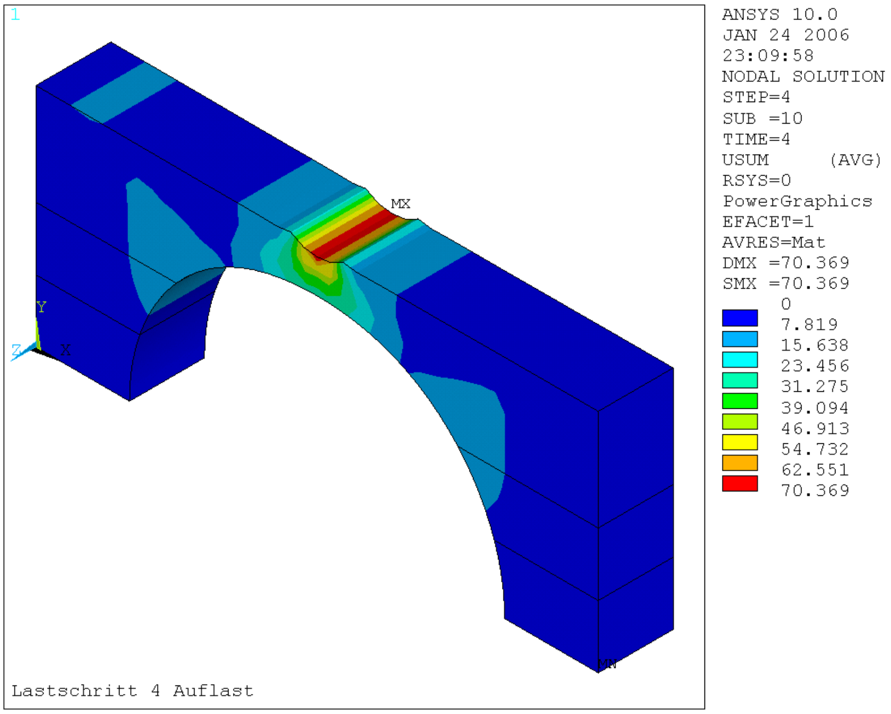

Total deformation usum (mm)

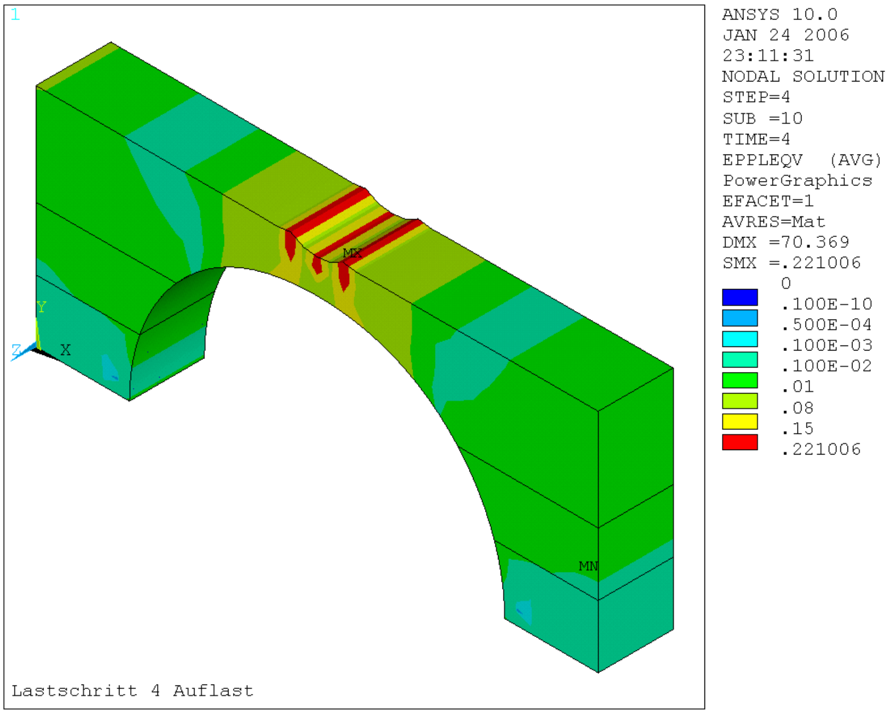

Equivalent plastic strain

5.4 Example 9 - MOHR-COULOMB anisotropic

(bsp9.dat)

3000 kN/m²

1850 kN/m²

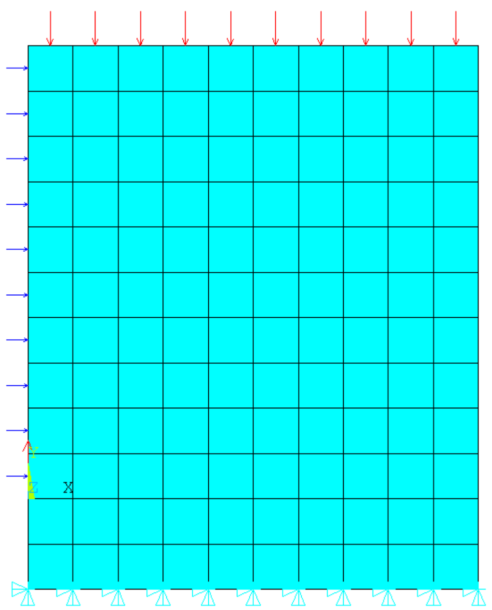

Rock with 2 joint blades

1st joint α = 85°, β = 0°
2nd joint α = -5°, β = 90°

Elements: SOLID 45

test_Mohr-Coulomb_anisotrop 2 TF LAW=10

FE-model

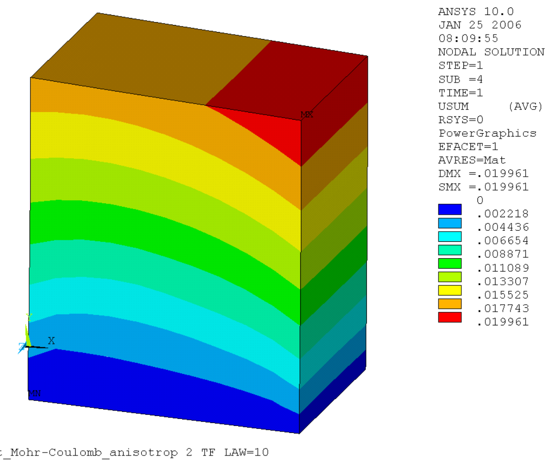

Total deformation usum (m)
max usum = 0,019961 m

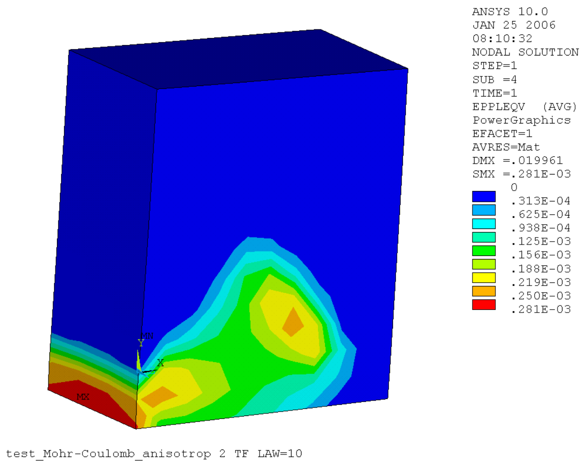

Equivalent plastic strain EPPL,EQV
max eppl = 0,281 E-03

5.5 Example 10 – Concrete-model DRUCKER-PRAGER singular (LAW=9)

(eld.dat)

Uniaxial compressive tests:

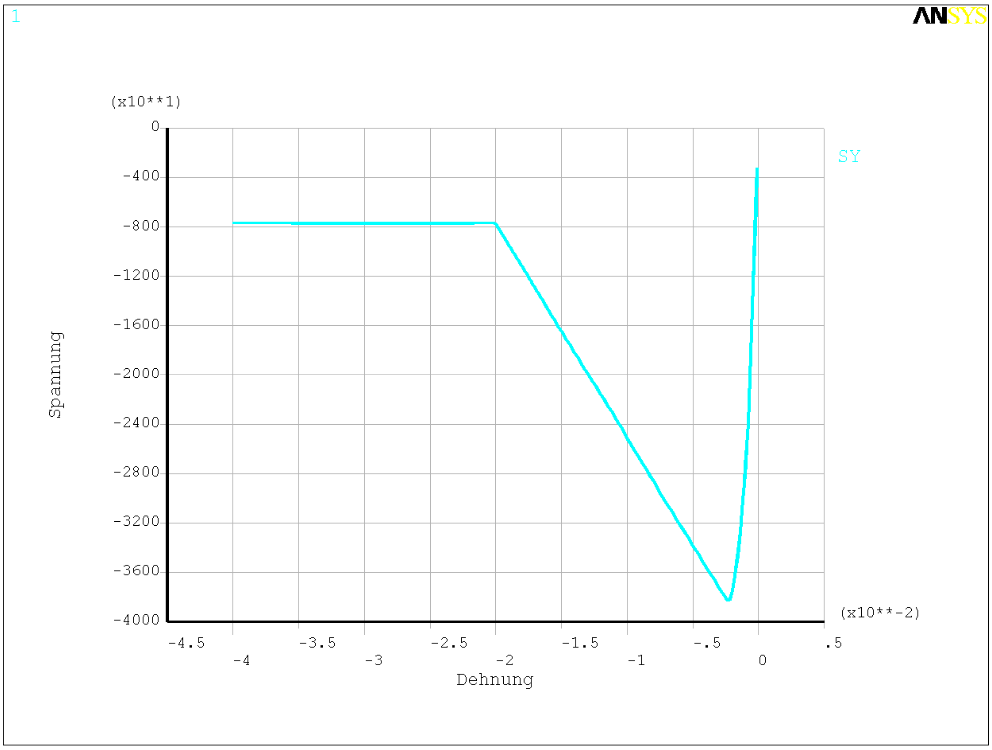

Stress-strain diagram 20°C, mlaw = 0

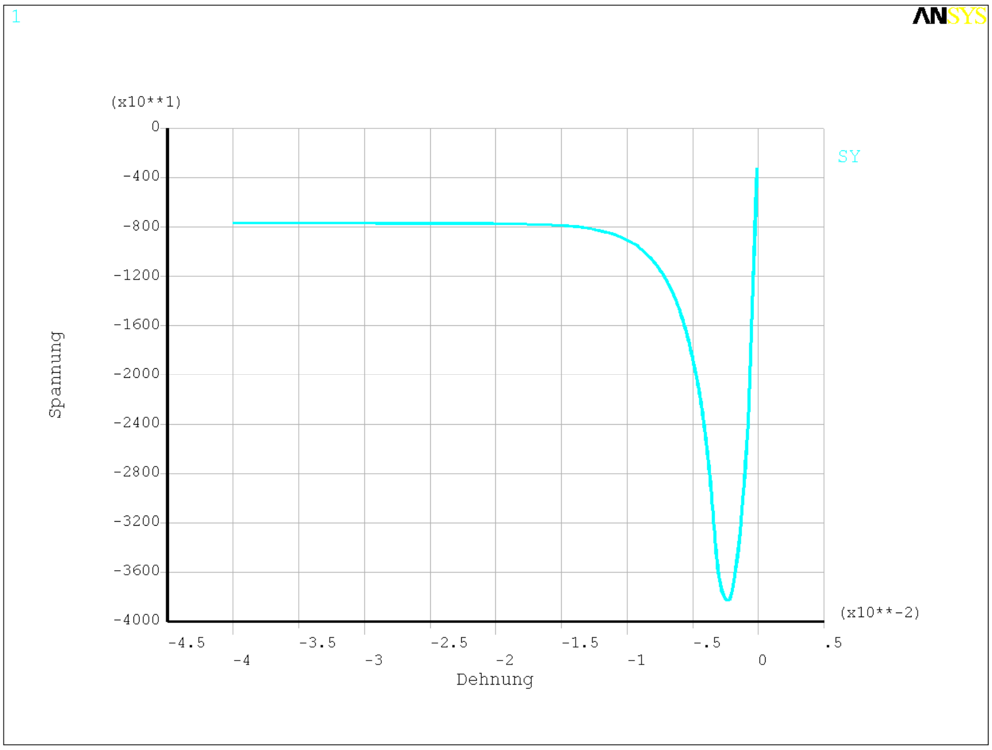

Stress-strain diagram 20°C, mlaw = 1

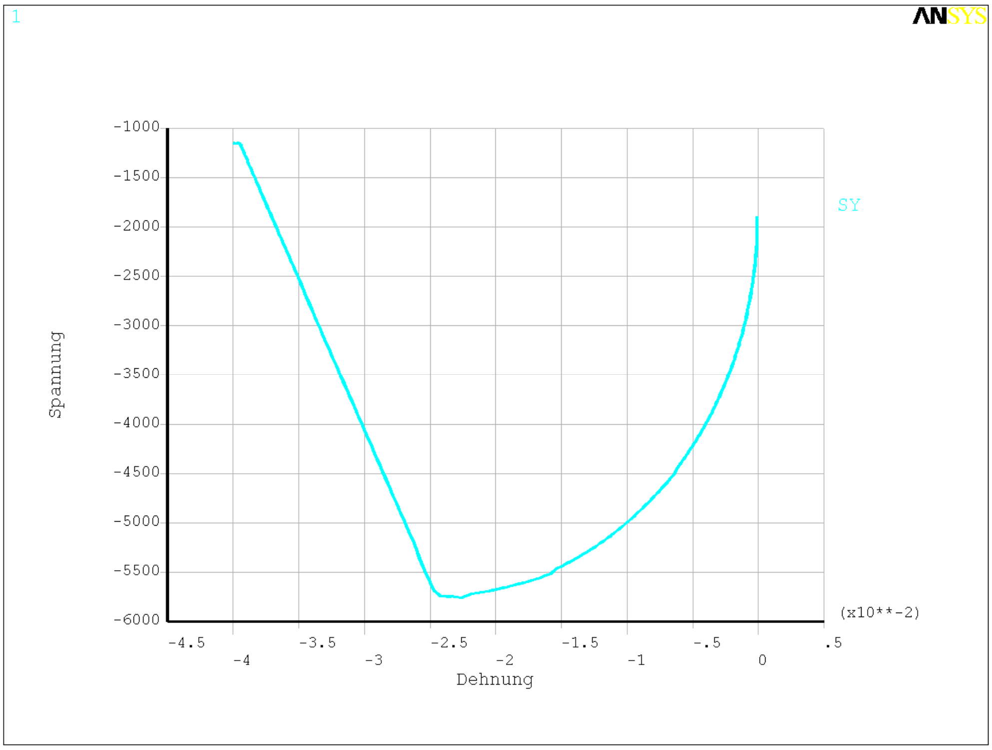

Stress-strain diagram 800°C, mlaw = 0

5.6 Example 11 – Concrete-model DRUCKER-PRAGER singular (LAW=9)

(elz.dat)

Uniaxial tensile tests:

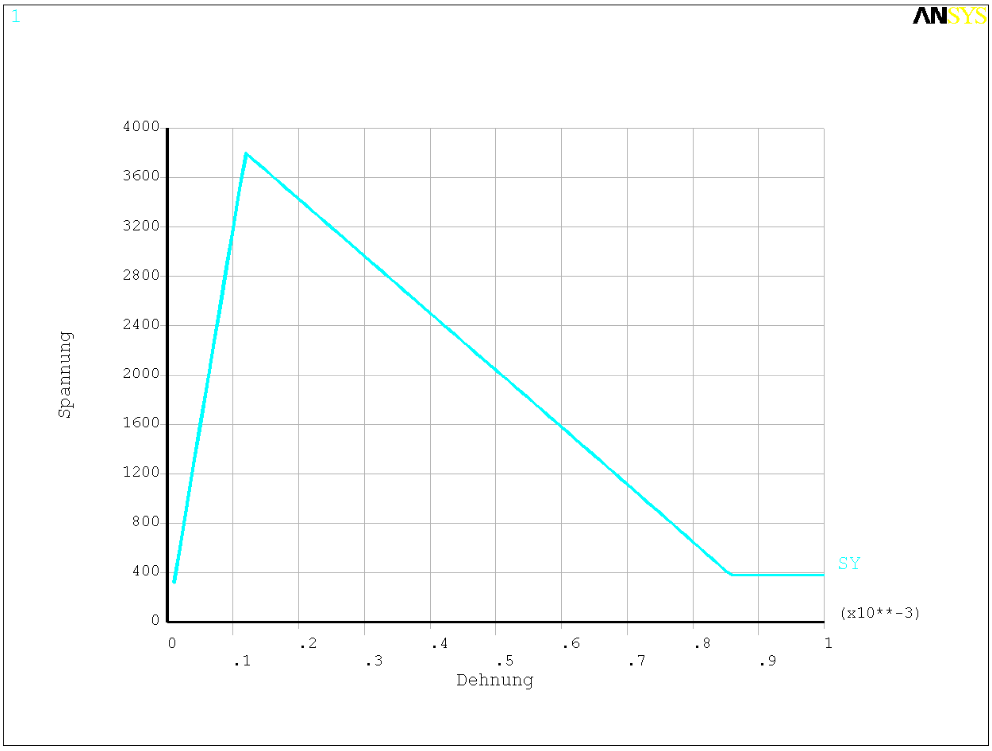

Stress-strain diagram 20°C, mlaw = 0

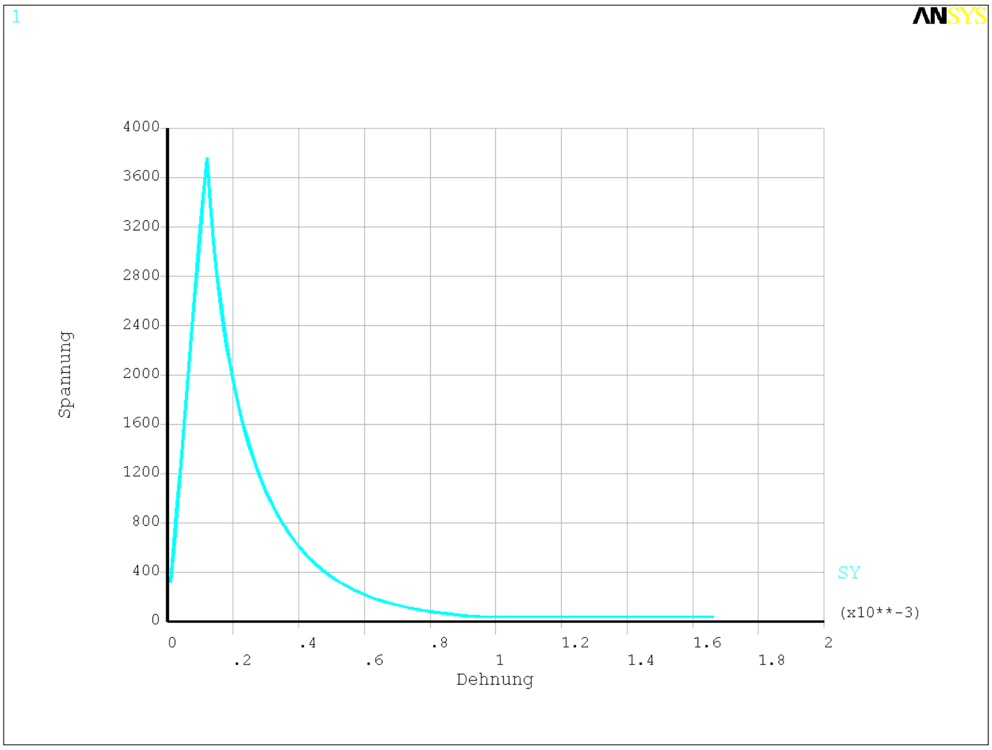

Stress-strain diagram 20°C, mlaw = 1

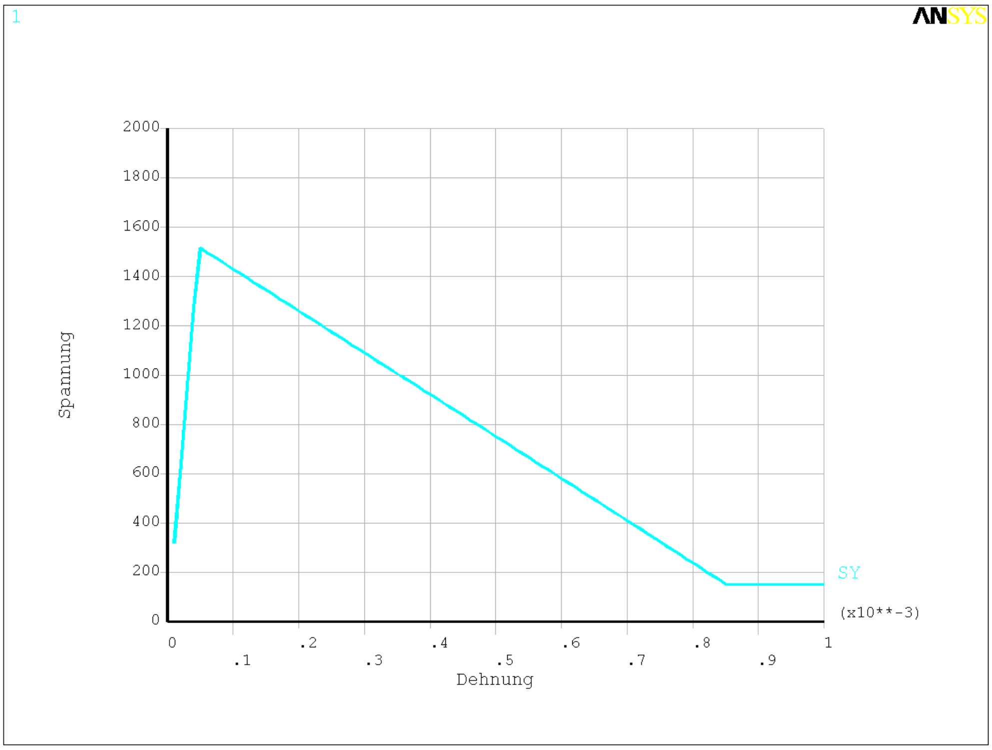

Stress-strain diagram 400°C, mlaw = 0

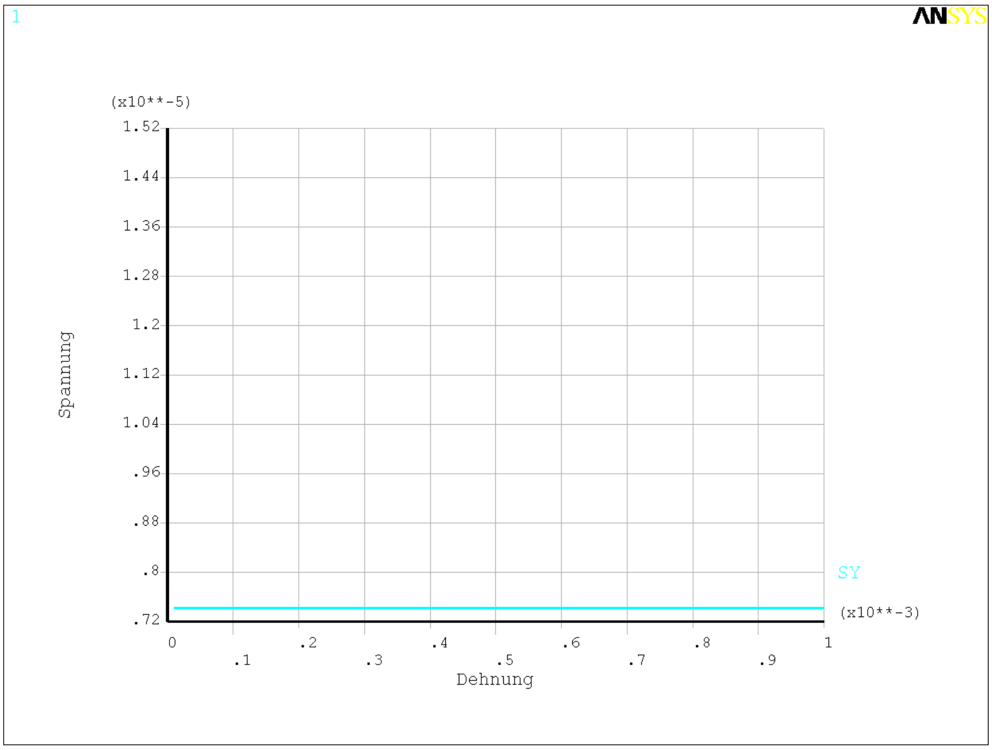

Stress-strain diagram 800°C, mlaw = 0

5.7 Example 12 – Masonry-model with softening (LAW=20)

(eld.dat)

Uniaxial compressive test, vertical:

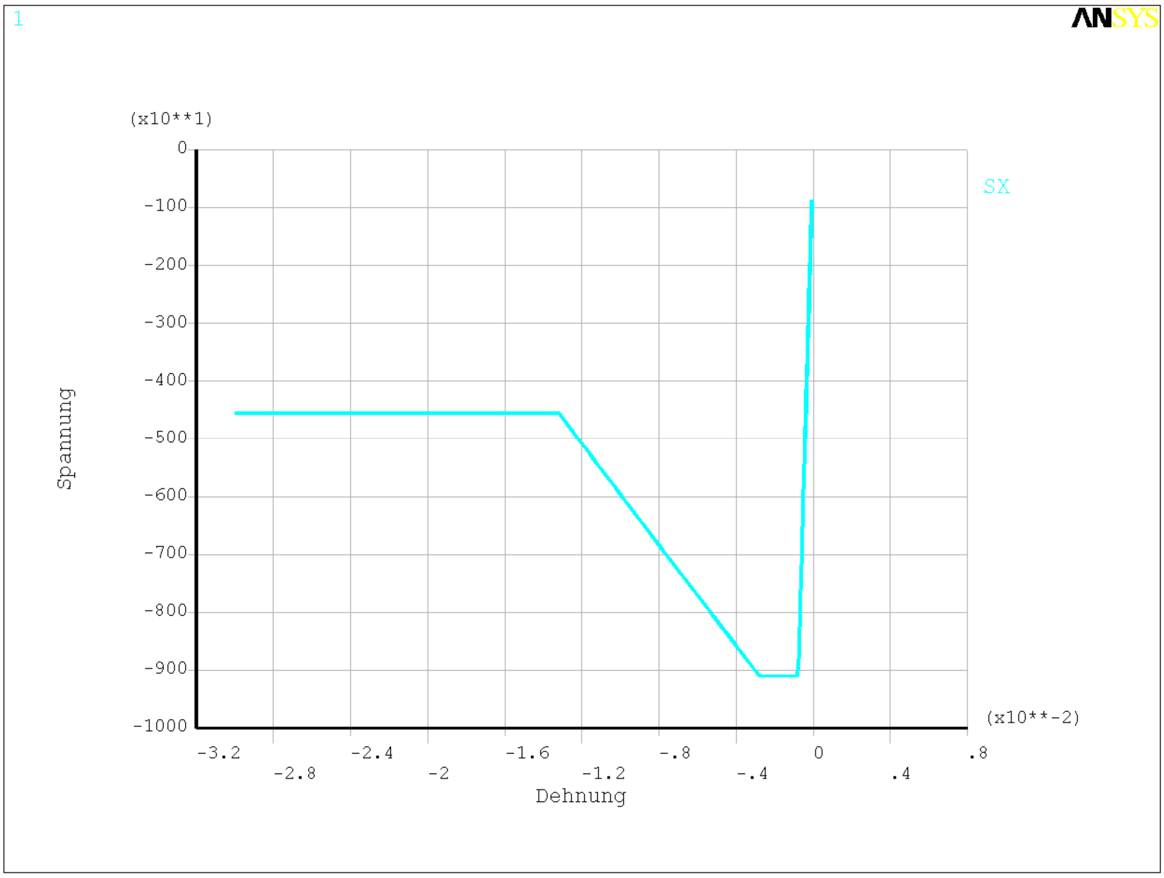

5.8 Example 13 – Masonry-model with softening (LAW=20)

(eld.dat)

Uniaxial compressive test, horizontal:

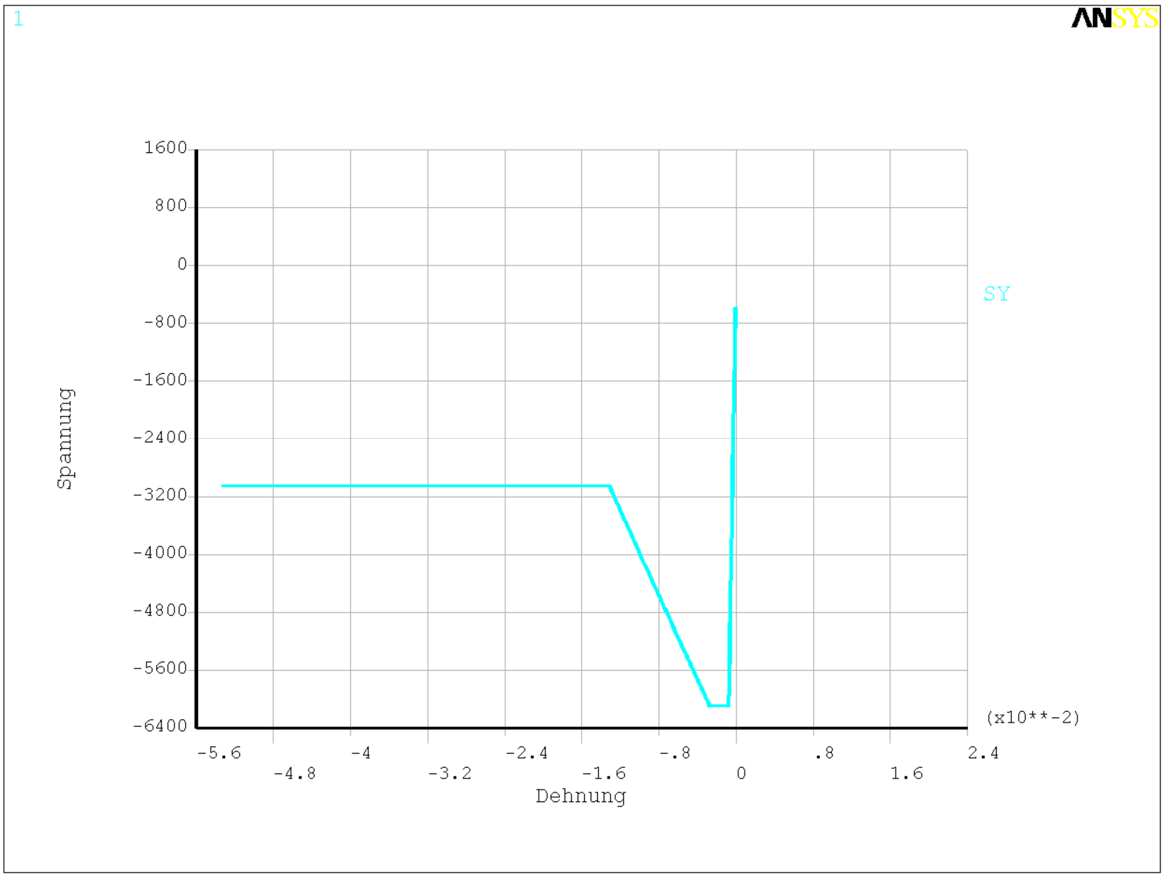

5.9 Example 14 – Masonry-model with hardening and softening (LAW=22)

(eld.dat)

Uniaxial compressive test, vertical:

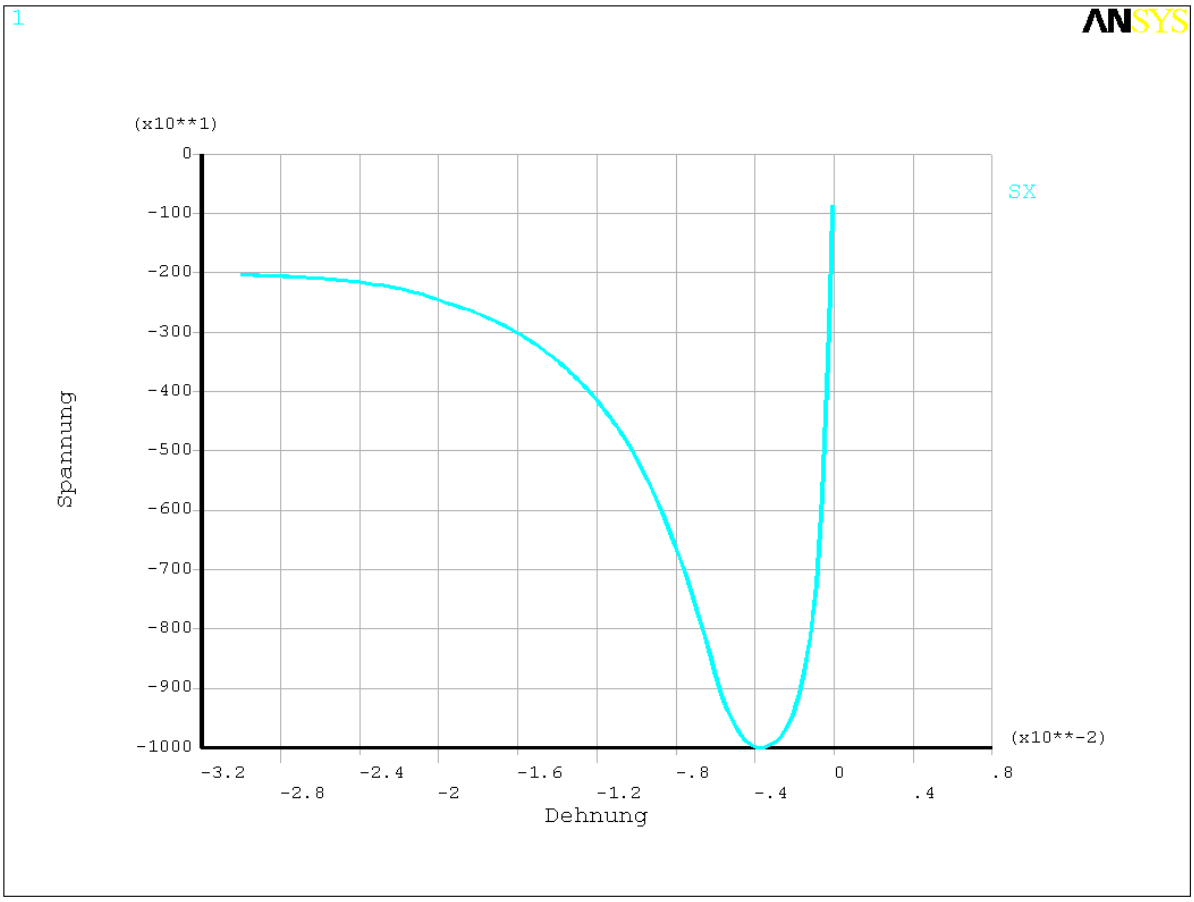

5.10 Example 15 – Masonry-model with hardening and softening (LAW=22)

(eld.dat)

Uniaxial compressive test, horizontal:

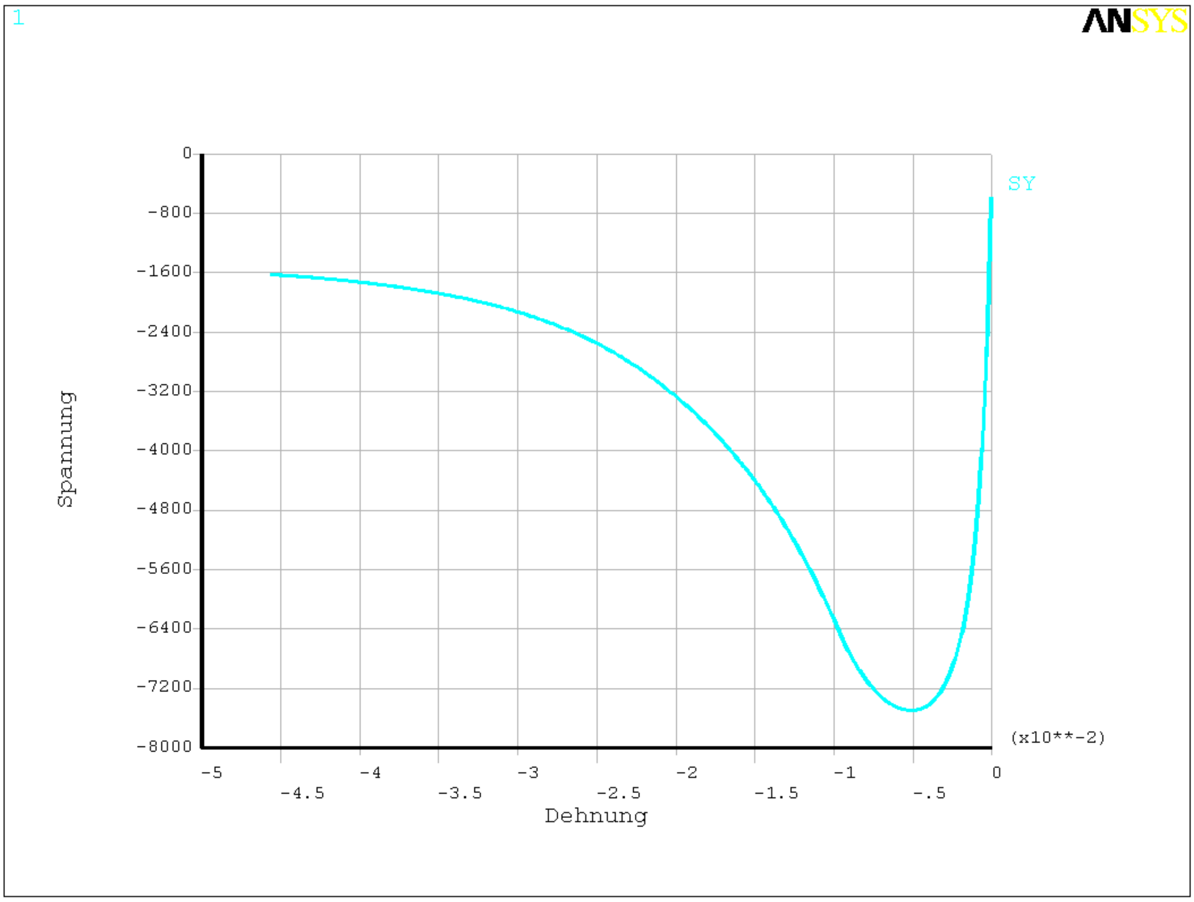

5.11 Example 16 – Masonry-model with hardening and softening (LAW=22)

(elz.dat)

Uniaxial tensile test, vertical:

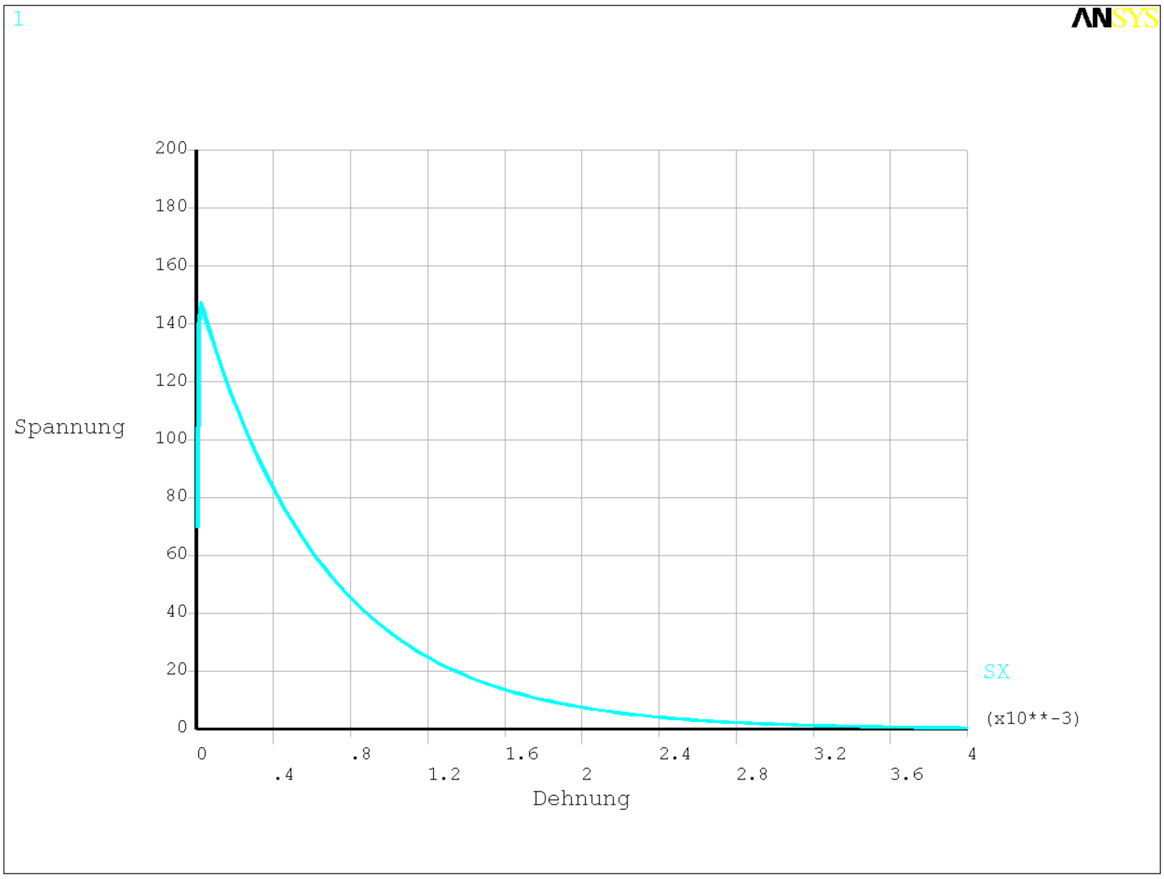

5.12 Example 17 – Masonry-model with hardening and softening (LAW=22)

(elz.dat)

Uniaxial tensile test, horizontal:

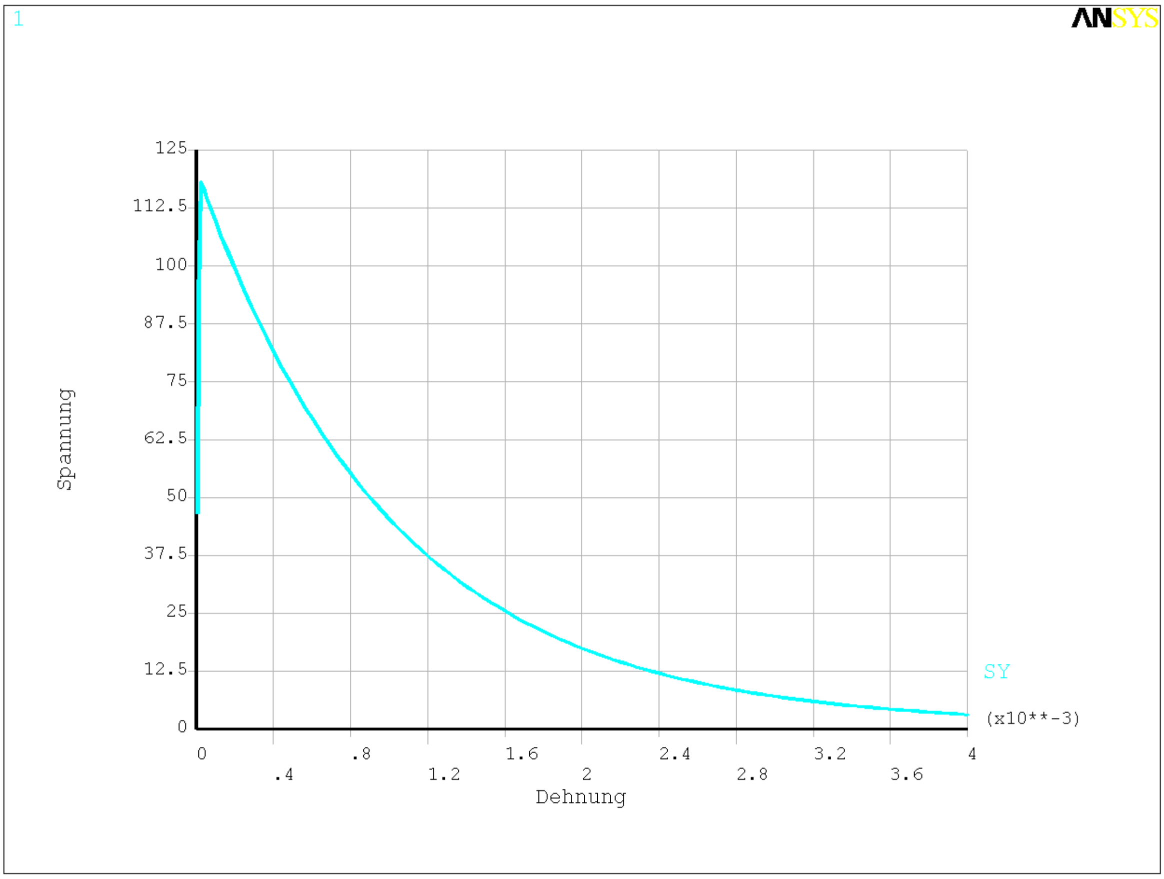

5.13 Example 18 – Masonry-model (LAW=20) shear test 1

Benchmark test according to [6-17], S.140f.

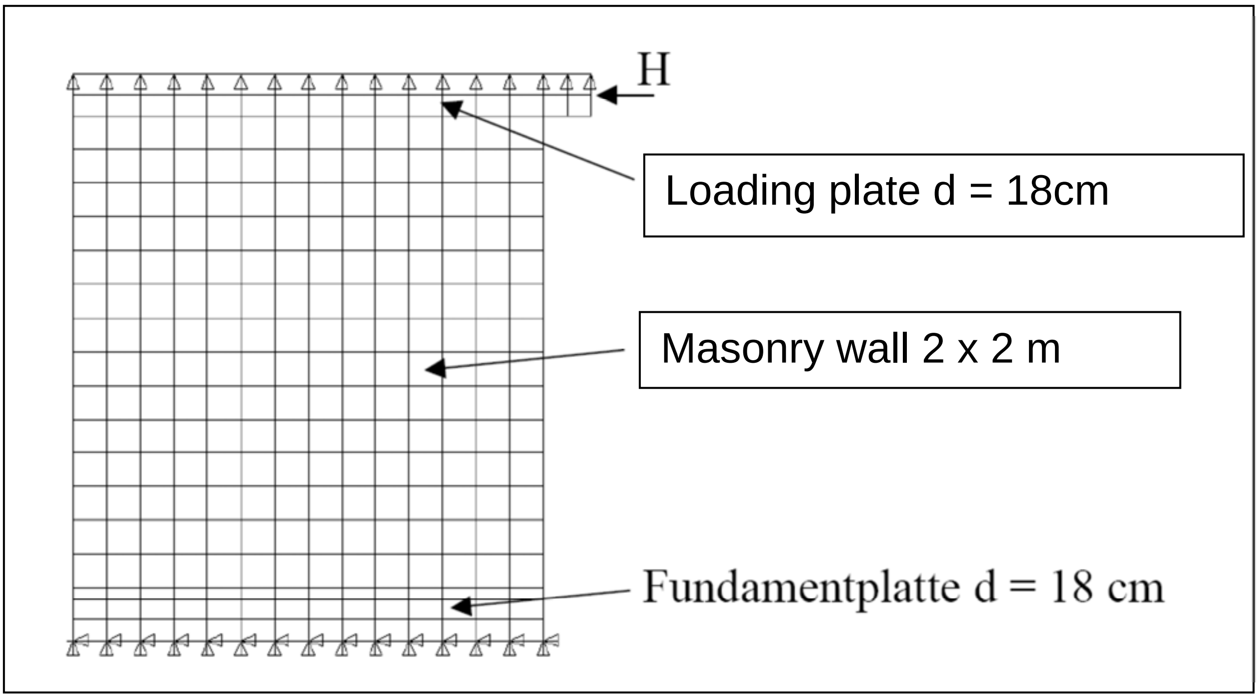

Stone format: 40x20

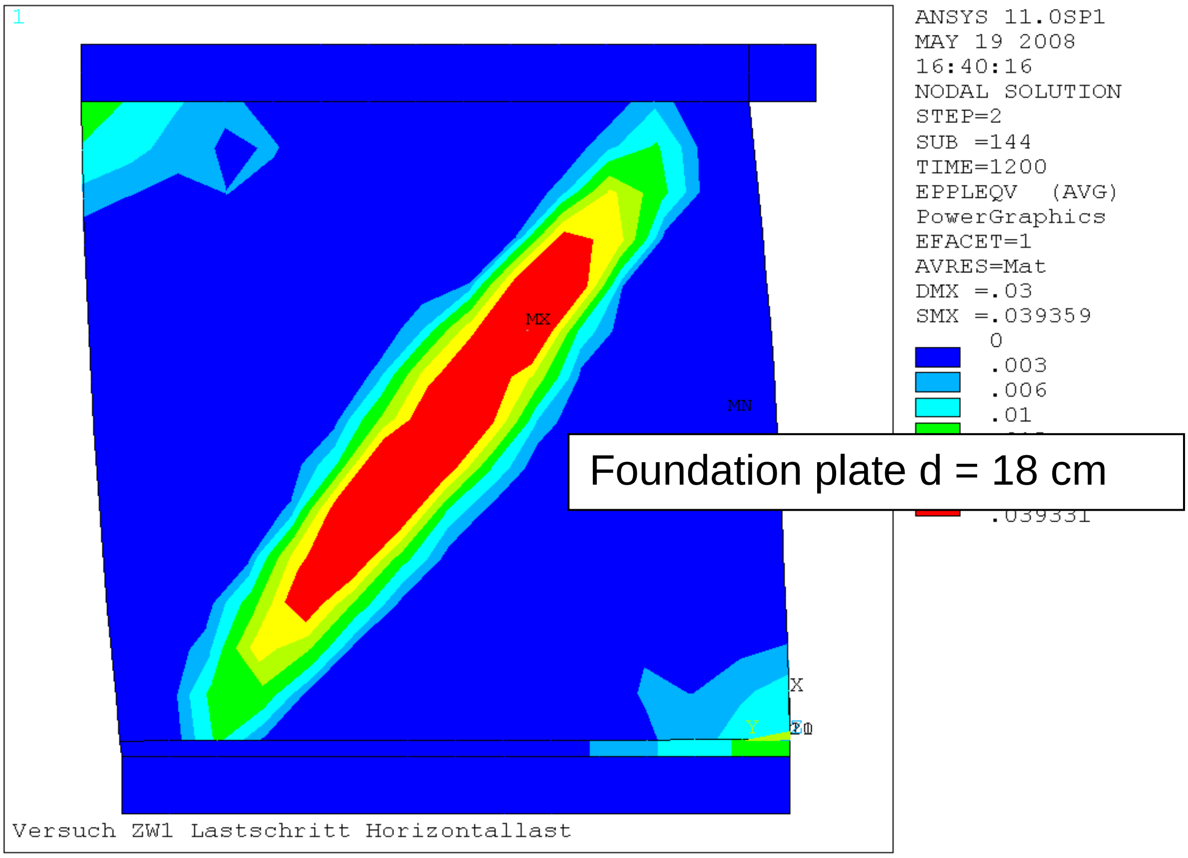

5.14 Example 19 – Masonry-model (LAW=20) Shear test 2

Benchmark test according to [6-17], S.140f.

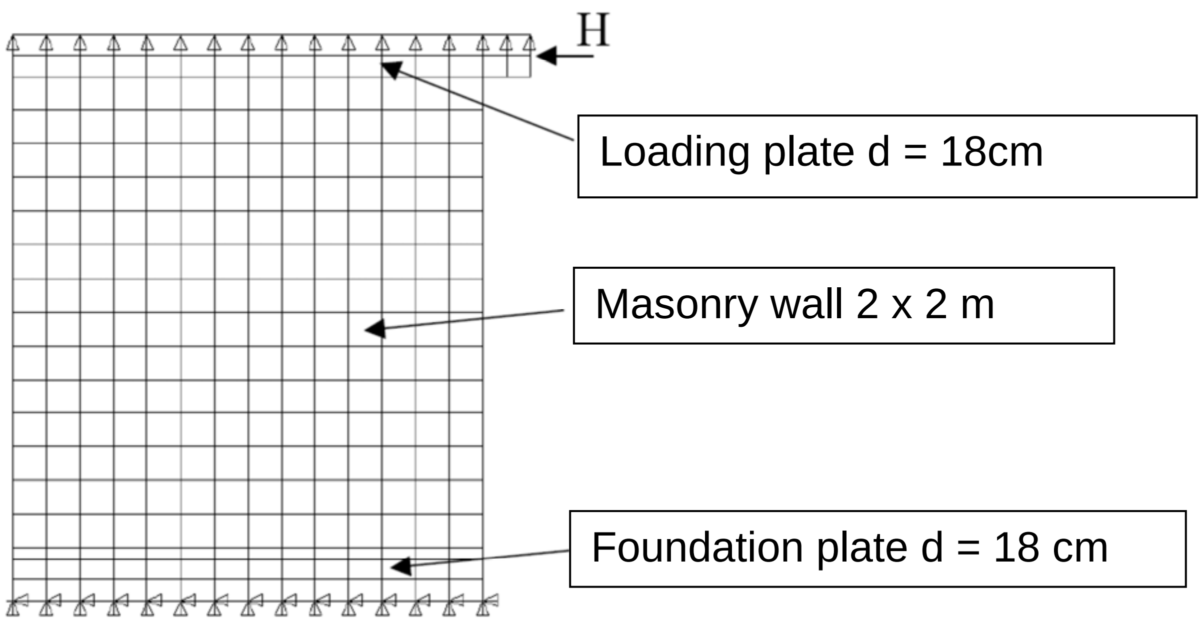

Stone format 20x20

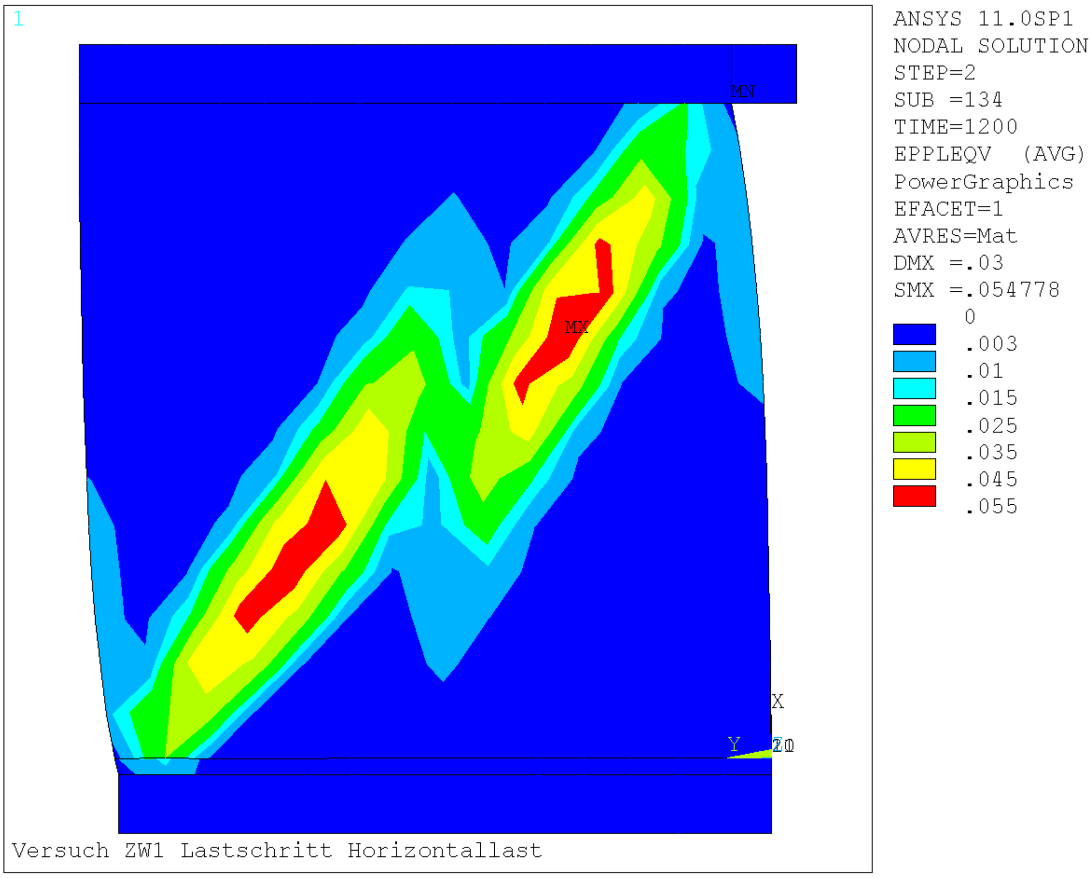

5.15 Example 20 – Wood-model (LAW=33) uniaxial compressive tests

(el_test_holz33.dat)

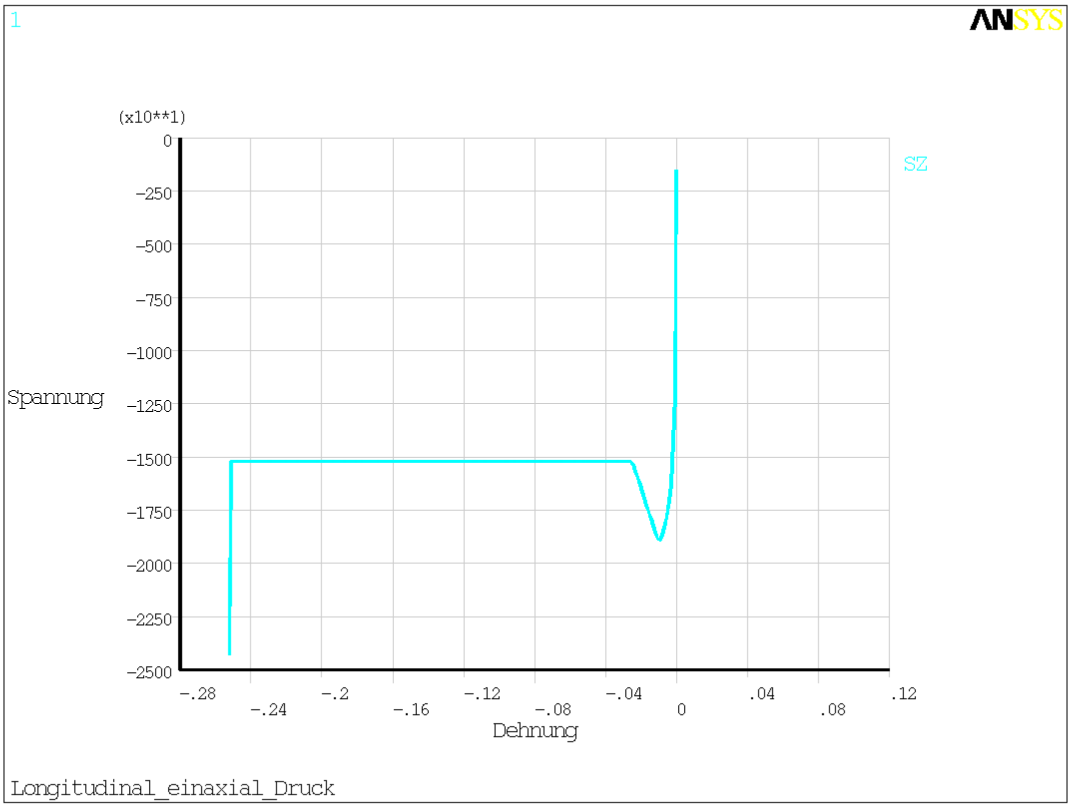

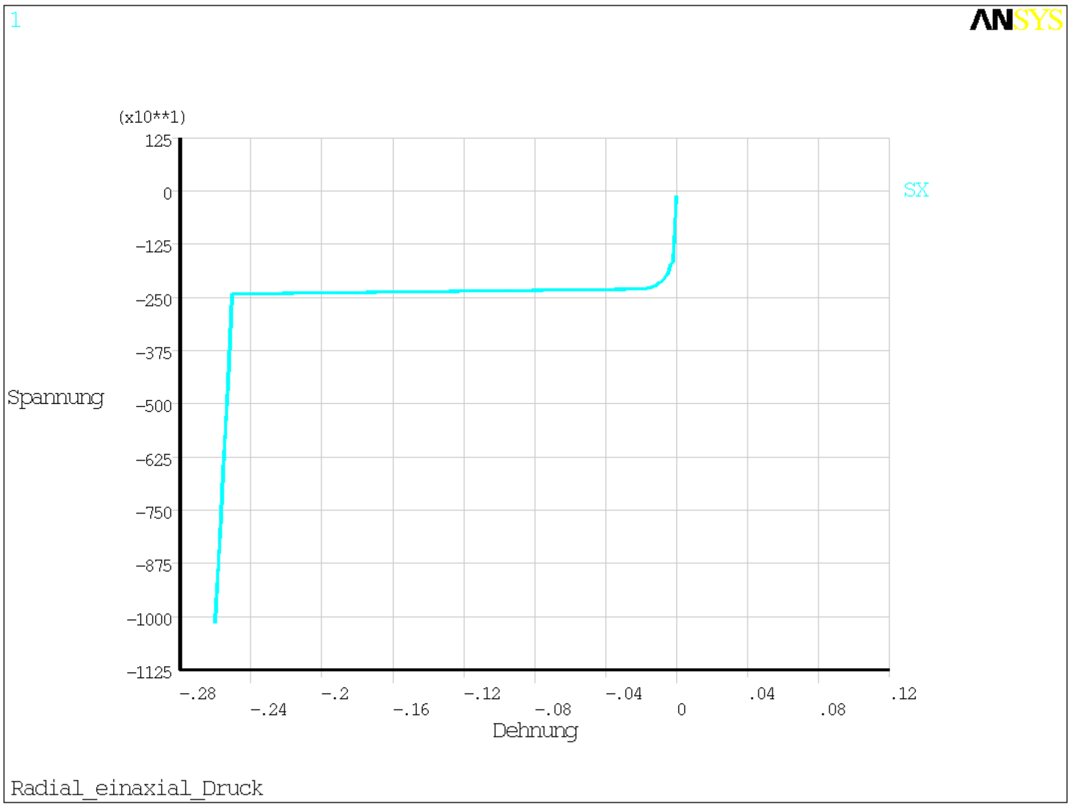

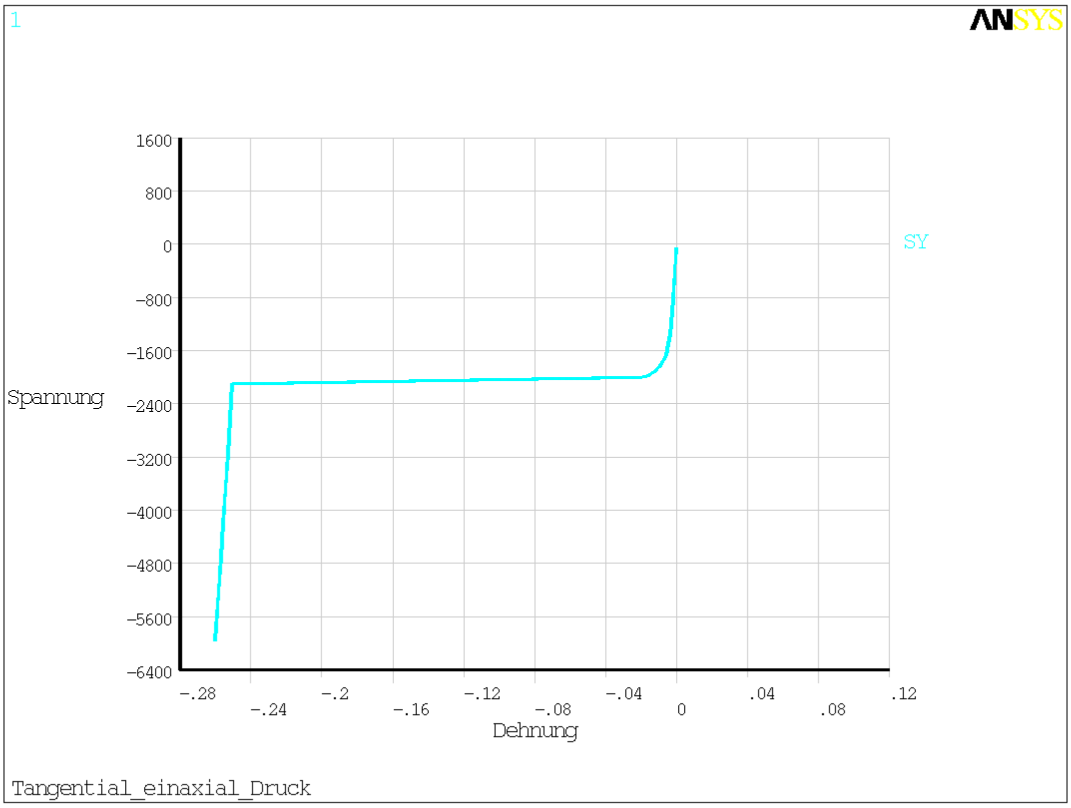
1
ANSYS
1600
800
0
-800
-1600
-2400
-3200
-4000
-4800
-5600
-6400
Spannung
SY
-.28
-.24
-.2
-.16
-.12
-.08
-.04
0
.04
.08
.12
Dehnung
Tangential_einaxial_Druck

5.16 Example 21 – Wood-model (LAW=33) uniaxial tensile tests

(el_test_holz33.dat)

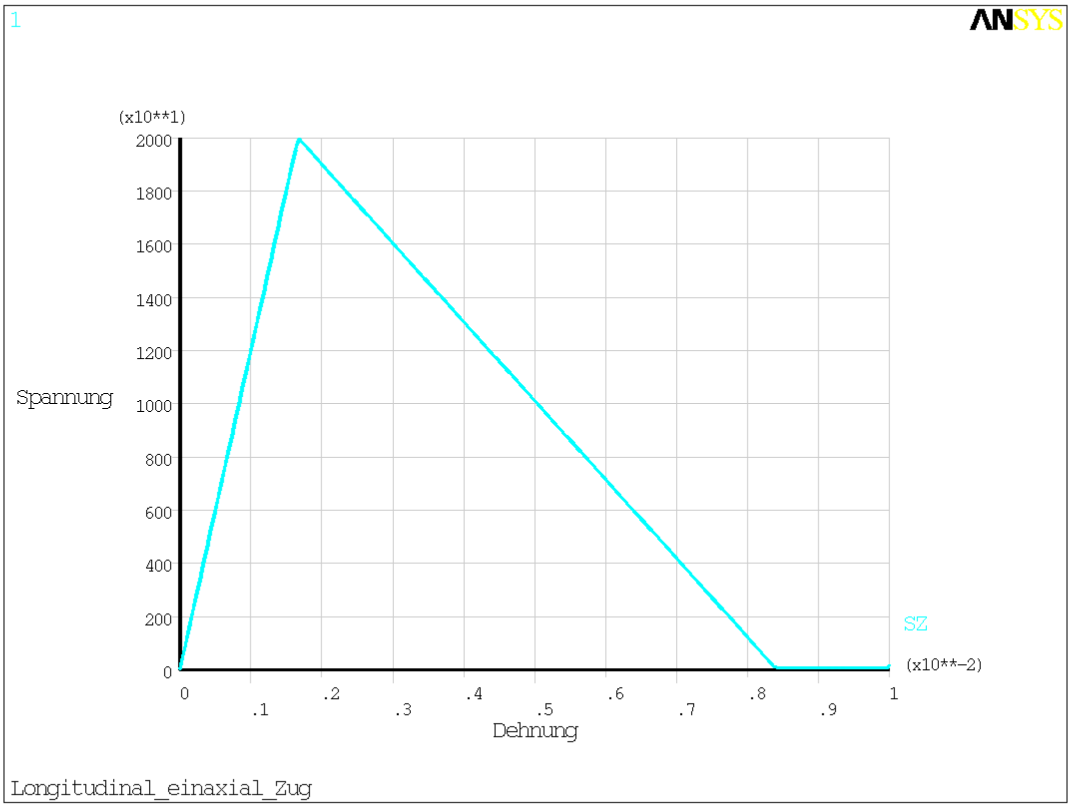

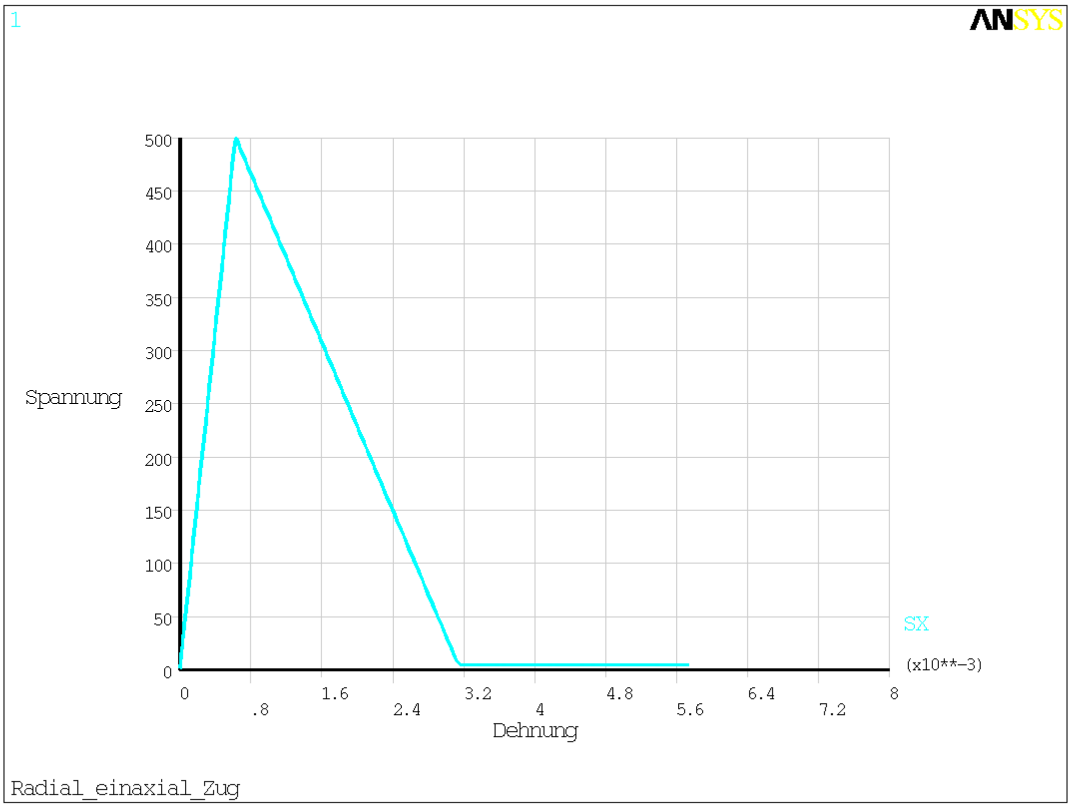

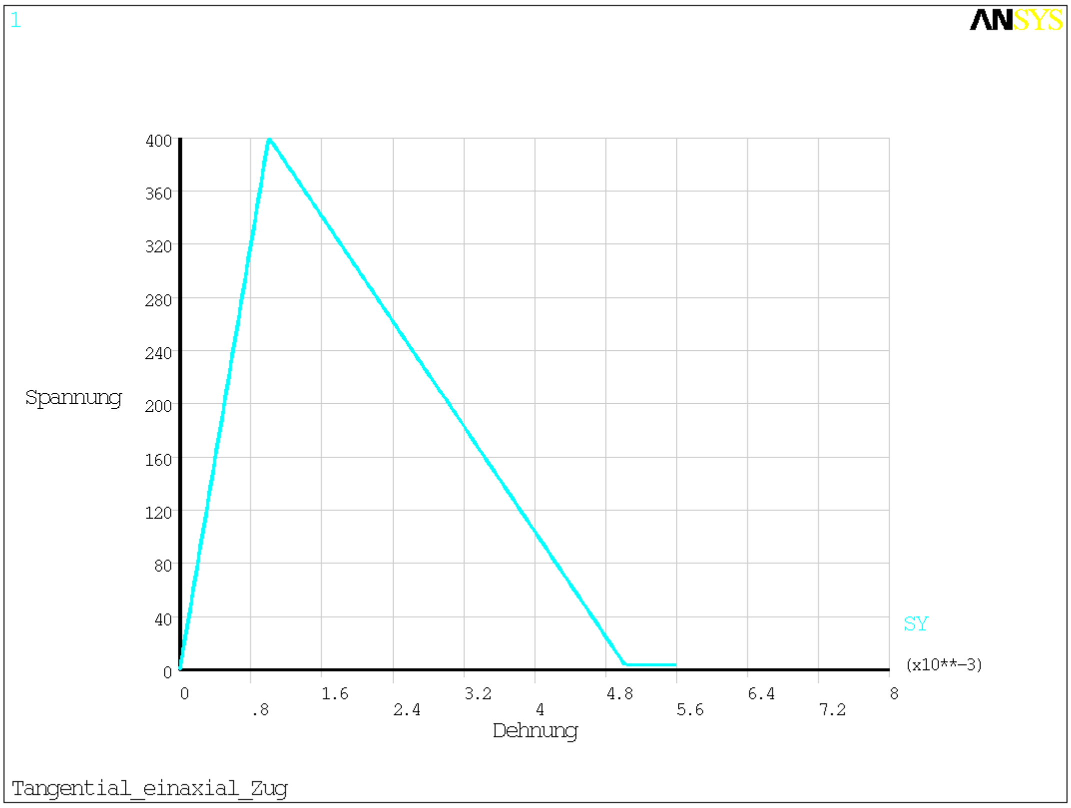
1
ANSYS
Spannung
400
360
320
280
240
200
160
120
80
40
0
SY
(x10**-3)
0
.8
1.6
2.4
3.2
4
4.8
5.6
6.4
7.2
8
Dehnung
Tangential_einaxial_Zug

5.17 Example 22 – Single Joint Shear-Test (LAW=1, 10)

(bsp22.dat)

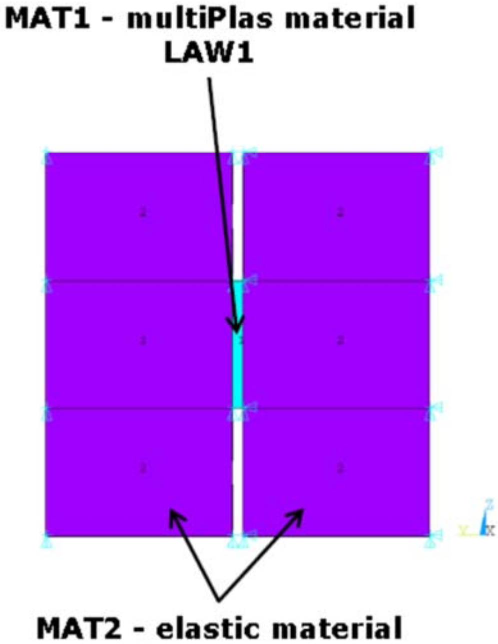

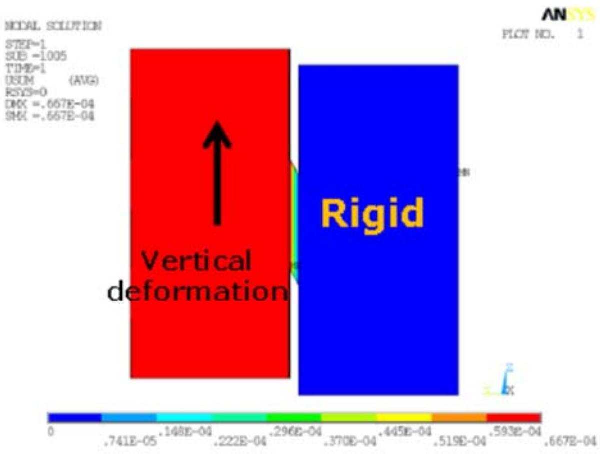

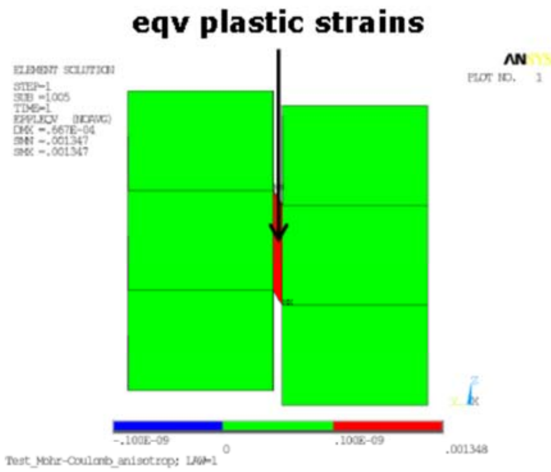

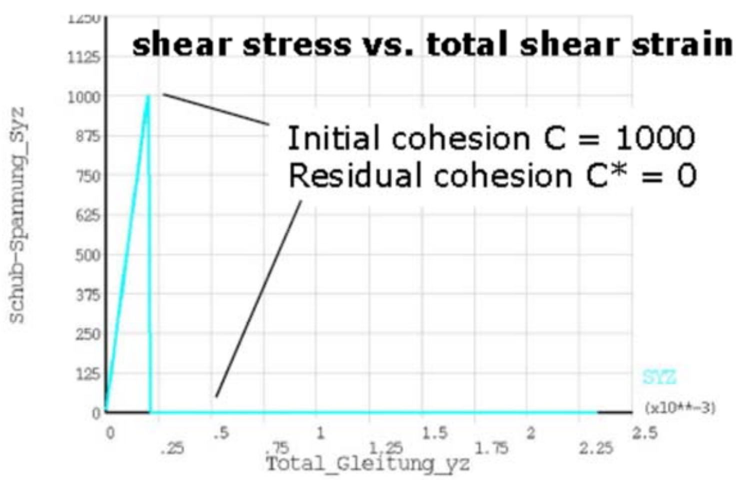

5.18 Example 23 – Single Joint Tensile-Test (LAW=1, 10)

(elz.dat)

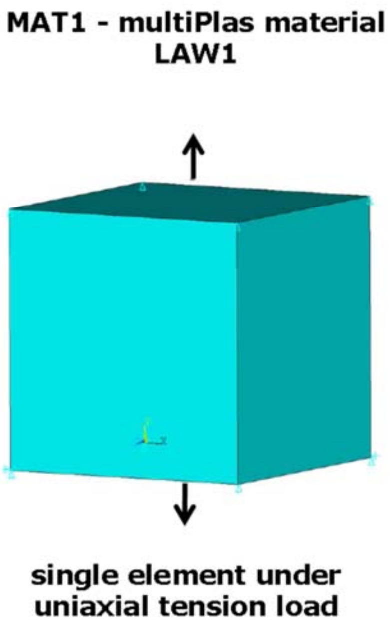

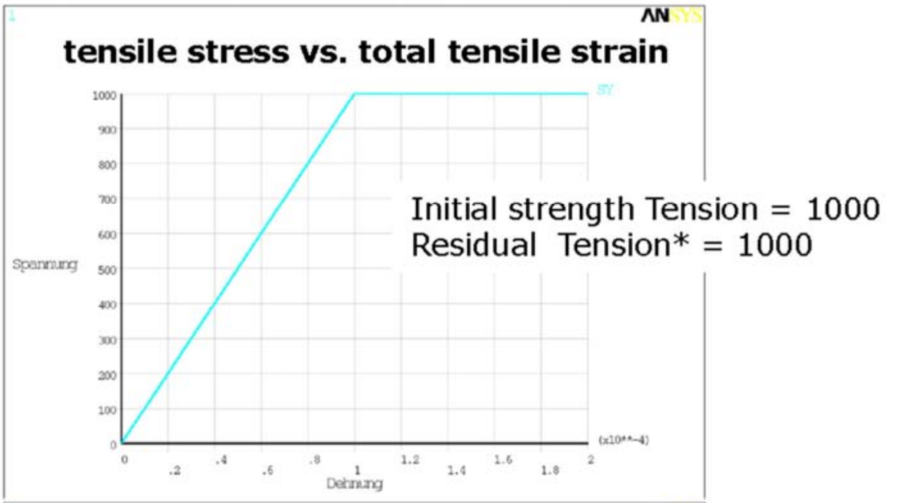

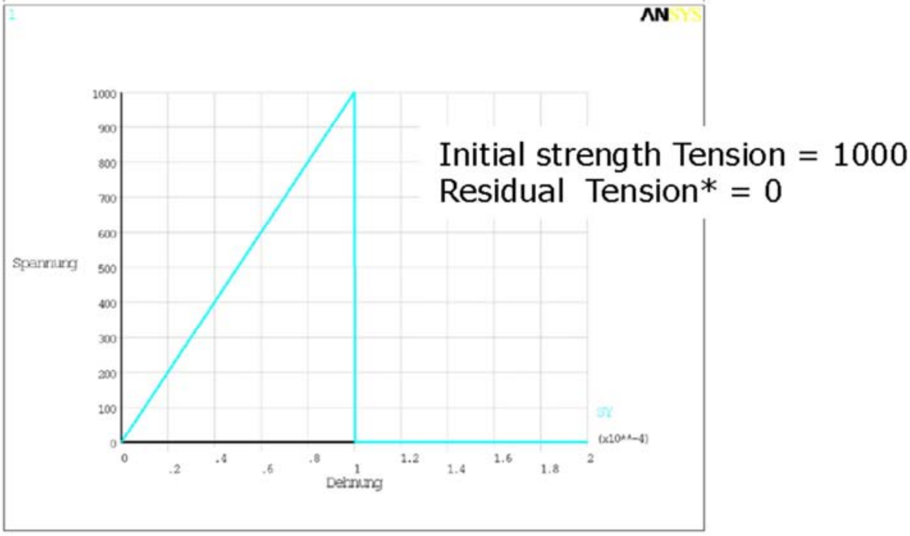

6 REFERENCES

[6-1] ANSYS Users Manual for ANSYS Rev. 11.0, Analysis Guides, ANSYS Inc., Houston, Canonsburg

[6-2] ANSYS Users Manual for ANSYS Rev. 11.0, Commands, ANSYS Inc., Houston, Canonsburg

[6-3] ANSYS Users Manual for ANSYS Rev. 11.0, Elements, ANSYS Inc., Houston, Canonsburg

[6-4] ANSYS Users Manual for ANSYS Rev. 11.0, Theory, ANSYS Inc., Houston, Canonsburg

[6-5] ANSYS Users Manual for ANSYS Rev. 11.0, Verification, ANSYS Inc., Houston, Canonsburg

[6-6] Bažant, Z.P.; Oh, B.H.: Crack band theory for fracture of concrete. Materials and Structures, RILEM, 93 (16), S. 155-177

[6-7] Chen, W.F.: Constitutive Equations for Engineering Materials. Vol. 2 Plasticity and Modeling. Elsevier Amsderdam - London - New York - Tokyo, (1994)

[6-8] Deutscher Ausschuss für Stahlbeton, Heft 525 - Erläuterungen zu DIN 1045-1, Ausgabe 2003, Beut-Verlag

[6-9] DIN 1045-1 Tragwerke aus Beton, Stahlbeton und Spannbeton, Teil1: Bemessung und Konstuktion, Beuth-Verlag, Ausgabe Juli 2001

[6-10] DIN EN 1992-1-1 Eurocode 2: Bemessung und Konstruktion von Stahlbeton- und Spannbetontragwerken. Teil 1-1: Allgemeine Bemessungsregeln und Regeln für den Hochbau, Ausgabe Oktober 2006

[6-11] DIN EN 1992-1-2 Eurocode 2: Bemessung und Konstruktion von Stahlbeton- und Spannbetontragwerken. Teil 1-2: Allgemeine Regeln – Tragwerksbemessung für den Brandfall, Ausgabe Nov 2005

[6-12] Hintze, D.: Zur Beschreibung des physikalisch nichtlinearen Betonverhaltens bei mehrachsigem Spannungszustand mit Hilfe differentieller Stoffgesetze unter Anwendung der Methode der finiten Elemente. Hochschule für Architektur und Bauwesen Weimar, Dissertation (1986)

[6-13] Kienberger, H.: Über das Verformungsverhalten von biegeweichen, im Boden eingebetteten Wellrohren mit geringer Überschüttung. Rep. Österreich, Bundesministerium f. Bauten u. Technik Straßenforschung, Heft 45, 1975

[6-14] Krätzig, W.; Mancevski, D.; Pölling, R.: Modellierungsprinzipien von Beton. In: Baustatik-Baupraxis 7. Hrsg. Meskouris Konstantin (RWTH Aachen). Balkema Verlag, Rotterdam 1999. S. 295-304

[6-15] Ottosen, N.S.: A Failure Criterion for Concrete. Journal of the Eng. Mech. Div. ASCE. 103, EM4, S. 527-535 (1977)

[6-16] Pölling, R.: Eine praxisnahe, schädigungsorientierte Materialbeschreibung von Stahlbeton für Strukturanalysen. Ruhr-Universität Bochum, Dissertation (2000)

[6-17] Schlegel, R.: Numerische Berechnung von Mauerwerkstrukturen in homogenen und diskreten Modellierungsstrategien. Dissertation, Bauhaus-Universität Weimar, Universitätsverlag (2004), ISBN 3-86068-243-1

[6-18] Simo, J.C.; Kennedy, J.G.; Govindjee, S.: Non-smooth multisurface plasticity and viscoplasticity. Loading / unloading conditions and numerical algorithms. Int. Journal for numerical methods in engineering. Vol. 26, 2161-2185 (1988)

[6-19] Vermeer, P.A.: Materialmodelle in der Geotechnik und ihre Anwendung. Proceedings Finite Elemente in der Baupraxis 1995

[6-20] Vonk, R.A.: Softening of concrete loaded in compression. Dissertation, Delft University of Technology (1992)

[6-21] Weihe, S.: Modelle der fiktiven Rissbildung zur Berechnung der Initiierung und Ausbreitung von Rissen. Ein Ansatz zur Klassifizierung. Institut für Statik und Dynamik der Luft- und Raumfahrtkonstruktionen, Universität Stuttgart, Dissertation (1995)

[6-22] Will, J.: Beitrag zur Standsicherheitsberechnung im geklüfteten Fels in der Kontinuums- und Diskontinuumsmechanik unter Verwendung impliziter und expliziter Berechnungsstrategien: Bauhaus Universität Weimar, Dissertation 1999, Berichte Institut für Strukturmechanik 2/99

[6-23] Ganz, H.R.: Mauerwerkscheiben unter Normalkraft und Schub. ETH Zürich, Institut für Baustatik und Konstruktion. Dissertation. Birkhäuser Verlag Basel (1985)

[6-24] Mann,W.; Müller,H.: Schubtragfähigkeit von gemauerten Wänden und Voraussetzungen für das Entfallen des Windnachweises. Berlin: Ernst u. Sohn. In: Mauerwerk-Kalender (1985)

[6-25] Berndt, E.: Zur Druck- und Schubfestigkeit von Mauerwerk – experimentell nachgewiesen an Strukturen aus Elbsandstein. Bautechnik 73, S. 222-234 Ernst & Sohn, Berlin (1996)

[6-26] Grosse, M.: Zur numerischen Simulation des physikalisch nichtlinearen Kurzzeittragverhaltens von Nadelholz am Example von Holz-Beton-Verbundkonstruktionen. Dissertation, Bauhaus-Universität Weimar (2005)

[6-27] Pluijm, R. van der: Shear behaviour of bed joints. Proc. 6th Noth American Masonry Conference, S. 125-136 (1993)

7 APENDIX USER INFERFACE - USERMPLS

7.1.1 **LAW = 99 – User-Material**

Feld	1	2	3	4	5	6	7	8	9	10
0-10 isotrop	LAW	up1	...							
11-20 1.TF										
21-30 2.TF										
31-40 3.TF										
41-50 4.TF										
51-60									up58	wr
61-70	Elem	Intpt	eps	geps	maxit	cutmax	dtmin	maxinc		ktuser
71-80										

User Parameter up1 – up58

up1 – 58 - free definable material parameters

7.1.2 **Requirements of ANSYS (Release 13)**

Installation Guides | ANSYS, Inc. Windows Installation Guide |

Table 2.1 Operating System Requirements

Platform/OS	ANSYS/Workbench Compilers*
Intel EM64T, AMD64 / Windows XP x64 Edition Version 2003 Intel EM64T, AMD64/Windows Vista x64	Intel Fortran v10.1 Microsoft Visual Studio 2005 Professional Edition
Intel IA-32 bit / Windows XP (Build 2600) Version 5.1 Intel IA-32 bit / Windows Vista	Intel Fortran v10.1 Microsoft Visual Studio 2005 Professional Edition

* Compilers are required only if you will be using User Programmable Features or other customization options.

Advanced Guide | Chapter 14. User-Programmable Features and Nonstandard Uses |

14.1. User-Programmable Features (UPFs)

User-programmable features (UPFs) are ANSYS capabilities for which you can write your own FORTRAN routines. UPFs allow you to customize the ANSYS program to your needs, which may be a user-defined material-behavior option, element, failure criterion (for composites), and so on. You can even write your own design-optimization algorithm that calls the entire ANSYS program as a subroutine. UPFs are available in the ANSYS Multiphysics, ANSYS Mechanical, ANSYS Structural, ANSYS PrepPost, and ANSYS Academic (Associate, Research, Teaching Advanced, and Teaching Mechanical versions) products. For detailed information, see the *Guide to ANSYS User Programmable Features*.

7.1.3 **User materials in multiPlas**

The user interface „usermpls“ is in the actual version multiPlas Release 2.0 a non-sufficient tested β-Feature. This interface offers the user a personal enhancement of the material library multiPlas in ANSYS.

The results of own implementations are in the responsibility of the user.

```
      SUBROUTINE usermpls (LAW,up,F,DF,ka,eppli,FK,DK,nfail,eps,ncomp,
     x             sigtr,sigm,sigdev,inv2,inv3,sigs,ta0,iott,wr)
c
c *** User definierte (mehrflaechige) Fliessbedingung in multiplas
c *** mehrflaechige Fliessbedingung mit max. 18 Flieskriterien
c *** Basis: userpl
c
c  input arguments:
c     variable (type,sze,intent)    description
c
c     LAW     (int,sc,in)         - Materialmodell-Nr. hier =99
c     up      (dp,ar(58),in)      - tbdata-Input-Werte
c     eppli   (dp,ar(18,6),in)    - Vektor plastischer Dehnungskomponenten
c                                   d. einz. Fliesskriterien
c     eps     (dp,sc,in)          - Abbruch-Toleranz f. F>0
c     sigtr   (dp,ar(ncomp),in)   - Trial-Spannungsvektor
c     sigm    (dp,sc,in)          - Hydrostat. Spannung
c     sigdev  (dp,ar(6),in)       - Deviatorspannung
c     inv2    (dp,sc,in)          - J2 zweite Deviatorinvariante
c     inv3    (dp,sc,in)          - J3 dritte Deviatorinvariante
c     ta0     (dp,sc,in)          - ta0=sqrt(2.0d0/3.0d0*inv2)
c     iott    (int,sc,in)         - Ausgabesteuerung
c     wr      (int,sc,in)         - Schalter fuer Ausgabeumfang
c
c  output arguments:
c     variable (type,sze,intent)    description
c
c     F       (dp,ar(18),out)     - Fliesskriterien
c     DF      (dp,ar(6,25),out)   - Partielle Ableitungen
c                                   d. Fliesskriterien u. plast. Potentiale
c     ka      (dp,ar(5),inout)    - History-Variablen kappa
c                                   (plast. Dehnungsanteile Ver-/Entfest.)
c     FK      (dp,ar(18),out)     - Partielle Ableitungen dF/dkappa
c     DK      (dp,ar(5,18),out)   - Partielle Ableitungen dkappa/dLambda
c     nfail   (int,sc,inout)      - Zaehler verletzter Fliesskriterien
c
c
      INTEGER LAW,nfail,wr,iott
      DOUBLE PRECISION up(58),F(18),DF(6,25),ka(5),eppli(18,6),
     x FK(18),DK(5,18),eps,sigtr(6),sigm,sigdev,inv2,inv3,sigs,ta0,
     x hyd

c *** Funktionen von ANSYS (s. ANSYS UPF-Programmers-Manual)
cc      EXTERNAL VZERO

c *** weitere erf. interne Variablen
c     DOUBLE PRECISION F1,ftx

c  *** Bsp. fuer Kontrollausgabe (Entwickler-Mode)
cc      if (wr.ge.1) then
cc      write(iott,*)
cc     x '***************** START usermpls ****************************'
cc      endif

C  *** update strain-Softening parameter kappa
cc      ka(1)=ka(1)+eppli(1,1)
cc      Oftx=dexp(-h*ftx/G(1)*ka(1))

c  *** Bsp. fuer Kontrollausgabe (Entwickler-Mode)
cc   if (wr.ge.4) then
cc        write (iott,*) '*** Kontrollausgabe Softeningfkt. in jexp ***'
cc        write (iott,2000) Oftx
cc        write (iott,2010) (ka(1))
cc       endif
cc2000  format('2000 Oftx ',1(1x,F14.7))
cc2010  format('2010 kappa(1) = ',1(1x,1pe14.7))

C *** Abfrage Kriterium F1
cc      ftx=up(1)
cc      F1=sigtr(1)-ftx*Oftx

cc      IF (F1.ge.eps) THEN
C *** Zugversagen (Kriterium F1)
cc         F(1)=F1
```

```
cc      nfail=nfail+1
C *** dF/dS (assoziiert)
cc          DF(1,1)=1.0d0
cc          DF(2,1)=0.0d0
cc      DF(3,1)=0.0d0
cc      DF(4,1)=0.0d0
cc      DF(5,1)=0.0d0
cc      DF(6,1)=0.0d0
C *** dF1/dKappa1
cc          FK(1)=ftx**2*h*Oftx/G(1)
C *** dkappa1/dLambda
cc          DK(1,1)=1.0d0
cc       ENDIF

C *** Abfrage Kriterium Fn
c     ...
cc       IF (Fn.ge.eps) THEN
C *** Versagen (Kriterium Fn
cc          F(n)=Fn
cc      nfail=nfail+1
C *** dF/dS
cc          DF(1,n)=...
cc          DF(2,n)=...
cc      DF(3,n)=...
cc      DF(4,n)=...
cc      DF(5,n)=...
cc      DF(6,n)=...
c *** z.B. nicht assoziierte Fliessregel
C *** dQ/dS
cc          DF(1,20)=...
cc          DF(2,20)=...
cc      DF(3,20)=...
cc      DF(4,20)=...
cc      DF(5,20)=...
cc      DF(6,20)=...

C *** dFn/dKappa
cc          FK(n)=...
C *** dkappa/dLambda
cc          DK(...,...)=...
cc       ENDIF

      RETURN
    END
```

Contact & Distributors

Germany & worldwide
Dynardo GmbH
Steubenstraße 25
99423 Weimar
Tel.: +49 (0)3643 900 830
Fax. +49 (0)3643 900 839
www.dynardo.de
contact@dynardo.de

Dynardo Austria GmbH
Office Vienna
Wagenseilgasse 14
1120 Vienna
Austria
www.dynardo.at
contact@dynardo.at

Germany
CADFEM GmbH
Marktplatz 2
85567 Grafing b. München
Germany
www.cadfem.de

science + computing ag
Hagellocher Weg 73
72070 Tübingen
Germany
www.science-computing.de

Austria
CADFEM (Austria) GmbH
Wagenseilgasse 14
1120 Wien
Austria
www.cadfem.at

Switzerland
CADFEM (Suisse) AG
Wittenwilerstrasse 25
8355 Aadorf
www.cadfem.ch

Czech Republic, Slovakia, Hungary
SVS FEM s.r.o.
Škrochova 3886/42
615 00 Brno-Židenice
Czech Republic
www.svsfem.cz

Russia
CADFEM CIS
Suzdalskaya Str. 46-203
111672 Moscow
www.cadfem-cis.ru

India
CADFEM Engineering Services India
6-3-887, MCP Arcade 4th Floor
Raj Bhavan Road, Somajiguda
Hyderabad 500 082
www.cadfem.in

USA
CADFEM US, Inc.
3 Research Drive
Greenville, SC 29607
www.cadfem-us.com

Japan
TECOSIM Japan Limited
Mimura K2 Bldg. 401
1-10-17 Kami-kizaki
Urawa-ku, Saitama-shi
Saitama 330-0071 Japan
www.tecosim.co.jp

Korea
CAE Technology Inc.
A-208, Seoul Hightech Venture
Center
29, Gonghang-daero 61-gil,
Gangseo-gu, Seoul 157-030, Korea
www.caetech.co.kr

TaeSung S&E Inc.
Kolon Digital Tower 2
10F, Seongsu-dong 2 ga
Seongdong-gu
Seoul 333-140, Korea
www.tsne.co.kr

China
PERA GLOBAL Holdings Inc.
Standard Chartered Tower 201
Century Avenue, Suite 7 B-C
Shanghai, 200120
www.peraglobal.com